MODULATION AND ROLES OF STRESS-RESPONSIVE PROTEINS IN COXSACKIEVIRUS INFECTION

by

Ye Qiu

B.Sc., Peking University, 2010

A THESIS SUBMITTED IN PARTIAL FULFILLMENT OF

THE REQUIREMENTS FOR THE DEGREE OF

DOCTOR OF PHILOSOPHY

in

THE FACULTY OF GRADUATE AND POSTDOCTORAL STUDIES

(Pathology and Laboratory Medicine)

THE UNIVERSITY OF BRITISH COLUMBIA

(Vancouver)

August 2017

Abstract

Viral myocarditis is an inflammatory heart disease caused by viral infection, which is a major cause of sudden death in children and young adults. Among the various viruses, coxsackievirus B3 (CVB3) is a predominant pathogen of viral myocarditis. As CVB3 replication is tightly tangled with signaling pathways in host cells, an in-depth study of CVB3-host interactions would promote the understanding of the pathogenesis of viral myocarditis and provide critical drug targets for the development of therapeutics. CVB3 infection induces different types of stress in host cells, and in turn, the cells respond to the stress via expressing certain stress-responsive proteins (SRPs) to counteract the stress for cell survival. During the co-evolution of virus and host, CVB3 has developed sophisticated strategies to modulate and utilize SRPs to benefit its own replication. The main **objective** of this dissertation is to investigate the modulation and functional roles of SRPs in CVB3 infection and CVB3-induced myocardium damage. I **hypothesize** that 1) CVB3 infection differentially regulates the expression and activity of SRPs at transcription, translation or post-translation level; 2) the dysregulation of SRPs benefits CVB3 replication and promotes CVB3-induced cell damage. This dissertation mainly focuses on two SRPs, the inducible heat shock 70 kDa protein (Hsp70) and nuclear factor of activated T-cell 5 (NFAT5), during CVB3 infection. Using *in vitro* (cell culture) and *in vivo* (mouse) models, I demonstrated an increase of Hsp70 but a decrease of NFAT5 during CVB3 infection. Further studies elucidated the mechanism underlying such changes as well as the feedback effects on CVB3 replication. Hsp70 was upregulated via CaMKII-HSF1 signaling cascade activated in CVB3 infection and in turn promoted CVB3 infectivity via stabilizing viral genome and benefiting viral translation. NFAT5 was cleaved by CVB3 proteases 2A and 3C, generating a 70 kDa

dominant negative truncate, which inhibited the iNOS-mediated anti-viral activity of NFAT5. Together, my findings have uncovered the new roles of SRPs in CVB3 infection and potential novel drug targets for CVB3-induced myocarditis.

Lay Summary

Heart diseases are a major threat to the public health around the world. Viral infection is an important cause of lethal heart diseases. Among different viruses, coxsackievirus B3 (CVB3) is one of the most common pathogens detected in patients with acute or chronic heart diseases in North America. Unfortunately, there is no effective drug available for the treatment of CVB3-induced heart diseases recently.

The classical anti-virus drugs killing viruses directly failed to inhibit CVB3 infection. In my study, I demonstrated a novel anti-CVB3 strategy which was aimed at enhancing the defense of the host cells against the virus. Briefly, I have found two human proteins critical for CVB3 survival in the heart. By modulating these proteins with specific treatment, CVB3 could not survive in the heart cells anymore and thus the heart damage caused by viral infection was blocked. These findings provided new ways for the development of anti-CVB3 drugs.

Preface

This dissertation is built mainly upon the research work of two manuscripts supported by one CIHR research grant [MOP125995].

Chapter 1 is an introduction of the background of the research project.

Chapter 2 is based upon an original research article entitled *Hsp70-1: upregulation via selective phosphorylation of heat shock factor 1 during coxsackieviral infection and promotion of viral replication via the AU-rich element,* (2016). Cell Mol Life Sci. 73(5):1067-84. I designed the majority of the experiments and contributed to 90% of the data. Dr. Xin Ye came up with the initial idea of this project and produced the data of upregulation of Hsp70 in HeLa cells as shown in Figure 2.1A in this dissertation. Dr. Paul Hansen produced the images of the immunohistochemical (IHC) staining as shown in Figure 2.1E. I interpreted the data and drafted the whole manuscript. Dr. Decheng Yang did the revision and proofreading of this manuscript. Copyright permissions have been obtained from the journals.

Chapter 3 is based upon an unpublished original research article titled "*Cleavage of osmosensitive transcriptional factor NFAT5 by Coxsackieviral proteases promotes viral infectivity and cardiac cell damage*", which has been submitted for publication but it is still under review. I designed all the experiments, generated all the data and drafted the whole manuscript with Dr. Decheng Yang's revision.

I also worked closely with Dr. Fengping Wang, a visiting scholar in our lab, and Dr. Mary Zhang, a Research Associate in our lab, on the manuscript entitled *Heat shock protein 70 promotes coxsackievirus B3 translation initiation and elongation via Akt-mTORC1 pathway depending on activation of p70S6K and Cdc2,* (2017) Cell Microbiol. Epub ahead of print. In

this manuscript, I contributed to ~30% of the experimental design and data production, and I am listed among the three co-first authors. The major results of this manuscript is briefly described in the "Limitations and future directions" part of this dissertation.

In addition to the work described above, I also conducted the literature review about the therapeutic application of RNA nanotechnologies and published two first-author book chapters: 1) Ye Qiu et al., *Application of microRNAs in RNA nanotechnology and antiviral therapeutics.* (2012) RNA Nanotechnology and Therapeutics, Taylor & Francis Books, Page 513-532; 2) Ye Qiu et al., *Small RNA molecules in antiviral therapy,* (2012) RNA nanotechnology, Pan Stanford Publishing Pte. Ltd., Page 287–316. Meanwhile, during the collaboration with other members in our laboratory and with other research groups, I co-authored in another 9 peer-reviewed articles.

All animal experiments were carried out in accordance with the Guide to the Care and Use of Experimental Animals – Canadian Council on Animal Care, and all protocols were approved by the Animal Care Committee, Faculty of Medicine, University of British Columbia (protocol number: A16-0093).

Table of Contents

List of Tables

List of Figures

List of Abbreviations

ADP: adenosine diphosphate

ATF: activating transcription factor

ATP: adenosine triphosphate

AED: auxiliary export domain

Akt: protein kinase B

AR: aldose reductase

BGT-1: betaine/GABA transporter

CAR: coxsackievirus-adenovirus receptor

CHOP: CCAAT-enhancer-binding protein homologous protein

CPE: cytopathic effect

CREB: cyclic AMP responsive element binding protein

CVB: coxsackie group A serotypes

CVB: coxsackie group B serotypes

DAF: decay-accelerating factor

DAP5: death associated protein 5

DCM: dilated cardiomyopathy

DMEM: Dulbecco's modified Eagle's medium

eIF4G: eukaryotic initiation factor 4G

ER: endoplasmic reticulum

ERAD: ER-associated protein degradation

ERK1/2: extracellular signal regulated kinase 1/2

FBS: fetal bovine serum

FL: full-length

GEF: guanine nucleotide exchange factor

GRP78: 78 kDa glucose-regulated protein

GSK3β: glycogen synthase kinase 3β

HCV: hepatitis C virus

H&E: hematoxylin and eosin

HIV-1: human immunodeficiency virus 1

HRV: human rhinovirus

Hsc70: heat shock 70 kDa cognate

HSP: heat shock protein

Hsp27: heat shock 27 kDa protein

Hsp70: heat shock 70 kDa protein

HSS: hypertonic saline solution

IA: immunoadsorption

IL: interleukin

IFN: interferon

iNOS: indicible nitric oxide synthase

IP: intraperitoneal

IRE1: inositol-requiring enzyme 1

IRES: internal ribosomal entry site

IVIG: intravenous immunoglobulins

JNK: c-Jun N-terminal kinase

kDa: kilodalton

KO: knockout

LTR: long terminal repeat

LV: left ventricular

LVEF: left ventricle ejection fraction

MAPK: mitogen-activated protein kinase

MEK: mitogen-activated protein kinase kinase

MHC: major histocompatibility complex

MRI: magnetic resonance imaging

MTb: *Mycobacterium tuberculosis*

Mut: mutant

MOI: multiplicity of infection

MTS: (3-(4,5-dimethylthiazol-2-yl)-5-(3-carboxymethoxyphenyl)-2-(4-sulfophenyl)-2H-tetrazolium, inner salt)

NES: nuclear export signal

NFAT5: nuclear factor of activated T-cells 5

NFκB: nuclear factor κB

NLS: nuclear localization signal

NK cells: natural killer cells

NO: nitric oxide

nt: nucleotides

OCT-1: octamer-binding protein

ORF: open reading frame

Osp94: osmotic stress protein of 94 kDa

PABP: poly(A)-binding protein

PBS: phosphate buffer saline

PCBP2: poly (rC)-binding protein 2

PERK: PKR-like ER protein kinase

pfu: plaque forming units

pi: post infection

pt: post transfection

PI3K: phophatidyl-3-kinase

PKR: protein kinase R

PTB: polypyrimidine tract binding protein

qPCR: quantitative real-time PCR

RHD: REL-homology domain

SBD: substrate binding domain

Ser: serine

SIDS: sudden infant death syndrome

siRNA: small interfering RNAs

ShcA: Src homology and collagen A

SMIT: sodium/myo-inositol transporter

Src: non-receptor tyrosine kinase protein encoded SRC gene

TAD: transactivation domain

TauT: taurine transporter

TBP: TATA-box binding protein

TGF: transforming growth factor

Thr: threonine

TLRs: Toll-like receptor

TNF: tumor necrosis factor

UPR: unfolded protein response

UTR: untranslated region

UV: ultraviolet

VPg: viral genome linked protein

WT: wild type

XBP1: X box binding protein 1

Acknowledgements

I offer my enduring gratitude to my supervisor Dr. Decheng Yang for supporting my graduate study and research work at UBC. He mentored me with extensive knowledge, exceptional patience and an impressive sense of responsibility. During the past six years, Dr. Yang instructed me to do scientific research, to draft manuscripts and to write grant proposal, helping me seize necessary skills for initializing my academic life. Meanwhile, he offered me the chance to participate in supervision of new lab members and lab management, greatly improving my leadership, communication and management ability. In addition, he also helped me settle down in Canada, a place thousands of miles away from my hometown. His excellent guidance has laid a solid foundation for my future career.

I would like to thank my supervisory committee (Dr. Ed Pryzdial, Dr. Honglin Luo, and Dr. Scott Tebbutt) for their instruction, advice and comments to improve my research and to optimize the pace of my graduate study. I also want to thank Dr. Haydn Pritchard and Dr. Bruce McManus for their guidance at the key steps in my study.

I am also very grateful to the current and former colleagues in the Centre for Heart Lung Innovation (HLI). Our Research Associate Dr. Mary Zhang directly trained me with various experimental techniques and helped me with my daily life. Dr. Xin Ye, the previous graduate student in our lab, contributed a lot to the successful application of Hsp70 grant which is the major support of my research, and he also guided me to initialize my research projects. My peers Paul Hanson, Fengping Wang, Helen Yao, Lei Tong, Hongxin Sheng, Brian Cho, Ronald Xie and Guangze Zhao provided valuable suggestions and technical support for my study and made our lab a fun place. I am truly grateful to Jingchun Zhang, Haoyu Deng and

Gabriel Fung of Dr. Luo's Lab for their technique support and idea sharing. I also appreciate the animal work support from Claire Smits and Tatjana Bozin in GEM Facility of HLI.

I also show my sincere gratitude to all my friends in UBC and Vancouver, especially Auntie Wang, Auntie Zhou, Sister Liu and Xining Yang, without whom I could not enjoy the colorful life during my graduate study.

The research project in this dissertation was funded by a CIHR grant [MOP125995].

For my dear parents

For your genome, for your nurturing, and for your enlightening

I love you forever

Chapter 1 Introduction

1.1 Viral Myocarditis

1.1.1 Definition and epidemiology

Myocarditis is an acute or a chronic inflammatory process in the myocardium [9, 10]. This disease is an ancient term used to refer to almost all heart diseases before early nineteenth century [11]. The modern concept myocarditis was first introduced by Sobemheim in 1837 **[12]**. Then, the disease was further defined by Feidler in 1899 **[13]** and classified by Saphir in 1942 **[14]**. Currently, the widely accepted diagnostic standard for myocarditis is the Dallas criteria established in 1986, which defines myocarditis as inflammatory cell infiltration of the myocardium with non-ischemic damage to cardiomyocytes [15, 16].

Viral infection is the most common cause of myocarditis [17], which is specifically referred to as viral myocarditis. Epidemiological studies suggest that up to 50% of the general public is exposed, typically early in life, to cardiotropic viruses and that approximately half of these individuals may have an episode of acute viral heart infection at some points in their lives [18, 19]. Although majority of these individuals recover spontaneously, certain acute viral myocarditis may progress into dilated cardiomyopathy (DCM), a severe heart disease characterized by heart enlargement, left ventricle (LV) chamber dilation, and systolic dysfunction [3, 20, 21]. In patients less than 40 years of age, virus-induced DCM is one of the major natural causes of sudden, unexpected death, accounting for approximately 20% of all such cases.[9, 19, 22]. To date, there is no specific therapy or vaccine for these virus-induced heart diseases. For patient with DCM, the only treatment thus far is heart transplantation[3, 20, 21].

1.1.2 Etiology

Various viruses can cause viral myocarditis and the types of virus detected in myocarditis vary with time and geographic locations. In developed countries, until the 1990s, the most frequently identified viruses were enteroviruses, particularly coxsackievirus group B serotypes (CVBs), accounting for 30% - 50% of all myocarditis cases in North America [23]. Thus, early understanding of pathogenesis of viral myocarditis came almost entirely from experimental models of acute CVB infection. Regardless, studies after year of 2000 have indicated that parvovirus B19 (PVB19) and human herpes virus 6 (HHV6) are the viruses most frequently found in patients with acute and chronic myocarditis, followed by enterviruses as the third predominant pathogen of viral myocarditis (**Figure 1.1**) [3, 24-27]. However, it is still controversial to bridge the causality between PVB19 and myocarditis. Firstly, the major infectious targets of PVB19 in the heart are endothelial cells but not cardiomyocytes, the loci where pathological change of myocarditis occurs [28]. This finding suggests that PVB19 is probably not capable of causing damage in myocardium directly and may facilitate the progress of inflammation via enhancing immune infiltration. Secondly, PVB19 genome, protein and specific serum IgG were detected in the heart tissue of patients without evidence of myocarditis or DCM, which reached as high as 85% among 100 samples detected in a study [29, 30]. These reports indicate that the present of PVB19 in myocarditis is likely to be a coincidence and detection of PVB19 only is not diagnostically helpful for determining the etiology of adult myocarditis [31]. Similar dilemma also occurs on HHV6, since the well documented infectious loci of HHV6 are also endothelial cells [32, 33] and there is lack of evidence for the expression of HHV6 receptor CD46 on cardiomyocytes [34, 35]. Therefore, enteroviral infection is still an important model used in the study of viral myocarditis currently, among which coxsackievirus B3 (CVB3) is the most widely studied

serotype in the CVB group. In addition to viruses described above, other viruses reported to be detected in myocarditis include adenovirus [36], hepatitis C virus (HCV) [37], Epstein-Barr virus (EBV) [38] and human immunodeficiency virus (HIV) [39].

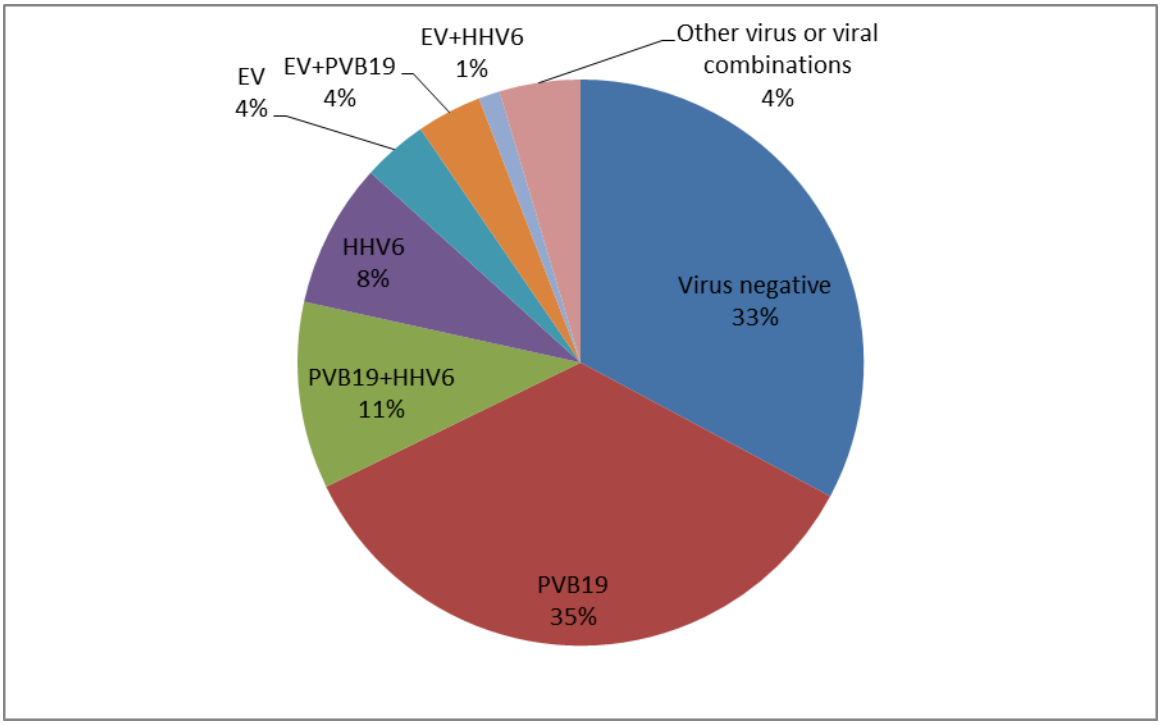

Figure 1.1. Prevalence of different virus or viral combinations detected in patients with myocarditis. The graph is made based on the report of Kuhl et al. [3].

1.1.3 Pathogenesis of viral myocarditis

The development of viral myocarditis, such as CVB3-induced myocarditis can be typically described as two stages, the pre-cardiac stage and the cardiac stage. The pre-cardiac stage is the process of initial viral entry, viral spread in the circulatory system and entry into myocardium. The cardiac stage is the period in which the pathological change of myocardium occurs and is further divided into three phases: 1) the acute phase characterized by active viral replication in

cardiomyocytes, 2) the sub-acute phase characterized by with immune infiltration and inflammation and 3) the chronic or remodeling phase [7, 40] (**Figure 1.2**).

1.1.3.1 Pre-cardiac stage

Since the heart is a well-protected organ shielded by the blood–heart barrier, the virus can hardly reach the myocardium directly. The initial infectious loci vary among different viruses. For example, enteroviruses enter the host via the oral cavity and/or respiratory tract, then reproduce in the upper respiratory tract and small intestine but usually lead to no serious symptoms [41]. Viruses then invade into the bloodstream by which they disseminate to a variety of target organs, such as heart. The spread of viruses in the circulatory system typically result in a minor viremia, but high viral load in the blood or exaggerated immune response to the virus may lead to sepsis with symptoms like fever, increased heart rate, increased breathing rate, and confusion [42, 43]. The mechanism underlying the transmission of viruses from the blood to the myocardium has not been well elucidated. For CVB3, most studies attribute this step to simple diffusion of extracellular viral particles but some believe that macrophages play as a critical vehicle in delivering the virus to myocardium [44]. After viruses invade into cardiomyocytes, the major viremia occurs in the heart and the cardiac stage starts.

1.1.3.2 Cardiac stage

In murine models with CVB3-induced myocarditis, the acute phase of cardiac stage lasts for 3 to 4 days after the initial viral infection in the myocardium. In this phase, active viral replication proceeds in cardiomyocytes and stimulates different responsive signalings. Intense viral replication directly inflict protein overload and protelytic damage to the host cells, subsequently

inducing apoptosis and/or necrosis of cardiomyocytes [45-47]. Meanwhile, the pathogen-associated molecular patterns on the viral capsid are recognized by cardiac Toll-like receptors (TLRs) [48] on cardiac resident myocytes, fibroblasts, endothelial cells, and dendritic cells. The TLRs activates these cells to express proinflammatory cytokines including interleukin-1b (IL-1b), IL-6, IL-18, tumor necrosis factor-α (TNF-α), and type I/ type II interferons (IFNs) [49, 50]. These cytokines exert a range of effects on myocardium. For instance, the high level of cytokines triggers the remodeling of the extracellular matrix (ECM) [51]; Type I IFN blocks protein synthesis, stimulate p53-mediated apoptosis, and upregulate the immunoproteasome and major histocompatibility complex (MHC) classes I and II [52]; the cytokines activate local macrophages, endothelial adhesion molecules, chemokines and chemokine receptors, contributing to the recruitment of innate immune cells [53].

The sub-acute phase ranged from day 4 to day 14 post infection (pi) commences with immune response and elimination of myocardial viruses [54]. The innate immune response is evoked first featured by infiltration of innate immune cells, such as natural killer (NK) cells. These innate immune cells are capable of recognizing and killing infected cells, which is the key step for viral clearance [55]. The innate immune response is later followed by accumulation of adaptive immune cells in the infected myocardium, including both T and B lymphocytes. $CD8^+$ cytotoxic T cells directly bind and eliminate infected cells by recognizing MHC class I antigens on infected cardiomyocytes, assisted by the cytokines TNF-α and IFN-γ [52], while CD4+ T helper cells facilitates the antigen presenting to cytotoxic T cells and B cells, and the latter produce neutralizing antibodies to limit the dissemination of extracellular viral particles [53]. The active immune response during the sub-acute phase lowers the active viral progeny to undetectable

level [54], but it kills infected cardiomyocytes which can barely regenerate, causing irreversible cardiac damage.

The third phase is featured by cardiac repair and remodeling after complete clearance of active viral particles. Acute immune response is subsided due to expression of anti-inflammatory cytokines such as transforming growth factor-β (TGF-β) and IL-10 secreted by regulatory T cells and M2 macrophages are activated to promote the replacement of dead tissue with fibrotic scar [53]. Large-scale myocardial repair may lead to cardiac dilation and compensatory hypertrophy, resulting in contractile dysfunction for long term [52]. Alternatively, viral RNA and viral proteins may still persist in cardiomyocytes though the viral replication is restricted to RNA synthesis [56, 57]. Viral persistence continues inducing pro-inflammatory cytokines, such as IL-18 and TNF-α [58], resulting in chronic inflammation which finally progresses to DCM [24, 56].

1.1.4 Treatment of viral myocarditis

Long-term follow-up studies indicated a rate of 40 – 60% of spontaneous recovery of myocardial function of patients with suspected viral myocarditis [59] for whom no treatment was needed. However, it is extremely risky to rely on the spontaneous recovery of myocarditis, since the development of myocarditis is hard to predict. Therefore, prompt treatment is necessary for symptomatic viral myocarditis. The antiviral treatment seems to be plausible in the early stage of viral infection. Vaccination for CVB3 has been tried in murine models, including a subunit vaccine from a non-virulent strain of CVB3 [60] and an inactivated CVB3 [61]. Both trials were promising with dramatically lower mortality of mice with CVB3-induced myocarditis. Anti-enterovirus compounds such as pleconaril, WIN 54954 and soluble CAR-Fc have also been tested in animal models for relieving viral myocarditis. For instance, pleconaril binds to CVB3

capsid proteins, prevents CVB3-receptor binding, and thus blocks the infectivity of CVB3 [62, 63]; WIN 54954 inhibits early events of CVB3 replication and reduces cardiomyocyte apoptosis [64-66]; a soluble IgG1-Fc fusion protein CAR-Fc neutralizes the extracellular viral particles and attenuates CVB3-induced myocarditis [67]. However, these treatments have not been applied to humans due to the high mutation rates of the viruses and the epidemiological shift from enteroviruses to PVB19 and HHV6 in the late 1990 (described above). Interferon-β is a broad-spectrum antiviral agent subduing viral mutation, which has been proved to be effective in acute entero- and adenoviral myocarditis [68] but not in chronic PVB19 myocarditis [69]. These results were probably not due to the virus types but to that antiviral therapy is only effective in cases with active viral infection. Intravenous immunoglobulins (IVIG) is another promising therapy for myocarditis due to its antiviral effect as well as immunomodulation properties which prevent the formation of proinflammatory cytokines [70]. Though several trials have shown benefit of IVIG on the treatment of viral myocarditis, the effect of IVIG is still controversial since no viral etiology was assessed in those trials [71, 72]. Immunoadsorption (IA) is a therapeutic technique to eliminate cardiotoxic autoantibodies together with cytokines, which is a major cause of myocardium damage in viral myocarditis. IA has been tested in patients with DCM which showed a marked reduction of ß-receptor autoantibodies and a significant improvement of cardiac function [73-75], but it was not confirmed that the DCM was caused by viral myocarditis and IA's effect on viral myocarditis is still obscure. Nevertheless, considering viral myocarditis can be a rapidly progressed lethal disease, easily accessible therapy is still in demand for this disease.

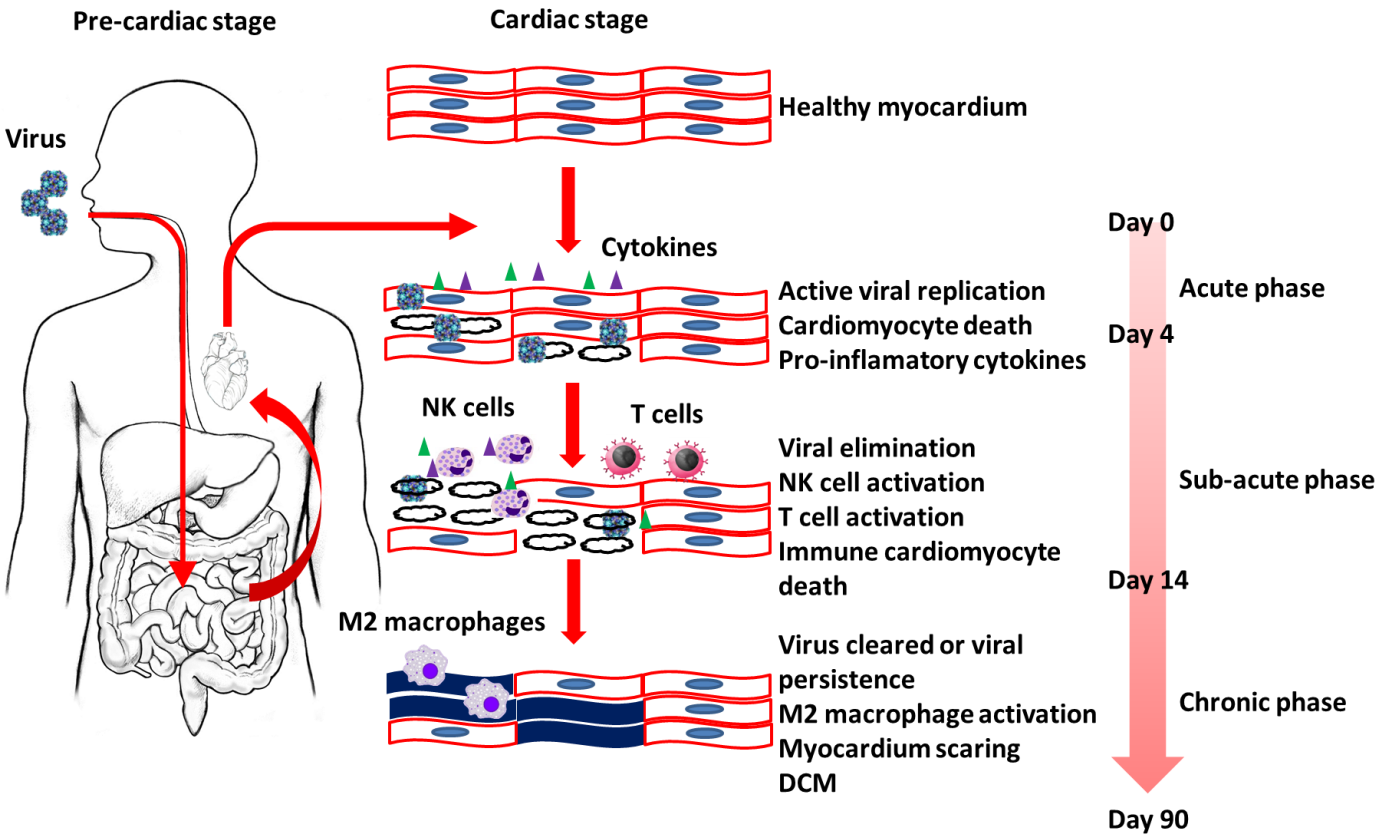

Figure 1.2. Pathogenesis of CVB3-induced viral myocarditis. In the initial infection or pre-cardiac stage, the virus enters the blood via small intestine and disseminates to different organ including the heart. In the heart, the virus starts the secondary infection or cardiac stage which can be further divided into three phases: 1) the acute phase with active viral replication, 2) the sub-acute phase with immune infiltration and 3) the chronic or remodeling phase. The time points of each phase were captured from murine models. This graph was developed based on the reviews of Liu et al. [7] and Yajima et al. [8].

1.2 Coxsackievirus B3 (CVB3)

1.2.1 Discovery and classification of coxsackieviruses

Coxsackieviruses were first reported in sudden death of an adult male in 1944 and characterized as a filter-passing agent causing interstitial myocarditis in different animal models [76]. The first isolated strain of coxsackieviruses, coxsackievirus A (CVA), was obtained by Dalldorf and Sickles in 1948. In a trial to search for mouse-adaptive poliovirus, they isolated the virus from the feces of children with paralysis showing unique features different from poliovirus and suggested name the new virus as coxsackievirus after Coxsakie, a small town in New York where specimens were obtained [77]. In 1949, Melnick et al. isolated the second coxsackiviral strain, CVB, from patients with non-paralytic poliomyelitis or aseptic meningitis, and pointed out that the virus was widespread in the public during the summer of 1948 [78]. From then on, CVA and CVB has been referred to as two groups of coxsackieviruses since different serotypes within them were further identified, including 23 serotypes for CVA and 6 for CVB [79-81].

Coxsackieviruses are classified to the genus of enterovirus of *Picornaviridae* family, regarding their fecal-oral transmission route [82] and their genetic homology to typical enteroviruses such as enterovirus 71 (**Figure 1.3**) [6]. Actually, the nomenclature of CVA and CVB is not based on the homology in their genomic sequence but on their pathogenicity. CVA was first noted in a flaccid paralysis due to generalized myositis, while CVB was initially related to spastic paralysis due to focal muscle injury and degeneration of neuronal tissue [83]. Later clinical trials have suggested that CVAs tend to infect the skin and mucous membranes, causing herpangina, acute hemorrhagic conjunctivitis, and hand-foot-and-mouth disease, while CVBs tends to infect the heart, pleura, pancreas, and liver, causing pleurodynia, myocarditis, pericarditis, and hepatitis [84]. Especially, CVB1, CVB3, and CVB5 are the most commonly

identified in myocarditis [52] and CVB3 was detected in 20-40% of all cases in acute onset heart failure and DCM [85, 86].

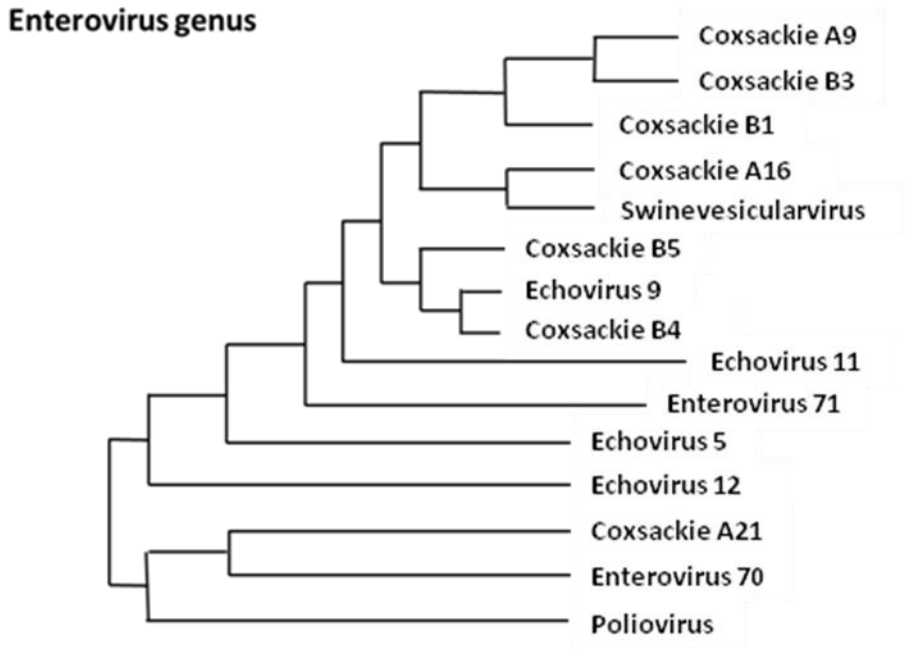

Figure 1.3. The genetic homology among common enteroviruses adapted from Donaldsom et al. [6]. The neighbor-joining tree was derived from an alignment of 196 base pairs of the 5' UTR from enteroviral standards. Notice that different serotypes within coxsackievirus A and B are not necessarily to be with higher genetic homology to their siblings than to non-coxsackieviral enteroviruses.

1.2.2 CVB3 genome and proteins

Similar to other picornaviruses, CVB3 is a small, non-enveloped virus with a single, positive-strand RNA genome of ~7400 nucleotides (nts). The genomic RNA of CVB3 contains a single open reading frame (ORF) flanked by 5' and 3' untranslated regions (UTR) (**Figure 1.4**) [87]. CVB3 genomic RNA is structurally similar to eukaryotic mRNA and can be translated directly using the host translational machinery. However, the 5' terminus of CVB3 genomic RNA lacks

the $m^7G(5')ppp(5')N$ cap structure present in cellular mRNAs, but instead, it is covalently bound to a viral protein VPg [88] which is essential for the initiation of viral transcription [89, 90]. The relative long 5' UTR (~740 nts) of CVB3 genome is highly structured to form some cis-elements critical for viral replication and translation. The cloverleaf structure harbored in the 5' UTR is the binding site of the viral RNA polymerase 3CD and plays important roles in the initiation and process of synthesis of negative-strand viral RNA in viral replication [91, 92]. Downstream of the cloverleaf structure locates an internal ribosome entry site (IRES) which is required for the cap-independent translation initiation of viral RNA distinct from normal cap-dependent translation utilized by most eukaryotic mRNA [88, 93]. The special translational mechanism of CVB3 is considered to be an evolutionary advantage which allows CVB3 to shut down the canonical cap-dependent translation of the host to release translational machinery for its own translation. The 3'UTR of CVB3 genome also harbors a binding site for 3CD. 3CD binding to both 5' and 3' termini is crucial for the circularization of viral genomic RNA which is key to the replication of both positive- and negative-strand viral RNAs [94]. In addition, the 3'UTR is ended with an poly(A) tail similar to cellular mRNAs which may be responsible for maintaining the stability of viral RNA [95-98].

CVB3 genomic RNA is translated into a single polyprotein. The polyprotein exerts auto-cleavage activity and is spontaneously cleaved into three precursor peptides, P1, P2 and P3, which are further cleaved by viral proteases to generate mature structural and non-structural viral proteins [52, 99, 100].

The P1 peptide is finally processed to full structural proteins VP1 – VP4 which are the components of viral capsid for the encapsulation of the viral genome. These four capsid proteins also determine the specific interaction between CVB3 and its primary receptor coxsackievirus-

adenovirus receptor (CAR) which is critical for viral entry, and especially, VP2 is capable of binding to the secondary receptor of CVB3, decay-accelerating factor (DAF), which is required for viral entry into cardiomyocytes where the CAR receptors are not well exposed [101].

The P2 peptide is further cleaved into two fragments, 2A and 2BC. 2A is a cysteine proteinase essential for viral polyprotein cleavage [94, 95] and 2BC is finally cleaved to 2B and 2C. 2BC and 2B are responsible for membrane alteration in infected cells, producing virus-induced vesicles where viral replication occurs [102]. Accumulation of 2BC and 2B changes the permeability of plasma membrane leading to cell lysis which is critical for viral progeny release [103]. Meanwhile, 2B/2BC complex also increases the efflux of Ca^{2+} from endoplasmic reticulum (ER) and Golgi complex, blocking protein transportation between ER and Golgi complex, which is speculated to inhibit the secretion of anti-viral agents such as interferons [103, 104]. 2C is an ATPase that interacts directly to the negative strands to facilitate viral RNA synthesis [105].

The P3 precursor is processed into two cleavage products, 3AB and 3CD. 3AB is reported to anchor the viral replication complex to the virus-induced vesicles via the hydrophobic interaction between the hydrophobic domain in the 3A portion and membrane vesicles [89]. 3AB is further cleaved and generate 3A and 3B. Similar to 2B, 3A disrupts ER-to-Golgi protein trafficking via redistribution of ADP-ribosylation factor (Arf) family, the important factors in protein secretion pathway [106]. 3B is also known as VPg, and it is covalently linked with the 5' terminus of viral genomic RNA and incorporates UMP to generate uridylylated VPg which is utilized as a primer for viral RNA synthesis [107]. 3CD is the precursor of 3C protease and 3D polymerase. 3CD exhibits protease activity which is responsible for processing P1 precursor [108]. 3CD does not exert polymerase activity but it was reported to contribute to circularization of the viral genome via interacting with both 5' and 3' ends in poliovirus [109]. 3D, the proteolytic product of 3CD, is an

RNA-dependent RNA polymerase which is the only RNA polymerase used by CVB3 to synthesize new RNA strands [110].

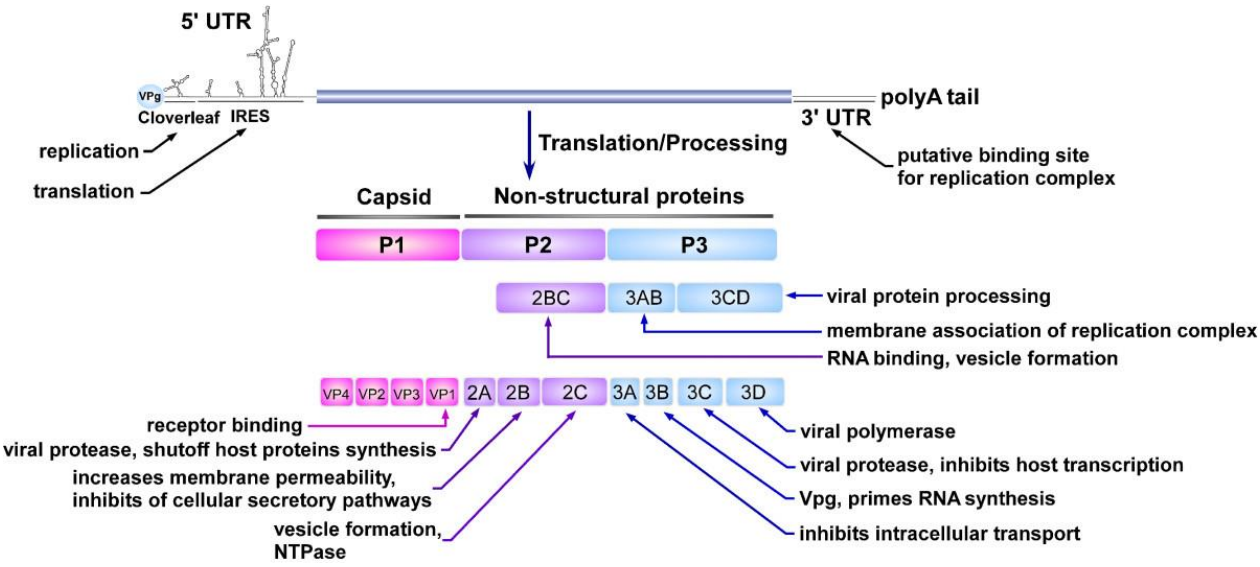

Figure 1.4. Schematic of enteroviral genome, the polyprotein processing and major functions of viral proteins adapted from Lin et al. [2]. The major cis-acting elements on viral genome, three main cleavage intermediates and 11 mature viral proteins are shown together with their major functions.

1.2.3 CVB3 life cycle

CAR is the primary receptor of CVB3 and binding to CAR is necessary for CVB3 internalization into cells [111]. CAR is a transmembrane protein of the immunoglobulin superfamily highly expressed in organs, such as heart and pancreas, sensitive to CVB3 [112-114]. However, in polarized cells like cardiomyocytes, CAR is exclusively located in the tight junction which is not accessible to extracellular viral particles [115]. To achieve the internalization into cardiomyocytes, CVB3 employs the auxiliary receptor DAF, a widely expressed

glycophosphatidylinositol (GPI)-anchored membrane protein located on the apical surface of cells [52, 100, 116]. Briefly, CVB3 binds to and clusters DAF to activate Abl, a tyrosine kinase, and activated Abl then induces actin polymerization and remodeling to facilitate the movement of CVB3-DAF complex to the tight junction where CVB3 binds to CAR and processes the internalization [102, 103, 117]. CVB3-DAF interaction also activates Fyn kinase which phosphorylates caveolin-1 and allows CVB3 to be internalized via caveolar vesicles [117]. As in nonpolarized cells such as HeLa cancer cells, since CAR is accessible on the cell surface, CVB3 can directly bind to CAR and enter the cell via endosomes independent of DAF and caveolin but requiring dynamin [118].

As shown in **Figure 1.5**, after internalization, CVB3 starts to uncoat its viral genome. The detailed mechanism underlying the uncoating step is still controversial but it is widely accepted that CVB3 externalizes the viral RNA and VP4 to the cytoplasm but remains the viral capsid in the endosome [119]. In the cytoplasm, the viral genomic RNA can be directly translated to viral proteins via a cap-independent IRES-driven mechanism using cellular translational machinery [120]. The viral proteins then induces the formation of single- and double-membrane compartments serving as a platform for viral replication [121]. The origin of such membrane structure is still unclear. Some reports claimed that it was derived from cellular organelles such as ER or Golgi complex via membranous alteration mediated by 2BC and 2B [122], while others suspected that the structure was persisting autophagosomes as a product of impaired autophagy in which the fusion between autophagosome and the lysosome is blocked [123]. Nevertheless, on the membrane vesicles, the viral replication complex is assembled and the replication of viral genomic RNA starts. The amplification of viral genomic RNA is well studied in poliovirus, another type of enteroviruses which shares much similarity with CVB3. During the genome replication, the parental RNA is

firstly transcribed to a complementary negative-strand RNA, and then the negative-strand RNA can be used as a template to produce nascent daughter positive-strand RNAs. Unlike translation, the amplification of CVB3 genomic RNA requires CVB3's own RNA-dependent RNA polymerase 3D, since 3D exerts the activity to uridylylate VPg to generate VPg-pUpU which can be used to initialize the synthesis of negative-strand RNA [124]. 3CD mediates the circularization of viral genomic RNA which delivers the replication complex to the 3' terminus where VPg-pUpU pairs the poly(A) tail as a primer and 3D polymerase elongates the new negative RNA strand until it reaches the 5' terminus of the parental strand [125]. After synthesis of negative RNA strand is completed, the negative strand is detached from the parental RNA and serve as a template for the production of new positive-strand viral genome [126]. The synthesis of new positive-strand RNA also requires 3D and VPg-pUpU but the efficiency is much higher than the synthesis of negative-strand RNA via a mechanism allowing to synthesize multiple positive-strand RNAs on a single copy of negative-strand template [127, 128]. The newly synthesized viral proteins and genomes are finally assembled to complete virions to be transmitted to other cells. As a cytolytic virus, the transmission of CVB3 is classically considered to depend on viral progeny release via induction of cell death and free diffusion in the extracellular fluid to surrounding cells [129]. However, a recent study indicated that the new CVB3 particles were transmitted to the adjacent cells without release via virus-induced cellular protrusions [130]. In addition, another study showed the presence of CVB3 progenies in extracellular microvesicles budding from neural progenitor and stem cells and myoblast cells [131]. These reports suggested novel routes of virus dissemination in non-cell-lytic patterns.

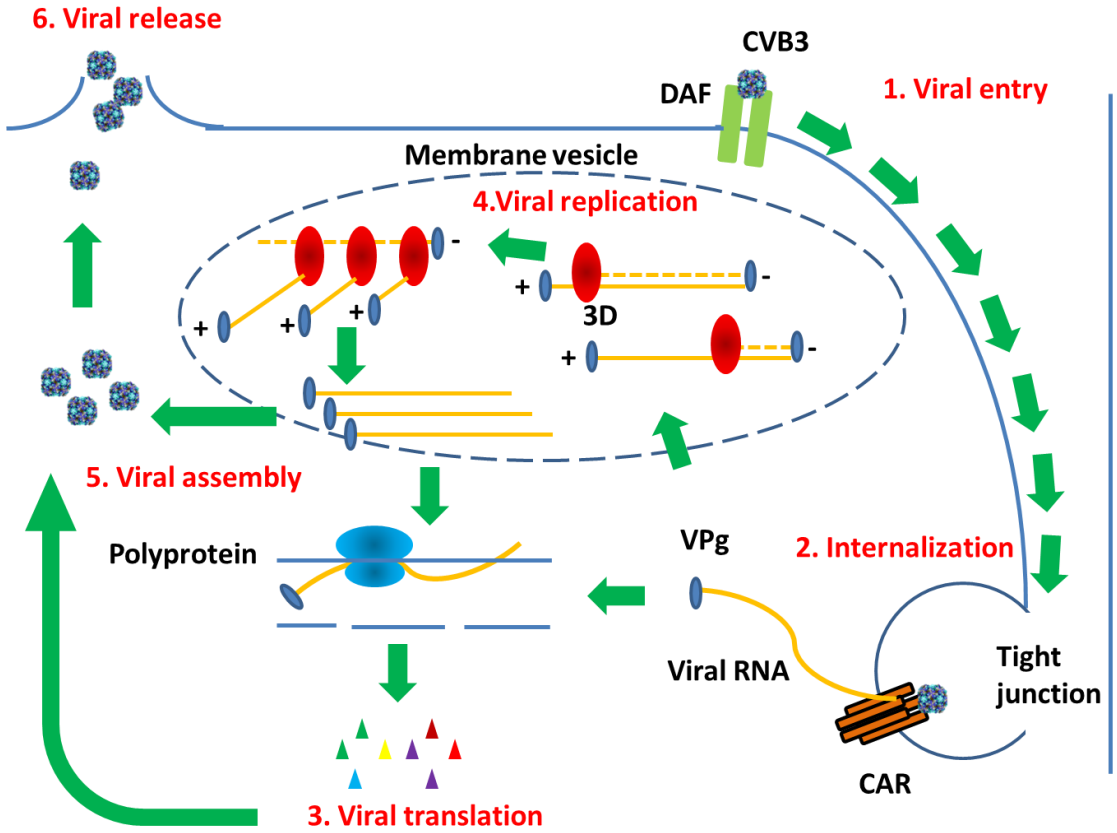

Figure 1.5. Brief flow chart of CVB life cycle. This figure was derived from Zoll et al. [1].

1.2.4 CVB3-induced cell stress

CVB3 infection induces various stresses in host cells, which is a major cause of CVB3 induced cell damage. The stresses trigger the defensive signals of the host cells and specific stress-responsive proteins (SRPs) are induced (**Figure 1.6**). These SRPs can be either adverse or beneficial for viral replication, which are potential drug targets for anti-CVB3 therapeutics.

ER stress is a cellular stress modulated in the infection of various viruses. ER stress is usually triggered by massive unfolded proteins accumulated in the ER, which activates unfolded protein response (UPR) [132]. In response to ER-stress, glucose-regulated protein 78 (GRP78), a master SRP of UPR in the ER, dissociates from the ER-stress sensors and thus is activated to facilitate protein folding [133-135]. Dissociation of GRP78 activates three ER-stress sensors, including ATF6a (activating transcription factor 6a), IRE1-XBP1 (inositol-requiring enzyme 1 and X box binding protein 1) and PERK (PKR-like ER protein kinase), resulting in attenuating new protein translation and removing misfolded proteins via ER-associated protein degradation (ERAD) pathway [136, 137]. A number of viruses have been shown to trigger ER stress upon infection. However, the pattern of molecular interactions that occurs within the UPR program differs depending on virus identity and type of host cell. Many viruses apparently activate only one or a subset of UPR pathways, and interestingly, some viral infections activate one pathway yet suppress others. For example, the expression of hepatitis C virus (HCV) proteins activates the PERK- and ATF6a-initiated pathways [138-140], yet suppresses the IRE1-XBP1 pathway [141]. Similarly, human cytomegalovirus (CMV) activates PERK and IRE1-XBP1 but suppresses the ATF6a pathway [142, 143]. Our laboratory has demonstrated that CVB3 infection triggers ER stress and differentially regulates the three arms of the unfolded protein [144]. Upon CVB3 infection, GRP78 expression was upregulated, and in turn ATF6a and XBP1 were activated via protein

cleavage and mRNA splicing, respectively, enhancing the expression of UPR target genes ERdj4 and EDEM1. Another UPR associated gene, $p58^{IPK}$, which often is upregulated during infections with other types of viruses, was downregulated at both mRNA and protein levels after CVB3 infection. In exploring potential connections between the three UPR pathways, we found that the ATF6a-induced downregulation of $p58^{IPK}$ is associated with the activation of PERK/protein kinase R (PKR) and the phosphorylation of eIF2a, suggesting that $p58^{IPK}$, a negative regulator of PERK and PKR, mediates cross-talk between the ATF6a/IRE1-XBP1 and PERK arms. Nevertheless, the ER stress induced in prolonged CVB3 infection eventually produced the induction of the proapoptoic transcription factor CHOP (CCAAT-enhancer-binding protein homologous protein), leading to cell apoptosis which benefits viral release.

Viral infection interplays a group of SRPs called stress-activated protein kinases (SAPKs), which are members of the mitogen-activated protein kinase (MAPK) family [145-149]. Typical SAPKs induced by CVB3 are c-Jun N-terminal kinase (JNK) and p38 mitogen-activated protein kinase (p38 MAPK) [150]. JNK1/2 and p38 MAPK are activated via phosphorylation during CVB3 infection and further activates their downstream signals ATF2 and heat shock protein 27 (Hsp27), respectively. In turn, p38 MAPK activation promotes CVB3-induced caspase-3 activation, enhancing cell apoptosis and viral progeny release.

It is well-documented that enteroviruses including CVB3 infection shuts down host protein translation by viral protease-mediated cleavage of cellular translation machinery, including eukaryotic initiation factor 4G (eIF4G), poly(A)-binding protein (PABP), and inhibits the cellular cap-dependent translation, which releases the translational machinery for viral cap-independent translation [151-153]. In addition, according to the studies on other enteroviruses, 3C protease is capable of entering nuclei through its precursor 3CD containing a nuclear localization

sequence [154, 155], where it cleaves numerous factors and regulators that are associated with cellular DNA transcription, such as TATA-box binding protein (TBP) [156], octamer-binding protein (OCT-1) [157], transcription activator p53 [158], cyclic AMP responsive element binding protein (CREB) [159], histone H3 [160] and DNA polymerase III [161]. The cleavage of these important factors responsible for gene expression will cause severe cellular stress.

Another major stress pathway induced by CVB3 infection is the PI3K (phophatidyl-3-kinase)/Akt pathway. Activation of PI3K/Akt cascade is induced at the later stage of infection [162], which further activates its downstream kinase glycogen synthase kinase 3β (GSK3β) via tyrosine phosphorylation, resulting in the degradation of β-catenin and subsequent cytopathic effect (CPE) in host cells [163].

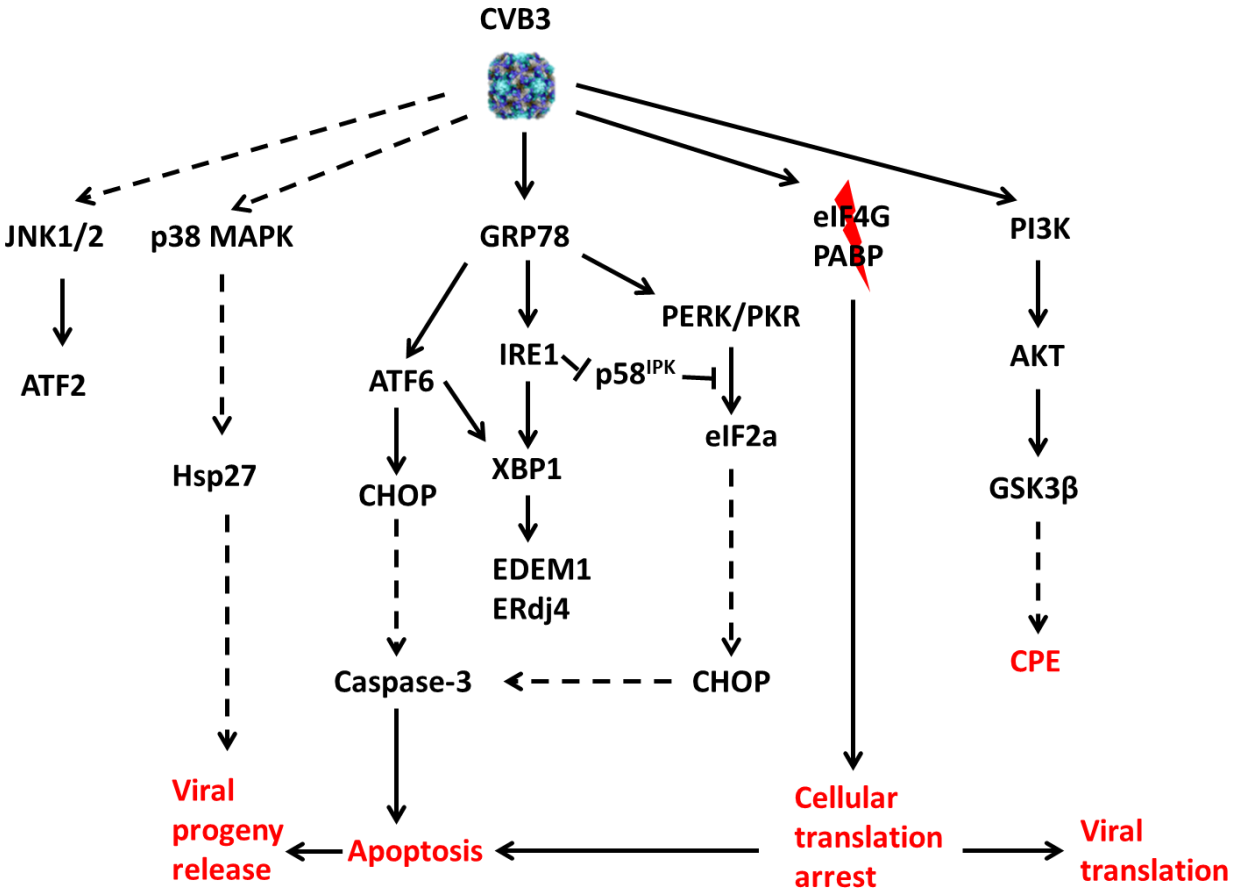

Figure 1.6. Brief summary of cell stress and SRPs induced by CVB3 infection. The dashed arrows indicate indirect regulation. The "lightning blot" indicates the cleavage of the protein.

1.3 Heat Shock Protein of 70 kDa (Hsp70)

1.3.1 Hsp70 family

Heat shock proteins (HSPs) are a family of SRPs important for protecting cells from stressful conditions. HSPs were originally recognized as proteins induced by high-temperature shock [164], but later more reports has claimed that HSPs were also upregulated during stresses caused by other stimulators such as cold [165], ultraviolet (UV) light [166] and wound [167]. Now most HSPs are considered as molecular chaperones induced by accumulation of unfolded and/or misfolded proteins which occurs in different stress conditions. The major function of HSPs is to facilitate the folding of newly synthesized proteins or refolding of misfolded proteins [168].

HSP family is a large protein family consisting of various proteins expressed by tens of different genes located on almost all chromosomes. To clarify and simplify the nomenclature, HSPs are usually classified into five groups according to their molecular weight: Hsp40s, Hsp70s, Hsp90s, small heat shock proteins and chaperonins[169, 170]. Hsp70s are one of the best characterized sub-families of HSPs. Seventeen genes, most of which are belonging to HSPA gene family, have been reported to express proteins of Hsp70 family so far (**Table 1.1**). Hsp70s are an important component of the cellular chaperone network, and help to protect cells from stress[171, 172]. Like other HSPs, Hsp70s mainly act as molecular chaperones facilitating protein folding, but several members have been reported to exert unique functions. For instance, Hsc70 encoded by HSPA8 is a constitutively expressed and multifunctional HSP which is involved in many non-stress cellular processes such as disassembly of clathrin-coated vesicles [173], protein degradation [174] and signal transduction [175]; GRP78 is a typical indicator of ER stress which facilitates folding and translocation of proteins and initiates unfolded protein response in the ER [133]. Especially, Hsp70-1 and Hsp70-2, encoded by HSPA1A and HSPA1B, respectively, are almost identical in their

amino acid sequences. These two proteins are inducibly expressed in response to different stresses and are both referred to as inducible heat shock protein. However, due to the differences in their gene promoters, only Hsp70-2 is induced in response to hypertonic stress [176].

Table 1.1. Genes and Proteins of Hsp70 Family [169]

Gene Symbol	Protein Name	Features	Reference
HSPA1A	HspA1, Hsp70-1		
HSPA1B	Hsp70-2	Response to hypertonic stress	[177]
HSPA1L	Hsp70-HOM, hum70t		
HSPA2	Hsp70A2		
HSPA4	HS24/P52, HSPH2		
HSPA4L	APG-1, Osp94, HSPH3	Response to hypertonic stress	[176]
HSPA5	GRP78, BiP	Facilitate diverse functions in the ER, an indicator of ER stress	[175, 178, 179]
HSPA6	Hsp70B’		
HSPA7	Hsp70B		
HSPA8	HspA10, Hsc71, Hsc70, Hsp73	Constitutively expressed chaperone protein, contributing to apoptosis, cell growth and differentiation	[175, 180]
HSPA9	HspA9B, Grp75, PBP74, mot-2, mtHsp75	Mitochondrial chaperone protein, controlling cell proliferation	[181-183]
HSPA12A	FLJ13874, KIAA0417		
HSPA12B	HspA12B, C20orf60		
HSPA13	STCH		
HSPA14	Hsp70-4, Hsp70L1		
HSPH1	Hsp105B, KIAA0201, Hsp105A, NY-CO-25		
HYOU1	Orp150, Hsp12A, Grp170	ER chaperone protein in response to hypoxia, inhibiting apoptosis	[184]

1.3.2 Function of Hsp70

Most Hsp70 proteins contains three major functional domains: 1) N-terminal ATPase domain which binds ATP (adenosine triphosphate) and hydrolyzes it to ADP (adenosine diphosphate), leading to conformational changes in the other two domains, 2) substrate binding domain (SBD) containing a groove with an affinity to peptides with neutral or hydrophobic amino acid residues and up to seven residues in length, and 3) C-terminal domain acting as a 'lid' for the substrate binding domain, which is open when an Hsp70 protein is ATP bound, allowing rapid peptide binding and release, and is closed when Hsp70 protein is ADP bound, restricting peptides to tightly bound to the SBD [185].

As protein chaperones, Hsp70 proteins interact with extended peptide segments of proteins as well as partially folded proteins to prevent aggregation, remodel folding pathways, and regulatory activity [186]. The activity of Hsp70 is modulated via the switch between ATP and ADP bound states which is affected by protein abundance in the cells. When the level of newly synthesized or misfolded proteins is low, Hsp70 is in an ATP bound state. As newly synthesized proteins emerge from the ribosomes, the SBD of Hsp70 recognizes sequences of hydrophobic amino acid residues and interacts with them in a weak and reversible pattern at the beginning since Hsp70 is still ATP bound. However, the presence of a peptide in SBD stimulates the ATPase activity of Hsp70, switching Hsp70 from ATP bound state to ADP bound state via ATP hydrolysis and resulting in tight binding to the peptide chain [186]. When high abundance of interacting peptides are present, the ATPase activity of Hsp70 will be enhanced by interacting with certain proteins called cochaperones, such as Hsp40, which further promotes peptide binding to SBD of Hsp70 [187, 188]. By binding tightly to partially synthesized or misfolded

peptides, Hsp70 prevents them from aggregating and being dysfunctional. Once the protein translation is completed or the misfolded protein is unfolded, the ADP will be released from Hsp70 by nucleotide exchange factors such as BAG-1 and HspBP1, and Hsp70 will switch back to ATP bound state to release the protein which will then fold on its own, or to be transferred to other chaperones for further processing [189].

In addition to chaperone activity, Hsp70 also modulates the turnover of mRNA via inhibiting mRNA degradation [5] (**Figure 1.7**). Many rapidly degraded mRNAs, especially those coding SRPs, nuclear transcription factors, and cytokines, harbor adenylate-uridylate-rich elements (AREs) in their 3'UTR. AREs are important determinants and regulatory elements of mRNA stability [190]. An ARE provides a binding site for ARE-binding proteins (AUBPs) which promote mRNA degradation [191]. The turnover of mRNAs can be thus modulated via regulating of AUBPs. ARE/poly(U)-binding/degradation factor 1 (AUF1) is one of the best-characterized AUBPs which further recruits other proteins related to mRNA stability, including eukaryotic translation initiation factor 4 G (eIF4G), poly(A)-binding protein (PABP), Hsp70 and many unknown proteins [192]. PABP is a protective protein shielding the poly-A tail of mRNA from deadenylases. On untranslated ARE-containing mRNAs, AUF1 interacts simultaneously with eIF4G and ARE, while PABP binds both eIF4G and poly(A) tail. After the translation starts, AUF1 and PABP are dissociated from eIF4G and AUF1 drags PABP away from poly(A) tail, resulting in exposure of the poly(A) tail to deadenylases which execute mRNA decay. This mechanism prevents excess gene expression at translational level. During stress, mRNA translation is deferred or blocked to avoid generation of misfolded proteins. However, in order not to synthesize the mRNAs again for future translation, Hsp70 stabilizes the untranslated mRNAs via AUF1. In this case, high level of Hsp70s bind to AUF1 and disrupt the AUF-PABP interaction, retaining PABP on the

poly(A) tail, thus masking it from ribonuclease [193]. Interestingly, the mRNA of inducible Hsp70s also contains ARE sites which elevate the stability of Hsp70 mRNAs in stress conditions [194-196].

Hsp70 also participates in disposal of damaged or defective proteins when the ADP bound state prolongs. Via interacting with CHIP, an E3 ubiquitin ligase, Hsp70 initializes the ubiquitination and proteolysis of the bound protein [197]. Moreover, Hsp70 proteins are widely considered as pro-survival proteins which inhibit apoptosis in multiple ways. Hsp70 directly suppresses the induction of reactive oxygen species (ROS) [198], the recruitment of procaspase-9 to the apoptosome [199, 200] and the cleavage of pro-caspase-8 [201], which are all triggers of apoptosis. In addition, Hsp70 is capable of relieving ER stress via interaction with ER stress sensor protein IRE1α and thereby protecting the cells from apoptosis caused by prolonged ER stress [202].

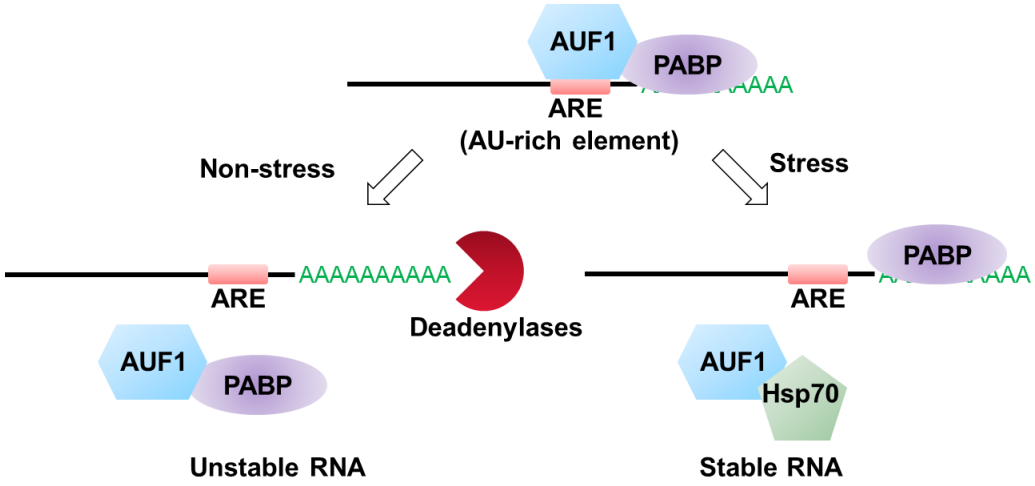

Figure 1.7. Schematic mechanism for stabilization of mRNAs via Hsp70-AUF1 interaction in stress. In non-stress condition, AUF1 hijacks PABP and exposes poly(A) tail to deadenylases for RNA degradation. In stress condition, Hsp70 removes the AUF1 from ARE and retains PABP on the poly(A) tail to prevent it. This figure was developed based on Grataco et al. [5].

1.3.3 Regulation of Hsp70

Similar to CVB3 genomic RNA, Hsp70 mRNA also contains an IRES element, which makes it possible for Hsp70 to be translated during CVB3 infection when the cap-dependent translation is compromised. The expression of Hsp70s is regulated by specific transcriptional factors. The major transcription factors for Hsp70s are the heat-shock factors (HSFs), which bind to the heat shock element (HSE), a cis-regulatory element within the HSP gene promoter [203]. Humans express nine HSFs, among which HSF1 is the most critical transcription factor for inducible Hsp70s, such as Hsp70-1 and Hsp70-2. The activity of HSF1 is mainly regulated via the serine (Ser) and threonine (Thr) phosphorylation by different protein kinases on different amino acid

sites. For instance, phosphorylation by kinases such as GSK-3β (at Ser303) [204], ERK1/2 (extracellular signal regulated kinase 1/2, at Ser307) [205], and JNK1/PKC (at Ser363) [206, 207] suppresses the HSF1 activity under normal conditions; whereas phosphorylation by JNK2 (at Ser444) [208], CaMKII (Ca^{2+}/calmodulin-dependent protein kinase II, at Ser230) [209] and CKII (casein kinase II, Thr142) [210] activates HSF1. These protein kinases are further subjected to sophisticated regulation by upstream signals. For example, GSK-3β is activated via PI3K/Akt cascade as mentioned above [162]; ERK1/2 is activated via the sequential phosphorylation of RAF kinase and MEK1/2 (mitogen-activated protein kinase kinase 1/2) [211]; JNK1/2 is activated by phosphorylation mediated by MEK4/7, PKC and ERK [212-214]; activation of CaMKII is initialized by elevated intracellular calcium/calmodulin (Ca^{2+}/CaM) and then sustained by threonine (Thr) phosphorylation and/or methionine (Met) oxidation [215-217]. Under non-stress conditions, HSF1 exists as an inactive form bound to Hsp40/Hsp70 and Hsp90 [218]; upon stress, HSF1 is released from the chaperone complex and tranlocated into the nucleus where it binds to HSEs.

In addition to HSFs, some Hsp70s in response to hypertonicity, such as Hsp70-2 and osmotic stress protein of 94 kDa (Osp94), employ the master hypertonicity-responsive protein NFAT5 as their transcriptional factor [176, 177], which will be discussed later.

1.3.4 Hsp70 and virus

Viral infections frequently induce HSPs due to the sudden increase of protein synthesis. During the co-evolution with the host, some viruses have developed different strategies to utilize HSPs to benefit their own survival. For example, Hsp70 and Hsp90 were reported to be transported to cell surface and may act as viral receptors/co-receptors responsible for viral attachment and entry [219-222]. After penetrating into the target cells, some DNA viruses such

adenovirus, polyomavirus and papillomavirus, require the assistance of Hsp70 to import their DNAs into nucleus, where replication takes place.[223, 224]. HSPs can not only bind to host gene expression machineries to enhance the viral gene expression [225-227] but also interact with viral polymerase to stimulate viral RNA synthesis [228, 229]. It has been reported that HCV replication was enhanced by inducible Hsp70 interactions with the HCV replicase complex containing nonstructural protein (NS)5A (polymerase), NS5B and NS3. The mechanism is likely via increasing the amount of replicase complex, leading either to the increased stability of viral replicase or to the enhanced efficiency of the IRES-mediated translation of HCV[230]. The roles of Hsp70s in other viruses are summarized in **Table 1.2**.

Table 1.2. Roles of Hsp70 in viral infection

Viral family	Virus, viral proteins	Functional interaction	References
Flaviviridae	HCV, E1, E2	Envelope protein maturation	231
	West Nile virus, Cp	Direct binding to inhibit infection	232
Picornaviridae	CVA9	Viral entry	222
	Poliovirus, CVB1, P1	Virion assembly	233
Paramyxoviridae	Canine distemper virus	Capsid protein maturation	234
Orthomyxoviridae	Influenza A	Present in virion particle; General regulation of translation	235
Retroviridae	HIV	Nuclear import of pre-integration complex	236

1.3.5 Hsp70 and heart diseases

Hsp70 can be induced in both vascular and cardiac compartments. The absolute cardiac level of Hsp70 correlates to the recovery of heart functions after a global ischemic insult [237-239]. Hsp70 can also reduce the infarct size in myocardial infarction [240, 241]. The protective roles of Hsp70 have also been observed in other cardiovascular stress conditions like cardioplegia [242] and endotoxin treatment [243]. Hsp70 is involved in regulating energy metabolism, calcium homeostasis, electronic stability, lipid metabolism and cell apoptosis in the heart [244]. The gradual decline of Hsp70s in heart is also associated with cardiac aging progress [245]. The presence of a high level of Hsp70 co-localized with infiltrating macrophages was observed in the center of atherosclerotic plaques in human blood vessels [246]. In addition, heat pretreatment has been indicated to benefit long-lasting hypothermic storage of cardiac tissue, which might be useful for heart transplantation [247].

Hsp70 is also associated with myocarditis, cardiac hypertrophy and cardiomyopathy. Induction of Hsp70 has been observed in myocarditis associated with foot-and-mouth disease virus (FMDV) infection [248]. Hsp70s have been found to be transiently upregulated in hypertrophic heart [249]. Whole body heat shock treatment can also induce higher levels of Hsp70s in cardiac hypertrophy models compared to normal, control animals [250, 251]. The major regulatory genes controlling the hypertrophy process are histone deacetylases (HDACs) [252, 253], particularly the HDAC2, which is a positive regulator of hypertrophy, accomplished by interacting with an atypical homeodomain protein, Hop [254, 255]. It was reported that multiple hypertrophic stimuli induce HDAC2 activation and up-regulation of hypertrophic makers correlated with Hsp70 [256]. Furthermore, Hsp70 was often detected in sera of patients with DCM as compared to healthy

controls [257]. The increase of both cardiac and serum Hsp70 was also demonstrated in patients with arrhythmogenic right ventricular cardiomyopathy [258].

1.4 Nuclear Factor of Activated T-cells 5 (NFAT5)

1.4.1 NFAT Family and Structure of NFAT5

The protein family of NFAT was named after its initial discovery as an inducible nuclear factor binding to the interleukin-2 promoter in activated T-cells [259]. Regardless of the name, as more proteins of NFAT family were indentified, it has been believed that the expression and function of NFAT protein are not limited to T cells and immune response [260-262]. Now NFAT proteins are characterized as a group of transcriptional factors containing a highly conserved DNA-binding domain homologous with the DNA-binding domain of REL-family transcriptional factors which is referred to as REL-homology domain (RHD) [263, 264]. Five members of NFAT5 family have been reported, among which four proteins, NFAT1-4, are regulated by calcium signaling [265, 266]. Unlike other members in NFAT family, NFAT5 activity is regulated in a calcineurin-independent manner due to lacking of the calcineurin-binding domain [4], and NFAT5 is the only NFAT protein activated in response to hypertonic stress [267].

Structurally, NFAT5 is a bipartite protein, with functional domains in the N terminus and regulatory domain toward the C terminus (**Figure 1.8**). As a member of NFAT family, NFAT5 employs an RHD as its DNA-binding domain. In the region upstream of RHD, NFAT5 harbors all the functional domains related to nucleus-cytoplasm translocation, including a canonical nuclear export signal (NES, amino acids 1–19), a consensus bipartite nuclear localization signal (NLS, amino acids 199–216) and an auxiliary export domain (AED, amino acids 132–156) [268, 269], making the N-terminal half (amino acids 1–543) of NFAT5 capable of nuclear localization

and DNA binding. As for the C-terminal half, there exists two long stretches (amino acids 1039–1249 and amino acids 1363–1476) of glutamine residues, acting as two transactivation domain (TADs) stimulated by hypertonicity and involved in activation of transcription [4, 270]. Due to such structure, the N-terminal fragment (amino acids 1–472) of NFAT5 can function as a dominant negative mutant [270].

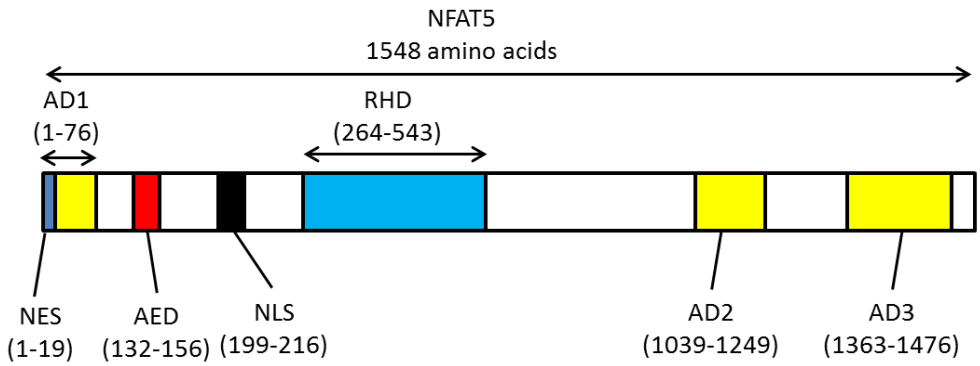

Figure 1.8. Schematic structure of NFAT5 protein adapted from Cheung et al. [4] REL-homology domain (RHD) is the DNA-binding domain of NFAT5. The region upstream of RHD contains a canonical nuclear export signal (NES, amino acids 1–19), a consensus bipartite nuclear localization signal (NLS, amino acids 199–216) and an auxiliary export domain (AED, amino acids 132–156). The region downstream of RHD harbors two transactivation domain (AD2 and AD3).

1.4.2 Hypertonic Stress and NFAT5-mediated Hypertonic Response

Osmotic pressure is the pressure required for a certain solution to prevent the inward flow of water across a semipermeable membrane [271]. The measure of osmotic pressure is often referred to as osmolality. Osmolality can serve as an indicator of solute concentration in a certain solution. Since cells in the body are exposed to soluble substance within extracellular fluid, stable osmolality of body fluid is critical for cell metabolism and homeostasis of the body. Hypertonicity refers to a physiological or pathological condition with an increase of osmolality in body fluid. Sudden increase in osmolality, such as exposure to high concentration of NaCl or urea, will induce hypertonic stress in cells featured by cell shrinkage, impaired function of intracellular proteins and disruption of the structural integrity of cell organelles[272]. Hypertonic stress further leads to increased reactive oxygen species formation, cytoskeletal rearrangements, increased mitochondrial depolarization, decreased DNA replication and DNA repair [273, 274]. Without proper protective response, hypertonic stress will eventually result in mitochondrial or death-receptor-mediated apoptosis of cells [275].

As mentioned above, NFAT5 is the master transcription factor regulating the expression of genes in response to hypertonic stress. All currently known signaling pathways in hypertonic response converge to NFAT5 to activate the expression of downstream genes (**Figure 1.9**). The detailed mechanism of NFAT5 activation in hypertonic stress is still controversial. The widely accepted sensor of hypertonicity is Brx, which is a guanine nucleotide exchange factor (GEF) localized on the plasma membrane and is stimulated by sensing hypertonicity-caused changes of cytoskeleton structure or interacting with certain osmosensor molecules near the plasma membrane [276]. Upon stimulation, as a GEF, Brx switches Rho-like GTPase from their inactive GDP state to active GTP state. Meanwhile, activated Brx recruits and interacts with JIP4, a p38-

MAPK-specific scaffold protein, which further binds to MKK3 and MKK6 kinases [277]. This complex then phosphorylates and activates p38 MAPK, subsequently inducing NFAT5 expression [276]. NFAT5 transcriptionally regulates the expression of various target genes involved in relieving hypertonic stress by directly binding to tonicity-responsive enhancer element (TonE) in the promoter, and thus, NFAT5 is also called tonicity enhancer binding protein (TonEBP) [278]. NFAT5 targets directly contributing to balancing cellular osmotic pressure are the genes responsible for the biosynthesis of organic osmolytes, including aldose reductase (AR)[279], taurine transporter (TauT)[280], betaine/GABA transporter (BGT-1)[270], and sodium/myo-inositol transporter (SMIT)[281, 282]. In addition to the organic-osmolyte-related genes, NFAT5 induces the expression of molecular chaperones, such as Hsp70-2[177] and Osp94[176], in order to prevent the accumulation of misfolding proteins in the stress condition. NFAT5 also modulates some immune responses in hypertonic stress. For instance, NFAT5 controls the osmotic stress-induced expression of several cytokines in lymphocytes, including tumor-necrosis factor (TNF) and lymphotoxin-β (TL-β)[283], which is evidenced by the fact that NFAT5-deficient mice have impaired T-cell function under hypertonic conditions and decreased cellularity of the thymus and spleen[284].

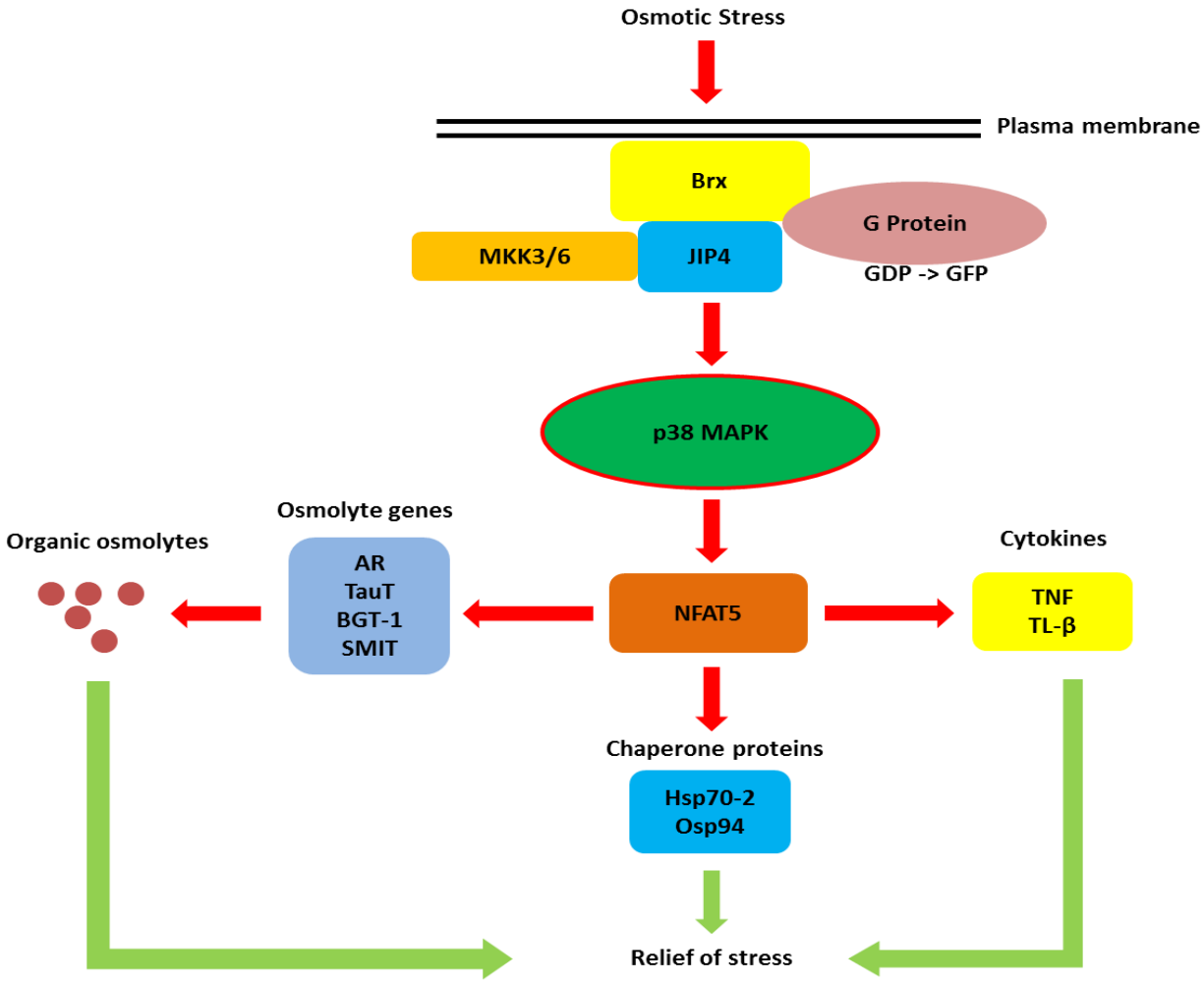

Figure 1.9. Activation of NFAT5 and its downstream genes in response to osmotic stress. This figure is modified based on the figure on Wikipedia (https://en.wikipedia.org/wiki/NFAT5).

1.4.3 NFAT5 and Viral Infection

The research on the anti-viral effect of hypertonicity can be dated back to the year 1975. In the study of Dr. Nuss and several later reports from other groups demonstrated that hypertonic medium is capable of inhibiting viral protein synthesis of different virus, including vesicular stomatitis virus (VSV)[285, 286], poliovirus[287, 288] and adenovirus[289]. However, those early studies barely elucidated the mechanism underlying the anti-viral effect of hypertonicity and none of them mentioned the role of NFAT5, the critical transcriptional factor involved in hypertonic response. After a more than 20-year gap, a couple of recent studies have started to link NFAT5 to viral infection. For instance, Goldfeld et al. reported that NFAT5 is highly expressed in terminally differentiated macrophages, the major target cells of human immunodeficiency virus 1 (HIV-1), and that NFAT5 is capable of binding to a conserved site harbored in the long terminal repeat (LTR) of HIV-1 genome specifically and functionally; lack of NFAT5 in the cells inhibits production of HIV-1 in human monocyte-derived macrophages[290]. In a more recent publication, the same research group further demonstrated a mutual regulation of NFAT5 and *Mycobacterium tuberculosis* (MTb)-stimulated HIV-1 replication in co-infected macrophages[291]. Briefly, NFAT5 expression is strongly induced by MTb infection via Toll-like-receptor-related innate immune response, and NFAT5 enhances the replication of HIV-1 via the direct interaction with the viral promoter. This model well explains the reason why HIV-1 replication is enhanced upon MTb infection. In addition to NFAT5 itself, the downstream signals of NFAT5 also play important roles in the infection of certain virus. For instance, NFAT5 expression is increased by NS5A, a nonstructural protein of hepatitis C virus (HCV), and it subsequently upregulates the expression of Hsp70. The binding between Hsp70 and NS5A is critical for viral RNA replication and virus production in HCV-infected cells [292].

1.4.4 NFAT5 and Heart Diseases

Heart is an organ barely exposed to hypertonic environment and thus, hypertonic response seems to barely occur in the heart. However, hypertonic saline solution (HSS, >5% NaCl solution), a common inducing agent of hypertonicity, has been used as a supplement for the routine drug furosemide to patients with refractory congestive heart failure. In this clinical trial, patients were treated with either high-dose furosemide plus small-volume HSS or high-dose furosemide only. The HSS-treated group showed a significant increase in daily diuresis and natriuresis, faster reduction of brain natriuretic peptide, and a better hydration state compared to non-HSS-treated group [293]. In addition, the readmission rate for heart failure and the mortality of HSS-treated patients are both half of that of patients treated with furosemide only[294]. Similar results favoring the therapeutic effects of HSS have also been reported in several other clinical trials [295, 296]. In another acute treatment case, a 90-year-old man with uncompensated heart failure was infused with 100 mL of 10% NaCl solution over a period of 10 minutes in the intensive care unit as a final, non-invasive approach to improve myocardial contractility. Less than three minutes after the infusion, the patient's breathing pattern, blood pressure, heart rate and capillary refill time were all improved [297]. Nevertheless, the mechanism underlying the effects of HSS treatment on heart has not been scientifically studied yet.

Induction of NFAT5 may be considered as an explanation, or at least partially, of the effects of HSS treatment on heart diseases. Though NAFT5 is usually recognized as a hypertonicity-responsive protein, it is ubiquitously expressed in almost all tissues including those not exposed to hypertonic environment, such as brain, heart, and skeletal muscle [298, 299]. In fact, some evidence supports that NFAT5 plays an important role in normal heart function and cardiotoxicity. Ito et al. reported that degradation of NFAT5 is induced in cardiomyocytes

treated with doxorubicin, a commonly used anti-tumor agent, and the decrease of NFAT5 exacerbates myocyte death upon doxorubicin treatment [300]. Another study using a NFAT5 knocked-out mouse model demonstrates that lacking of NFAT5 results in reduction of heart beating rate and abnormal Ca^{2+} signaling profile, which contributes to abnormal heart function [301]. A potential protein bridging NFAT5 and heart diseases is NFκB. NFAT5 enhances NFκB activity via forming NFκB-NFAT5 complexes which promotes NFκB's binding to κB elements of NFκB–responsive genes [302]. NFκB is generally considered as a transcriptional factor closely related to inflammation [303], and interestingly, NFκB has been reported to promote cardiomyocyte viability in CVB3 infection [304]. In addition to NFκB, NFAT5 is also critical for the expression of inducible nitric oxide synthase (iNOS) [305]. Activation of iNOS enhances the production of nitric oxide (NO), a major molecule controlling cardiomyocyte contractility and heart rate, limiting cardiac remodeling after an infarction and contributing to the protective effect of ischemic pre- and postconditioning [306]. Especially, in a murine myocarditis model, NO exerts an inhibitory effect on CVB3 replication and mouse mortality after viral infection [307].

1.5 Rationale, Hypothesis and Objectives

1.5.1 Project Background and Rationales

The high frequency and lethality of viral myocarditis is currently a major threat to public health, especially in children and young adults. Effective and accessible therapies are in urgent demand for the treatment of viral myocarditis. CVB3 is one of the predominant pathogens of viral myocarditis and is a widely used model for the research of this disease. As an RNA virus, the high mutation rate of CVB3 impedes the development of drugs by targeting the viral genome or viral protein directly. Certain host cellular components are critical for CVB3 infection, which

are relatively conserved for different CVB3 strains and may even be shared by other picornaviruses. Thus, the host-oriented strategy is probably a more efficient approach in the therapeutic development against CVB3 infection and viral myocarditis.

CVB3 infection frequently induces various stresses in cells. To avoid the adverse effects of these stresses, the host cells activate different responsive signaling pathways employing specific SRPs. However, during the long history of coevolution of the virus and the host, CVB3 is capable of utilizing or even depends on certain SRPs and the corresponding signaling pathways for its own replication. Comprehensive studies of the SRP-CVB3 relationship contributes to the understanding of CVB3 infection in host cells, which will provide potential drug targets for CVB3-induced myocarditis.

Our preliminary results showed significant changes of two SRPs, Hsp70 and NFAT5, during CVB3 infection *in vitro* and *in vivo*. These two proteins have been reported to play important roles in infection of other viruses as well as in heart disease. Therefore, I focused my study on Hsp70 and NFAT5 to uncover the modulation and roles of them in CVB3 infection.

1.5.2 Overall Hypothesis

CVB3 infection differentially regulates the levels of Hsp70 and NFAT5 in cells, which benefits viral replication and contributes to the pathogenesis of viral myocarditis.

1.5.3 Specific Aims and Experimental Design

Aim 1: To determine the changes of Hsp70 and NFAT5 expression during CVB3 infection and the underlying mechanisms

Live CVB3 viral particles were used to infect cell culture and A/J mice. Cellular proteins and mRNAs were extracted from cell culture or mouse heart. The expression of Hsp70 and NFAT5 was detected by quantitative real-time PCR (qPCR) for mRNA levels and western blot analysis for protein levels, in order to determine which step of expression was affected by CVB3. Then the upstream regulatory signals or downstream protein modulation of these two SRPs in CVB3 infection was analyzed to determine the mechanisms underlying the expression change.

Aim 2: To investigate the roles of Hsp70 and NFAT5 in CVB3 infection and the underlying mechanisms

The expression of Hsp70 and NFAT5 was artificially altered by plasmid-mediated overexpression or siRNA-mediated interference in CVB3-infected cells. The replication of CVB3 was evaluated at three levels: 1) western blot detection of viral protein, 2) qPCR quantification of viral RNA and 3) viral plaque assay of viral progeny release. The intermediate signals bridging the SRPs and CVB3 were then identified by detecting the roles of related cellular proteins.

Aim 3: To test the therapeutic potential of hyperosmotic agents in the treatment of CVB3 infection *in vitro* and in mice.

NFAT5 expression can be induced by hypertonic conditions. Thus, hypertonic reagents were used to treat CVB3-infected cell culture or A/J mice, and then the treatment effects on viral replication were evaluated by detecting viral protein, cell death and pathological changes of the heart tissue.

Chapter 2 CVB3 and Inducible Heat Shock 70 kDa Protein

2.1 Background and Rationale

2.1.1 CVB3 and Hsp70

Hsp70 is a key member of cellular chaperone system involved in response to various cellular stresses [244]. The Hsp70 protein family contains two major members, Hsp70-1 and Hsp70-2, which are encoded by gene HSPA1A and HSPA1B respectively. The proteins of Hsp70-1 and Hsp70-2 differ on two amino acids and both of them are induced in heat shock, but only Hsp70-2 is stimulated in response to hypertonicity since only HSPA1B contains a tonicity-responsive enhancer (TonE) in its promoter region[177].

Hsp70 has been reported to be induced in viral infection [308] and acts as a regulatory factor, either negative or positive, in viral life cycle [231, 232, 236, 309]. Similar to CVB3 genomic RNA, Hsp70 mRNA also contains an IRES element, which makes it possible for Hsp70 to be translated during CVB3 infection when the cap-dependent translation is compromised. Heat shock factor 1 (HSF1) is the major transcriptional factor of Hsp70-1 reported in various stress conditions [310, 311]. As described in Chapter 1, the transcriptional activity of HSF1 is modulated at multiple phosphorylation sites. Two serine (Ser) sites, Ser230 and Ser307, are phosphorylated and involved in the modulation of the activity of HSF1 primarily[209]. The phosphorylation at Ser230 is catalyzed by active calcium/calmodulin-dependent protein kinase II (CaMKII) [209], while activation of CaMKII is initialized by elevated intracellular calcium/calmodulin (Ca^{2+}/CaM) and then sustained by threonine (Thr) phosphorylation [215-217]. During CVB3 infection, increase of the efflux of Ca^{2+} from ER and Golgi complex [312] and generation of massive reactive oxygen species (ROS) [313] are likely to result in persistent CaMKII activation and induction of Hsp70. Unlike Ser230, phosphorylation at Ser307 represses transcriptional activity of HSF1 [314]. Ser307

phosphorylation is catalyzed by extracellular signal-regulated kinase (ERK) [315] and ERK has been reported to be activated in a biphasic pattern at early and late stages in CVB3 infection [162, 316]. As for Hsp70-2, its transcription is stimulated by NFAT5 via the interaction between NFAT5 and TonE [177], and the upstream signal of NFAT5 activation is p38 MAPK which is activated in CVB3 infection [150, 276],

2.1.2 CVB3 and Hsp70-AUF1-mediated RNA decay

Hsp70 has been reported to stabilize messenger RNAs (mRNAs) containing adenosine-uridine-rich elements (AREs) by preventing mRNA degradation. One explanation for Hsp70-mediated stabilization of ARE-containing mRNAs focuses on the interactions between Hsp70 and ARE/poly(U)-binding/degradation factor 1 (AUF1). It was reported that degradation of ARE-containing mRNAs is induced by the binding of AUF1 on the ARE site [317]. AUF1 has four isoforms (p37, p40, p42 and p45) due to alternative splicing, among which $p37^{AUF1}$ and $p40^{AUF1}$ are most strongly associated with ARE-mRNA decay [318]. Hsp70 can sequester AUF1 in nucleus to avoid the AUF1 and mRNA interaction in the cytoplasm [319]. Another explanation of Hsp70-mediated stabilization of mRNA is that Hsp70-1, but not Hsp70-2, binds to ARE directly and stabilizes the mRNA, which is supported by the highly selective binding of Hsp70-1 and ARE [320]. The genomic RNA of CVB3 contains an ARE site within the 3'UTR and it has been reported that AUF1 can bind to CVB3 genomic RNA [321]. Therefore, it is possible that the stability of CVB3 genomic RNA is also regulated by Hsp70.

2.2 Hypothesis and Specific Aims

The objective of this chapter is to investigate the interplay between Hsp70 and CVB3 during the viral infection. Based on the knowledge to date, I **HYPOTHESIZE** that CVB3 infection induces Hsp70 and Hsp70, in turn, promotes CVB3 replication via stabilizing the viral genome.

The **SPECIFIC AIMS** for this chapter are as follows:

Aim 1: To detect the upregulation of Hsp70 in CVB3 infection

Aim 2: To investigate the phosphorylation and activation of HSF-1 in CVB3 infection

Aim 3: To clarify the feedback effect of Hsp70 on the stability of CVB3 genomic RNA

2.3 Methods and Materials

2.3.1 Animals, cell culture and viral infection

This study was carried out in strict accordance with the recommendations in the Guide to the Care and Use of Experimental Animals – Canadian Council on Animal Care. All protocols were approved by the Animal Care Committee, University of British Columbia (protocol number: A11-0052). HeLa cells (ATCC) were cultured in Dulbecco's modified Eagle's medium (DMEM) supplemented with 10% fetal bovine serum (FBS) (Sigma). The HL-1 cell line, a mouse cardiac muscle cell line established from a cardiomyocyte tumor lineage, was a gift from Dr. William C. Claycomb (Louisiana State University Health Science Center). HL-1 cells were maintained in Claycomb medium (Sigma) supplemented with 10% fetal bovine serum (FBS) (JRH Biosciences), 0.1 mM norepinephrine (Sigma) and 2 mM L-glutamine (Invitrogen). SV40 immortalized human cardiomyocytes were purchased from Applied Biological Materials (Richmond, BC, Canada) and cultured in Prigrow I medium with 10% FBS. Primary rat neonatal cardiomyocytes were isolated from rat pups using commercial Neonatal Cardiomyocyte Isolation

Kit (Cellutron) according to the protocol provided. Briefly, hearts were dissected from 1-day-old Sprague–Dawley rats and transferred into a sterile beaker. Each heart was digested and stirred in the beaker at 37 °C for 12 min. The supernatant was then transferred to a new sterile tube and spun at 1200 × g for 1 min. The cell pellets were then resuspended in D3 buffer and the cells were seeded onto an uncoated plate, which was incubated at 37 °C for 1 h in a CO_2 incubator to allow the attaching of cardiac fibroblasts. The unattached cardiomyocytes were transferred onto precoated plates with NS medium supplemented with 10% FBS. After overnight culturing, the NS medium was replaced with a serum-free NW (without serum) medium. The cardiomyocyte cultures were ready for experiments 48 h after the initial plating. All these cells were sustained in a humidified incubator supplemented with 5% CO_2 at 37 °C. For heat shock, HeLa cells were incubated at 42 °C for different durations.

CVB3 (CG) strain was obtained from Dr. Charles Gauntt (University of Texas Health Science Center) and propagated in HeLa cells. Viral stock was prepared from the cells by three freeze-thaw cycles followed by centrifugation to remove cell debris and stored at -80 ºC. The titer of virus stock was determined by plaque assay as described below. Cell cultures were infected with CVB3 for 1 h (HeLa) or 1.5 h (HL-1, SV40 and primary rat neonatal cardiomyocytes) in serum-free medium, washed with phosphate-buffered saline (PBS), and then replenished with fresh medium containing FBS. The total proteins of CVB3-infected cells were extracted by lysing the cells with RIPA buffer (Santa Cruz) at different time points post infection (pi). Male A/J mice (4-week old) were purchased from Jackson Laboratory. Mice were infected by intraperitoneal (IP) inoculation with 5×10^3 plaque-forming unit (pfu) of CVB3 or sham-infected with PBS. Heart tissues were collected at day 7 pi for immunostaining.

2.3.2 Viral plaque assay

Samples were freeze-thawed and then centrifuged (4,000 × g) to isolate viruses. HeLa cells were seeded onto 6-well plates (8×10^5 cells/well) and incubated at 37 °C for 20 h to a confluence of approximately 90% and then washed with PBS and overlaid with 800 µl of virus-containing samples serially diluted in cell culture medium. After a viral adsorption period of 60 min at 37 °C, the supernatant was removed and the cells overlaid with 2 ml of sterilized soft Bacto-agar-minimal essential medium, cultured at 37 °C for 72 h, fixed with Carnoy's fixative for 30 min, and stained with 1% crystal violet. The plaques were counted and viral pfu per ml calculated.

2.3.3 UV irradiation of CVB3

One mL of CVB3 stock in a 2-mL tube was kept on ice. UV irradiation was conducted in a UV Stratalinker 1800 (Stratagene) for 30 min with the virus tube kept 5-cm from the UV bulb. The viruses were tested for successful irradiation by infection of HeLa cells and then western blot detection of the absence of CVB3 VP1 protein.

2.3.4 RNA extraction and quantitative real-time PCR

Total cellular RNAs were extracted using RNeasy mini kit (Qiagen) according to the manufacturer's instructions. cDNAs were then synthesized by reverse transcription using SuperScript III First-Strand Synthesis System (Invitrogen) and detected by qPCR using QuantiTect SYBR Green PCR kit (Qiagen). The mRNA level of glyceraldehyde 3-phosphate dehydrogenase (GAPDH) was detected as the endogenous control. All qPCR experiments were

performed in triplicates with the no-template as a negative control. The primers for the q-RT-PCR are showed in **Table 2.1**.

2.3.5 Western blot analysis

Cells were washed with cold PBS before the addition of an appropriate volume of RIPA lysis buffer (Santa Cruz). After incubation for 20 min on ice, the cell lysates were centrifuged at 13,000 × g for 15 min at 4°C, and protein-containing supernatant was collected. The isolated proteins were separated by 10% SDS-PAGE and transferred onto nitrocellulose membranes. Membranes were blocked with 5% skim milk in TBST and incubated with one of the following primary antibodies overnight: monoclonal mouse anti-VP1 (Novocastra); monoclonal mouse anti-Hsp70 (Enzo Life Sciences); monoclonal mouse anti-β-Actin, monoclonal mouse anti-Hsp70/Hsc70, monoclonal mouse anti-HSF1, polyclonal rabbit anti-Histone H1, polyclonal rabbit anti-phosphorylated-HSF1 (Ser230), polyclonal rabbit anti-phosphorylated-HSF1 (Ser307), polyclonal rabbit anti-ERK1/2 and polyclonal rabbit anti-NFAT5 (Santa Cruz); monoclonal rabbit anti-phosphorylated-ERK1/2 (Thr202/Tyr204), monoclonal rabbit anti-CaMKII (pan) and polyclonal rabbit anti-pCaMKII-Thr286 (Cell Signaling). After several washes with TBST, each blot was further incubated with an appropriate secondary antibody (goat anti-mouse or donkey anti-rabbit) conjugated to horseradish peroxidase (Amersham). Detection was carried out by enhanced chemiluminescence (Amersham) as per the manufacturer's instructions. β-actin was detected as a loading control. Signal intensities were quantified by using the ImageJ (NIH) program and normalized to the control samples (set as 1.00). All the Western blots were conducted in three biological repeats and subjected to statistical analysis.

2.3.6 Immunohistochemistry (IHC)

The collected mouse hearts were fixed in 10% buffered formalin and embedded in paraffin. The IHC analysis was performed using the MACH 4™ Universal AP Polymer Kit (Biocare Medical) as per the manufacturer's instructions. Brief, a set of 4-μm thick serial sections of the ventricular wall from each sample were dewaxed in two changes of CitriSolution (Biocare Medical) and hydrated by sequential incubation with 100%, 90%, 70% isopropanol and distilled water. The sections were then immersed in Tris-EDTA (pH 6.0) and autoclaved at 120 °C for 20 min to retrieve the antigen. Non-specific antibody binding was blocked with 1% bovine serum albumin (BSA) (Sigma) in Tris-buffered saline (TBS, pH 7.6) for 15 min at room temperature. After blocking, the sections were incubated overnight at 4 °C with the Hsp70 antibody (Cell Signaling, 1:500 dilution) mentioned above. After the first incubation, the sections were washed with TBS, incubated with MACH 4™ Probe for 10 min and then with MACH 4™ MR AP-Polymer for another 10 min at room temperature. Finally, the sections were again rinsed in TBS. The slides were developed with Vulcan Fast Red Chromogen 2 (Biocare Medical). After development, the slides were rinsed, counterstained with Mayer Haematoxylin for 5 s and dipped in saturated lithium carbonate for 5 s. The images were captured using a Nikon Eclipse E600 microscope.

2.3.7 Transfection of plasmids and siRNAs

All the siRNAs were purchased from Santa Cruz Biotechnology and transfected into cells using Oligofectamine^{TM} (Life Technologies) according to the manufacturer's instructions. Briefly, 2×10^5 HeLa cells were grown at 37 °C overnight to 30-40% confluence in 6-well plates, washed with PBS and overlaid for 6 h with transfection complex containing siRNAs and

Oligofectamine. The transfection medium was then replaced with DMEM containing 10% FBS and the incubation was continued for 48 h. The plasmids pEGFP-Hsp70-1 and pEGFP-Hsp70-1 (K71E) were a gift from Dr. Lois Greene (Addgene plasmid # 15216) [322]. The plasimds pFLAG-AUF1s was a gift from Dr. Robert J. Schneider [323]. These plasmids were transfected using the same procedures as those described for siRNAs except Lipofectamine™ 2000 (Life Technologies) was used as transfection reagent and the initial cell confluence was 80-90%. The following analyses were performed at 24 h or 36 h post transfection (pt).

2.3.8 Immunofluorescence and confocal microscopy

Cells cultured on glass cover slips (Thermo Fisher) were washed with PBS and fixed and permeabilized with methanol/acetone (1:1) for 20 min at −20°C. Cells were then washed with TBS twice and blocked with 2.5% BSA in TBS for 1 h at room temperature followed by incubation with monoclonal mouse anti-HSF1 antibody (Santa Cruz) diluted in blocking buffer overnight at 4°C. Cells were then washed with TBS five times at room temperature. Slides were stained with goat anti-rabbit IgG (H + L) labeled with ALEXA Fluor 488 and then incubated for 1 h at room temperature. After final wash with TBS, the slides were stained with DAPI (DAKO) and mounted onto microscope glass slides (Thermo Fisher) with nail oil. Images were captured using a Leica AOBS SP2 confocal microscope (Leica, Allendale, NJ) and analyzed by using the Volocity software as described previously [324].

2.3.9 Reporter construction, dual luciferase assay and mRNA turnover assay

The corresponding DNA fragments of wild-type (WT) or mutant CVB3 3'UTR were amplified by PCR using specific primers (**Table 2.1**) targeting the cDNA template of the CVB3-

genome. The synthesized DNA fragments were inserted into the EcoRI restriction site of the Dual-Luciferase Expression Vector C49, a kind gift from Dr. Joanna Floros's laboratory. C49 plasmid contains two tandem open reading frames encoding firefly luciferase and Renilla luciferase, respectively, with an EcoR I restriction site in between. We constructed our reporter plasmids by inserting the WT or mutant CVB3 3'UTR to the downstream region of Renilla luciferase coding sequence and the SV40 promoter to the upstream region of Renilla luciferase coding sequence, generating C49-WT-CVB3-3'UTR and C49-WT-CVB3-3'UTR, respectively. The reporter plasmids were co-transfected with Hsp70-1 siRNAss into HeLa cells. At 48 h pt, the cell lysates were used for luciferase assay to determine the relative luciferase activity (Renilla/Firefly) by using the Dual-Luciferase® Reporter Assay System (Promega) as per the manufacturer's instructions. Meanwhile, another batch of cells were subjected to the same transfection and then treated by actinomycin D at a dose of 2.5 ug/mL (Santa Cruz) for different durations or by 0.1% DMSO as a control, in order to do mRNA turnover assay. Then the total cellular RNAs were extracted, reversely transcribed and subjected to qPCR to detect the mRNA levels of Renilla luciferase as described above. Each treatment was verified by three biological repeats.

2.3.10 Statistical analysis

The graphic figures were drawn as means ± standard deviations (error bars) of three independent experiments. The unpaired two-tail student's *t* test was employed to analyze the data. A *p* value less than 0.05 was considered statistically significant.

Table 2.1. Primers used in Chapter 2

Experiment	Primer	Sequence
Q-RT-PCR	Human Hsp70 forward	ACTGCCCTGATCAAGCGC
	Human Hsp70 reverse	CGGGTTTGTCGGAGTAG
	Human Hsp70-1 forward	TGCATTTCCTAGTATTTCTGTTTG
	Human Hsp70-1 reverse	AGAAATAGTCGTAAGATGGCAG
	Human Hsp70-2 forward	TGTTTGTCTTTGAGGTGGAC
	Human Hsp70-2 reverse	AAGAATTCTAATGAACATATCGG TTG
	Mouse Hsp70 forward	GCCTGATCGGCCGCAAGTT
	Mouse Hsp70 reverse	GGAAGGGCCAGTGCTTCAT
	Renilla luciferase forward	GCAGAAGTTGGTCGTGAGG
	Renilla luciferase reverse	TCATCCGTTTCCTTTGTTCTG
	Human GAPDH forward	AATCCCATCACCATCTTCCA
	Human GAPDH reverse	TGGACTCCACGACGTACTCA
	Mouse GAPDH forward	GGCAAATTCAACGGCACAGT
	Mouse GAPDH reverse	AGATGGTGATGGGCTTCCC
	CVB3 2A forward	GCTTTGCAGACATCCGTGATC
	CVB3 2A reverse	CAAGCTGTGTTCCACATAGTCCTTCA
Molecular cloning	CVB3 3'UTR forward/EcoRI	GCCTTAAGAAGTGGTTGGACTCC TTTTAG
	CVB3 3'UTR reverse/EcoRI	GCCTTAAGTTTTTTTTTCCGCAC CGAATGCGGAG
	Mutant CVB3 3'UTR forward/EcoRI	GCCTTAAGAAGTGGTTGGACTCC TTTTAGATTAGAGACAATTTGAA ATACGGGAGATTGGCTTAACCCT AC

2.4 Results

2.4.1 Protein level of Hsp70 is increased during CVB3 infection *in vitro* and *in vivo*

To examine the association between viral infection phases and Hsp70 expression, we detected mRNA and protein levels of Hsp70 in HeLa cells at different time points pi of CVB3 at a multiplicity of infection (MOI) of 10. Hsp70 protein was evaluated by western blot analysis

using an Hsp70/Hsc70-specific antibody (**Figure 2.1A**, the upper panel). The quantification of Hsp70 was conducted by densitometric analysis and normalized to β-actin. We observed a 100% increase of Hsp70 protein at 6 h pi. However, Hsc70, a constitutively expressed cognate of Hsp70, showed less than 50% changes during CVB3 infection (**Figure 2.1A**, the lower panel). To further verify the change of Hsp70 expression in cardiomyocytes, we detected the Hsp70 protein levels in HL-1 mouse cardiomyocytes, SV40 immortalized human cardiomyocytes and primary neonatal rat cardiomyocytes after infection with CVB3 at 20, 50 and 50 MOI, respectively. Similarly, we found an approximately 100% increase of Hsp70 in HL-1 cells at 8 h pi and neonatal rat cardiomyocytes at 48 h pi (**Figure 2.1B and 2.1C**), and a more than 3-time increase in human cardiomyocytes (**Figure 2.1D**). The time points of significant up-regulation of Hsp70 varied due to different sensitivities of cell types to viral infection, which can be indicated by the expression levels of viral capsid protein VP1 (**Figure 2.1A, B, C and D**). To test whether CVB3 infection can induce up-regulation of Hsp70 *in vivo*, we performed CVB3 infection in A/J mice (a well-established viral myocarditis model) and IHC analysis using the ventricular wall tissue to detect Hsp70 protein expression (**Figure 2.1E**). In the IHC images, the blue dots indicate cellular nuclei and the red signal represents Hsp70 protein. At 7 d pi, there appeared immune infiltration featured by accumulation of immunocyte nuclei in the heart issue (**Figure 2.1E**, blue arrow), indicating that the heart was infected successfully. At the same point, we observed more red signals in cardiomyocytes compared with sham-infected tissue (**Figure 2.1E**, red arrow), indicating a higher expression level of Hsp70 in CVB3-infected heart.

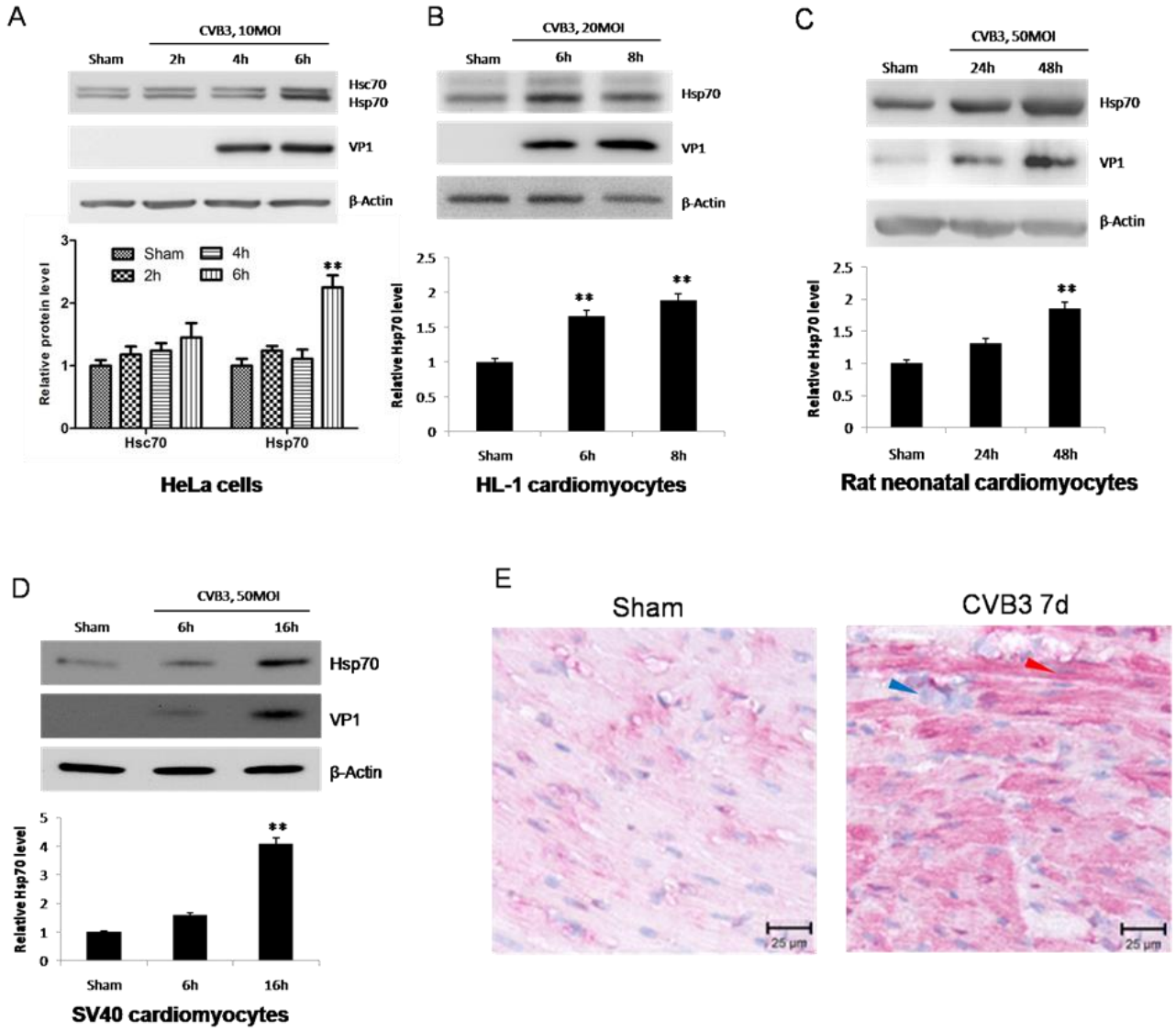

Figure 2.1. CVB3 infection induces upregulation of Hsp70 both *in vitro* and in vivo. HeLa cells (A), HL-1 cardiomyocytes (B), neonatal rat cardiomyocytes (C) and SV40 human cardiomyocytes (D) were infected by CVB3 at 10 MOI, 20 MOI, 50 MOI and 50MOI, respectively. Cell lysates were collected for western blot to detect the protein levels of Hsp70. Hsc70, a constitutively expressed cognate of Hsp70, was detected by a monoclonal mouse anti-Hsp70/Hsc70 antibody simultaneously (A). β-actin was detected as a loading control and cells treated with PBS (Sham) were used as a negative control. Band intensities were quantified using the ImageJ program, normalized against β-actin and shown as means ± SD (n=3) (see lower panels of A, B, C and D; **, $p<0.01$). (E) 4-week old A/J mice were infected with 105 pfu of CVB3 or sham infected with saline. At 4 days pi, mice were sacrificed and the ventricular wall tissue was fixed and subjected to immunohistochemical staining using an anti-Hsp70 antibody. The blue arrow indicates immune cell nuclei in the myocardium. The red arrow indicates a typical cardiomyocyte with Hsp70 protein upregulation (red).

2.4.2 CVB3 upregulates the expression of Hsp70-1 but not Hsp70-2

Our results showed that the protein level of Hsp70 was increased during CVB3 infection. However, Hsp70 family contains two major members, Hsp70-1 and Hsp70-2. We attempted to further confirm which isoform contributes to the increase. Hsp70-1 and Hsp70-2 differ from each other only on two amino acids; hence it is hard to distinguish them with antibodies. To detect these two isoforms specifically, we designed two sets of qPCR primers targeting them respectively based on the sequence difference in their 3'UTRs. Then we detected the mRNA levels of Hsp70-1 and Hsp70-2 in HeLa cells infected by CVB3. The qPCR results showed an approximately 100% increase of Hsp70-1 mRNA while there is no significant change of Hsp70-2 mRNA (**Figure 2.2A**), indicating a transcriptional enhancement of Hsp70-1 but not Hsp70-2 during CVB3 infection. To confirm that the primers we used were specific for the Hsp70 mRNAs, we extracted the RNAs from cells heat-shocked at 42 °C for 0.5 h and 1 h and then used the same primers to detect the mRNA of Hsp70-1 and Hsp70-2. The qPCR results showed that Hsp70-1 had a 8-fold induction after 1 h of heat shock while Hsp70-2 was upregulated 3 fold (**Figure 2.2B**), indicating that the primers we used are specific for heat-shock-induced proteins.

Since the transcription of Hsp70-1 and Hsp70-2 are stimulated by HSF1 and NFAT5, respectively [177, 325], we attempted to evaluate the transcriptional alteration of Hsp70-1 and Hsp70-2 by detecting the protein levels of HSF1 and NFAT5 in sham- and CVB3-infected HeLa cells. Unexpectedly, HSF1 showed modest increase at 4 h pi and slightly decreased thereafter. As for NFAT5, it underwent a robust decrease at those time points compared to sham-infected cells (**Figure 2.2C**), corresponding to no induction of Hsp70-2 transcription. Besides, the HSF1 bands showed a slow mobility on the gel, probably due to the post translational modification of

the protein, which may still affect the activity of HSF1 regardless of no change in total protein level. To confirm it, we detected the roles of HSF1 and NFAT5 in Hsp70 transcription by siRNA-mediated knocking-down of the genes. We observed a decrease of Hsp70 expression during CVB3 infection when HSF1 was knocked-down (**Figure 2.2D**). Conversely, in the case of NFAT5 knocking-down, the expression level of Hsp70 seemed not changed (or slightly increased) compared to cells transfected with scrambled siRNAs, further confirming that the Hsp70-2 is not inducible in CVB3 infection. The slight increase of Hsp70 protein is probably attributed to the enhancement of viral replication, which is evidenced by the increased VP1 production at 5 h pi (**Figure 2.2E**). These results indicate that CVB3 infection enhances the transcription of Hsp70-1 but not Hsp70-2.

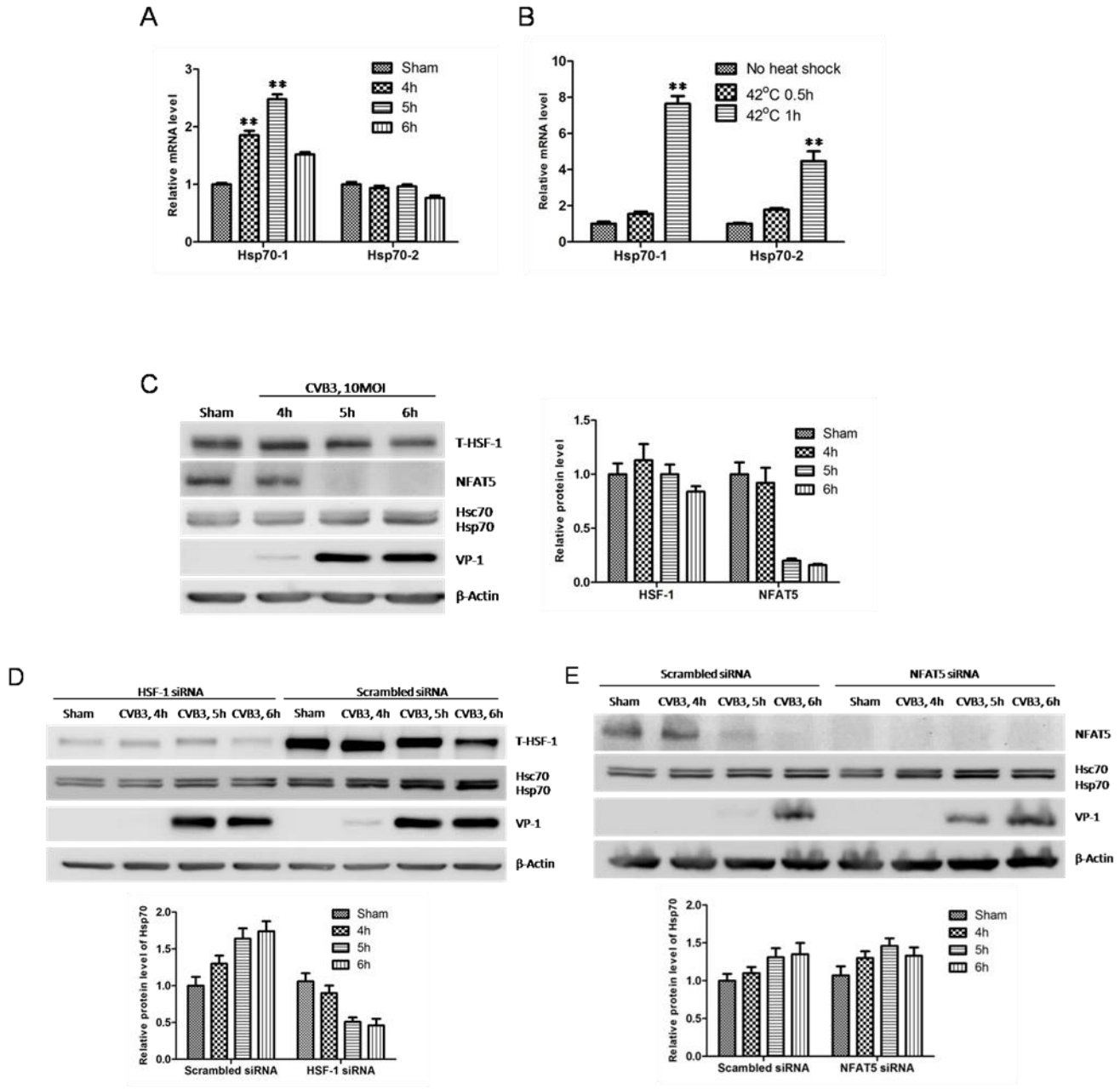

Figure 2.2. CVB3 infection stimulates the transcription of Hsp70-1 but not Hsp70-2. (A) HeLa cells were infected by CVB3 at 10 MOI for different time points and cellular total RNA was extracted. mRNA levels of Hsp70-1 and Hsp70-2 were detected by q-RT-PCR using primers targeting Hsp70-1 and Hsp70-2 specifically, and were normalized against those of GAPDH and shown as means ± SD (n=6). (B) HeLa cells were heat-shocked at 42 °C for 0.5 h and 1 h and cellular total RNA was extracted. mRNA levels of Hsp70-1 and Hsp70-2 were detected by qPCR. (C) HeLa cells were infected with CVB3 as described above. Cell lysates were extracted for western blot analysis using indicated antibodies and the results were quantified as described (lower panel). (D, E) HeLa cells were transfected with specific siRNAs to knock down HSF1 (D) or NFAT5 (E) and subjected to CVB3 infection at 10 MOI. Then the cell lysates were extracted for western blot analysis of indicated proteins. The quantification of Hsp70 is shown in the right panel (C) or the lower panels (D, E).

2.4.3 Phosphorylation of HSF1 at Ser230 is responsible for Hsp70-1 upregulation

Noting that the expression level of HSF1 was barely changed and there was a little shift of HSF1 band at 5 and 6 h pi (**Figure 2.3A**), we speculated that HSF1 was phosphorylated and led to the enhancement of the transcriptional activity of HSF1. Ser230 is a potential phosphorylation site in this case since such phosphorylation enhances the transcriptional activity of HSF1 [209]. To verify this hypothesis, we determined Ser230 phosphorylation during CVB3 infection by western blot using an antibody against phosphorylated HSF1 at Ser230 (p-HSF1 Ser230). Coinciding with Hsp70 up-regulation, HSF1 showed a significant increase of phosphorylation at 4 and 5 h pi (**Figure 2.3A**).

To further substantiate the role of such phosphorylation, we treated HeLa cells with 10 μM of KN62 (1-[N,O-bis-(5-Isoquinolinesulfonyl)-N-methyl-L-tyrosyl]-4-phenylpiperazine, Santa Cruz), a chemical that inhibits the phosphorylation of HSF1 at Ser230 [326], and then detect the phosphorylation of HSF1 at Ser230 as well as the mRNA level of Hsp70-1. Upon KN62 treatment, we observed that both phosphorylation of HSF1 at Ser230 and increase of Hsp70-1 mRNA were diminished during CVB3 infection (**Figure 2.3B and C**). In order to exclude the possibility that phosphorylated HSF-1 enhance transcription of Hsp70-1 via other mediators, we treated HeLa cells with 2 μM of KRIBB11 (N(2)-(1H-indazole-5-yl)-N(6)-methyl-3-nitropyridine-2,6-diamine), a specific inhibitor for the transcriptional activity of HSF1 but not the phosphorylation of HSF1 at Ser230 [327]. According to the results, though the treatment of HeLa cells with KRIBB11 didn't inhibit the phosphorylation of HSF1 at Ser230 (**Figure 2.3B**), it diminished the increase of Hsp70-1 mRNA induced by CVB3 (**Figure 2.3C**). Together, our results demonstrate that HSF1 is phosphorylated at Ser230 and such phosphorylation is responsible for transcriptional enhancement of Hsp70-1 during CVB3 infection.

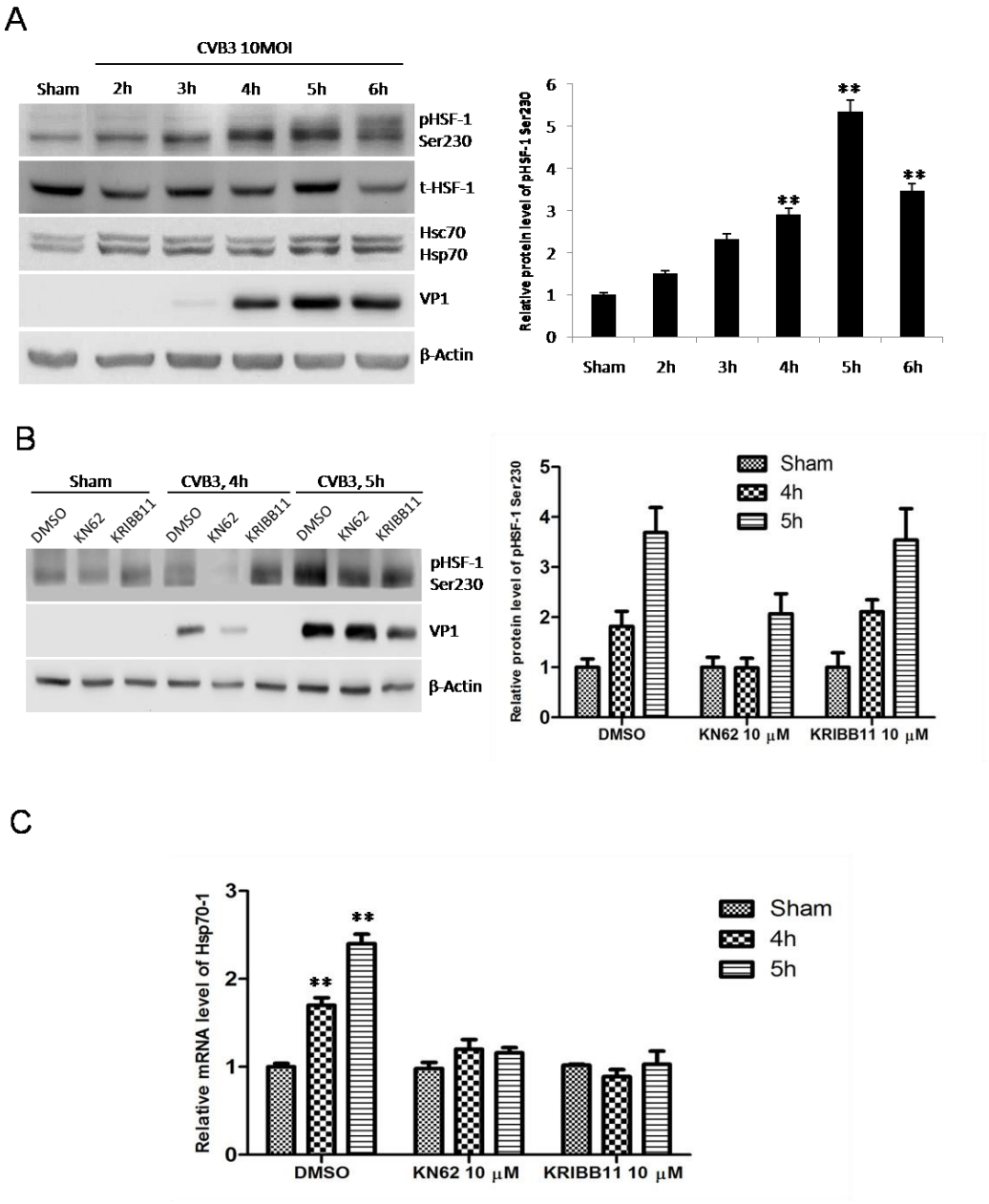

Figure 2.3. Phosphorylation of HSF1 at Ser230 up-regulates Hsp70-1 during CVB3 infection. (A) HeLa cells were infected with CVB3 and expression levels of phosphorylated HSF1 at Ser230 and Hsp70 were detected at different time points pi by western blot analysis. β-actin was used as a loading control. Quantification of band intensities was conducted as described in Fig. 1. (B, C) HeLa cells were treated with KN62, a CaMKII inhibitor and KRIBB11, an HSF1 inhibitor, 1 h before infection. Then the cells were infected with CVB3. At different time points pi, the cellular proteins and total RNA were extracted for western blot analysis of HSF1 phosphorylation at Ser 230 (B) and q-RT-PCR detection of Hsp70-1 mRNA (C), respectively.

2.4.4 CVB3-induced phosphorylation of HSF1 at Ser230 is via phosphorylation of CaMKIIγ

Previous studies showed that phosphorylation of HSF1 at Ser230 is catalyzed by CaMKII [209]. The family of CaMKIIs contains four isoforms [328], among which isoforms γ and δ are the predominant isoforms in the heart [329], thus we focused our studies on these two isoforms. CaMKIIδB is a sub-isoform of CaMKIIδ accumulated in the nucleus in response to stresses and contributing to phoshorylation of HSF1 [330]. However, to our surprise, western blot analysis showed a decrease of CaMKIIδB in HeLa cells during CVB3 infection (**Figure 2.4A**). Then we changed our focus onto CaMKIIγ. Activation of CaMKIIγ is initialized by binding to Ca^{2+}/CaM and retained by autophosphorylation at Thr286 due to persistent high level of Ca^{2+}/CaM [215]. Therefore, we hypothesized that CVB3 infection activated CaMKIIγ via Thr286 phosphorylation. we detected the phosphorylated CaMKII by western blot using a specific antibody and found that CaMKII was indeed phosphorylated at 3 h pi, a time point ahead of phosphorylation of HSF1 at Ser230 (**Figure 2.4B**). Furthermore, we knocked-down CaMKIIγ in CVB3-infected HeLa cells using specific siRNAs and found that phosphorylation of HSF1 at Ser230 was diminished (**Figure 2.4C**). These results indicate that CaMKIIγ activation is required for HSF1 phosphorylation at Ser230 during CVB3 infection.

Upon determining the role of CaMKIIγ, we next studied the upstream signal molecules. Since cytosolic calcium is a prerequisite for CaMKII phosphorylation, we cultured HeLa cells in calcium-free medium and detected the change of downstream signals during CVB3 infection. As expected, less phosphorylation of CaMKII at Thr286 and HSF1 at Ser230 was observed compared with cells cultured in normal calcium-containing medium (**Figure 2.4D**). Here we used phosphorylation of eukaryotic elongation factor 2 (p-eEF2) as a control for Ca^{2+}-free

condition since eEF2 phosphorylation requires the presence of calcium. It has been reported that active CVB3 replication induces increase of cytosolic calcium [103], thus we speculated that viral replication is required for activation of CaMKII and its downstream signals. Hence, we used UV-irradiated CVB3, which is capable of receptor binding and internalization but not able to replicate, to infect HeLa cells. Indeed, modest phosphorylation of CaMKII at Thr286 and HSF1 at Ser230 was observed upon infection of UV-irradiated CVB3 (**Figure 2.4E**). In all, these results reveal a signaling cascade in which CVB3 replication raises cytosolic calcium, activates CaMKII, and phosphorylates HSF1 at Ser230 and finally upregulates Hsp70-1.

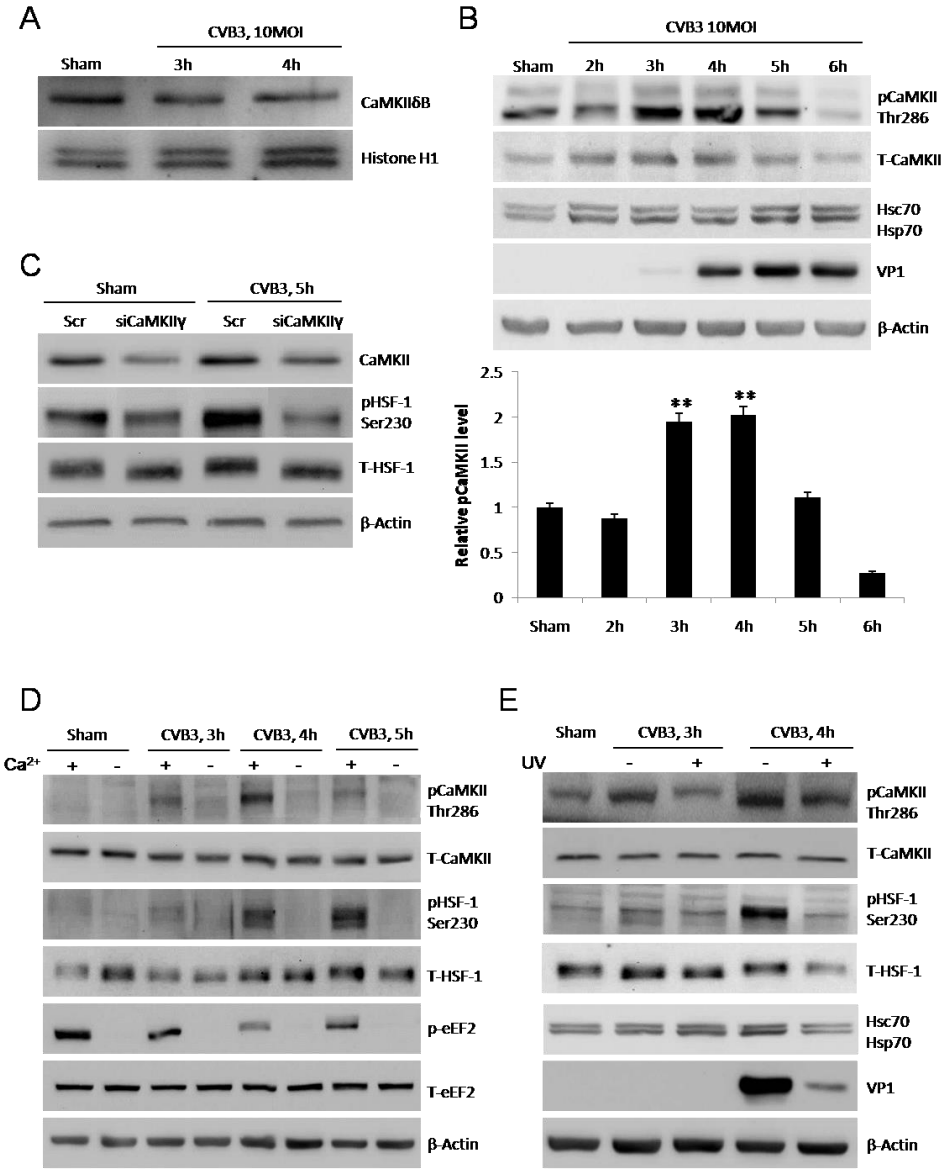

Figure 2.4. CaMKII is activated by phosphorylation and oxidation during CVB3 infection to phosphorylate HSF1 at Ser230. (A) HeLa cells were infected with CVB3 and expression levels of CaMKIIδB were detected by western blot using nuclear extracts. Histone H1 was detected as the loading control. (B) HeLa cells were infected with CVB3 and phosphorylation of CaMKII at Thr286 was detected at different time points pi. (C) HeLa cells were transfected with siRNAs targeting CaMKIIγ and then infected with CVB3 at 10 MOI. Cell lysates were used for western blot analysis of HSF1 phosphorylation at Ser230 and other indicated proteins. (D) HeLa cells were cultured in medium with or without calcium, a key factor of CaMKII phosphorylation (activation). Then the cells were infected with CVB3 or sham-infected with PBS for 5 h. Phosphorylation of CaMKII and HSF1 was detected by western blot analysis using the cell lysates. Phosphorylation of eEF2 was detected as a control indicating calcium-free environment. (E) HeLa cells were infected with alive or UV-irradiated CVB3 at 10 MOI and phosphorylation of CaMKII and HSF1 was detected in the cell lysate.

2.4.5 Phosphorylation of HSF1 at Ser307 is blocked during CVB3 infection

Unlike Ser230, phosphorylation of HSF1 at Ser307 inhibits the transcriptional activity of HSF1 [314]. Phosphorylation of HSF1 at Ser307 is catalyzed by active ERK1/2. However, ERK1/2 is substantially activated by phosphorylation at 5 h post CVB3 infection [316], the exact same time point when Hsp70-1 is upregulated, thus we cannot neglect the potential adverse effect of Ser307 phosphorylation of HSF1 on Hsp70-1 induction during CVB3 infection. To determine the possible contributions of Ser307 phosphorylation to the HSF-1 activity during CVB3 infection, we detected it as well as its upstream signal, phosphorylated ERK1/2, by western blot using specific antibodies. Surprisingly, though dramatic phosphorylation of ERK1/2 was observed at 5 h pi, coinciding with the previous study, phosphorylated HSF1 at Ser307 could be barely detected (**Figure 2.5A**), indicating that ERK1/2-mediated phosphorylation of HSF1 at Ser307 was blocked. However, when we detected the phosphorylation of HSF1 at Ser307 at very early time points of CVB3 infection (0.5-2 h pi, the time for CVB3 binding and internalization) during which ERK1/2 was also transiently phosphorylated, we observed phosphorylation of HSF1 at Ser307 (**Figure 2.5A**). We suspected that blocking of Ser307 phosphorylation at 4 h pi was resulted from translocation of HSF1 into the nucleus and isolation from ERK1/2 after phosphorylation at Ser230 [330]. This speculation was verified by western blot analysis using protein extracts isolated from nucleus and cytoplasm separately. We found that HSF1 increased dramatically at 4 h pi in the nucleus, coinciding with the time of HSF1 phosphorylation at Ser230, whereas ERK1/2 was mainly located in the cytoplasm (**Figure 2.5B**). This finding was solidified by immunofluorescence staining and confocal imaging, showing the accumulation of HSF1 in the nucleus at 4 h pi (**Figure 2.5C**), the time point when Ser230 was phosphorylated.

These data indicate that phosphorylation of Ser230 isolates HSF1 from ERK1/2 and avoids the negative regulation of Hsp70.

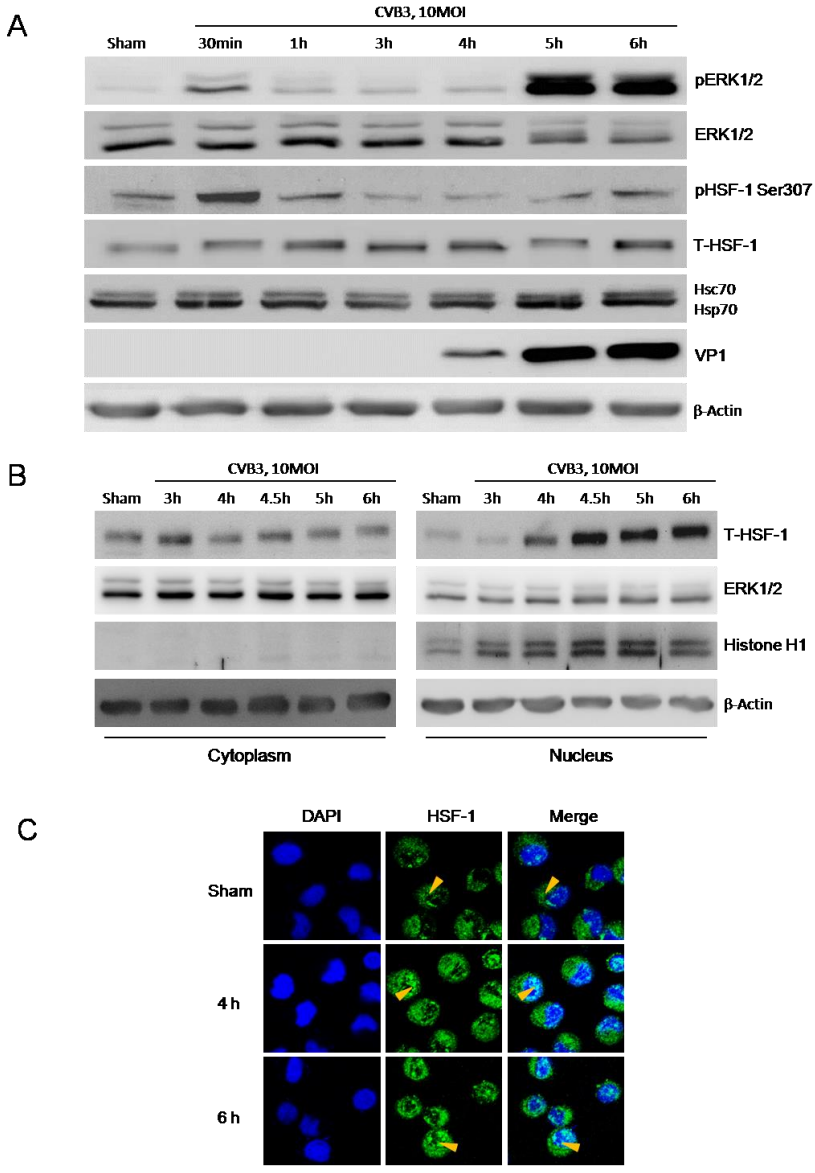

Figure 2.5. Phosphorylation of HSF1 at Ser307 was blocked by nuclear translocation of HSF1. (A) HeLa cells were infected with CVB3 at 10 MOI. Phosphorylation of both HSF1 at Ser307 and its upstream signal ERK1/2 was detected by western blot using indicated antibodies. (B) HeLa cells were infected with CVB3 or sham-infected with PBS. Nuclear and cytosolic proteins were isolated for detection of HSF1 and ERK1/2 respectively. Histone H1 protein was used as a purity control for nuclear fraction. β-actin was the loading control. (C) HeLa cells were infected with CVB3 at 10 MOI. At different time points pi, the cells were fixed for the immunostaining of HSF1. Nuclei were counter-stained with DAPI. The cellular localization of HSF1 was visualized by confocal microscopy.

2.4.6 Hsp70 favors CVB3 replication

To investigate the effect of Hsp70-1 on CVB3 infection, we first silenced Hsp70-1 expression by transfection of HeLa cells for 48 h with siRNAs targeting Hsp70-1 or scrambled control siRNAs and then infected with CVB3 for 2-6 h. Total cellular RNAs were extracted at different time points pi and then the levels of CVB3 genome were detected by q-RT-PCR using the primers targeting the coding region of one of 2A, one of the viral genes. We observed a dramatic decrease of 2A RNA in Hsp70-1 siRNAs-transfected cells compared to the control (**Figure 2.6A**). This negative effect of Hsp70-1 silencing on CVB3 replication was further solidified by western blot analysis of CVB3 VP1 protein using cell. As shown in **Figure 2.6B**, transfection of siRNA targeting Hsp70-1 resulted in a decrease in VP1 production.

To further confirm the positive effects of Hsp70-1 on CVB3 replication, we next overexpressed Hsp70-1 in HeLa cells using the plasmid pEGFP-Hsp70-1. Meanwhile, we transfected the cells with the empty vector pEGFP and pEGFP-Hsp70-1(K71E), a loss-of-function mutant of Hsp70-1, as negative controls. After transfection for 20 h and then infected with CVB3, viral RNA and VP1 levels were detected as described above. As shown in **Figure 2.6C and 6D** particularly at 4h pi, compared with controls, overexpression of WT Hsp70-1 enhanced viral replication at levels of transcription and translation, while overexpression of pEGFP-Hsp70-1(K71E) barely changed the levels of viral RNA and protein (**Figure 2.6C and E**).

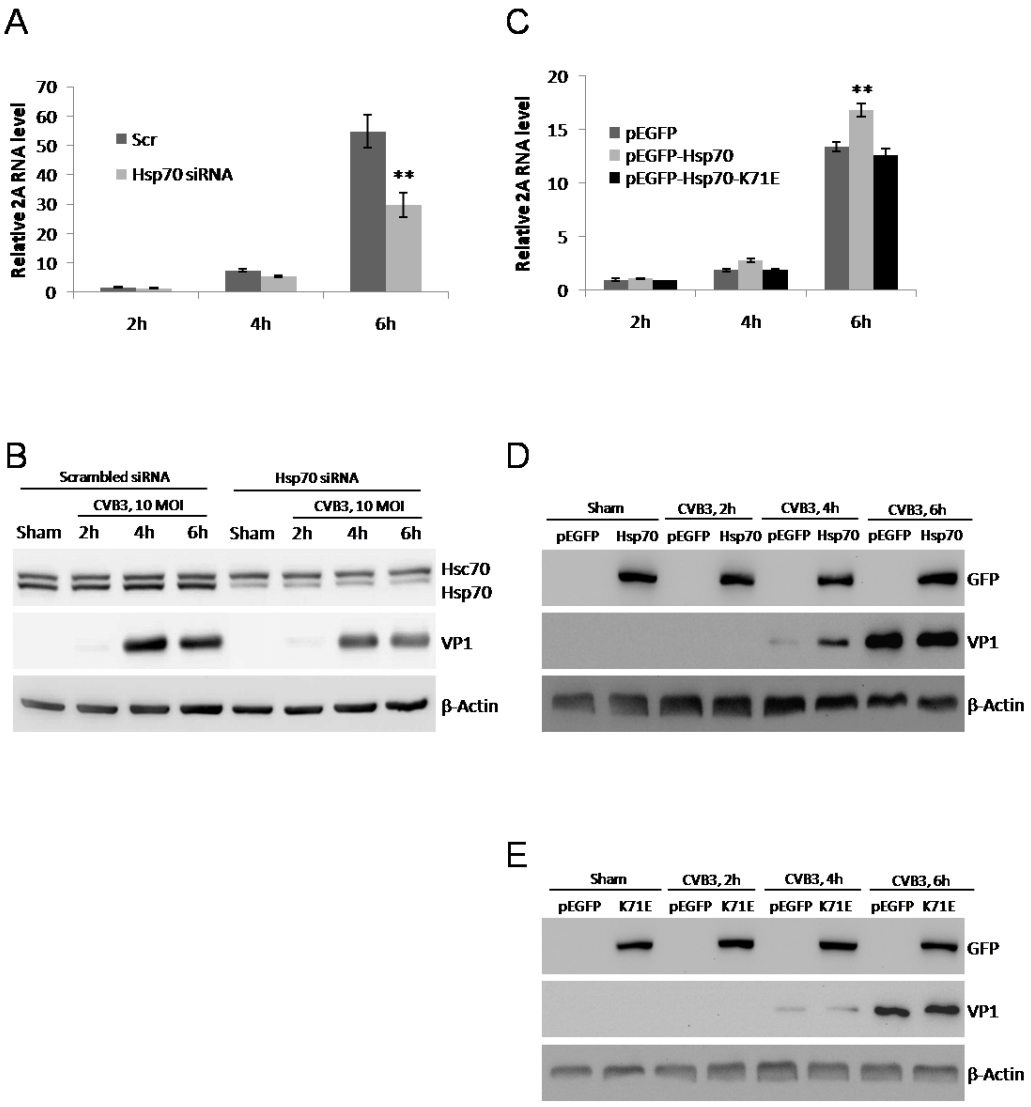

Figure 2.6. Hsp70-1 upregulation benefits CVB3 replication. HeLa cells were transfected with specific siRNAs to knock down endogenous Hsp70-1 and then infected with CVB3 at 10 MOI. Viral replication was evaluated by q-RT-PCR detection of 2A RNA (A) and western blot analysis of VP1 (B). Cells transfected with scrambled siRNAs served as the negative control. Meanwhile, HeLa cells were transfected with plasmid pEGFP-Hsp70-1 to overexpress Hsp70-1 and then infected with CVB3 at 10 MOI. Viral replication was measured by q-RT-PCR detection of 2A RNA (C) and western blot analysis of VP1 (D). Cells transfected with the empty vector pEGFP and pEGFP-Hsp70-1 (K71E) mutant plasmid served as negative controls (E). In both q-RT-PCR results, the RNA levels of CVB3 2A were normalized against the mRNA levels of GAPDH and shown as means ± SD (n=6, $p < 0.01$).

2.4.7 Hsp70-1 stabilizes CVB3 genomic RNA via the ARE site of CVB3 3'UTR

Hsp70-1 is known to play a role in stabilizing mRNAs containing an ARE site in its 3'UTR [319]. As shown in **Figure 2.7A**, CVB3 genomic RNA also contains an ARE sequence within its 3'UTR. Thus, I focused my attention to investigate whether Hsp70-1 enhances CVB3 replication via stabilizing viral genome. To this end, I constructed the dual-luciferase reporter plasmids, C49-WT-CVB3-3'UTR and C49-Mut-CVB3-3'UTR, by inserting WT and mutant 3'UTR of CVB3 RNA at the downstream of Renilla luciferase coding region, so that these two reporters contain a WT and a mutant ARE site, respectively (**Figure 2.7B**). I co-transfected the reporter plasmids and Hsp70-1 siRNAs or scrambled siRNA into HeLa cells. The knockdown efficiency of Hsp70-1 was confirmed by qPCR detecting Hsp70-1 mRNA, which showed that the mRNA levels of Hsp70-1 decreased more than 50% in Hsp70-siRNA-transfected cells compared to scrambled-siRNA-transfected controls (**Figure 2.7C**). Then I measured the activity of Renilla luciferase by luciferase assay, and the data were normalized to the activity of firefly luciferase. The results showed that knocking-down of Hsp70-1 decreased the expression of the luciferase with the wild-type ARE site, whereas the luciferase gene with the mutant ARE site was not sensitive to Hsp70-1 knocking-down (**Figure 2.7D**). To further confirm that Hsp70-1 is critical for the stability of mRNAs modulated by CVB3 3'UTR, I treated the reporter cells with 2.5 μg/mL of actinomycin D for 2 and 4 h to inhibit new transcription, and detected the mRNA levels of Renilla luciferase by qPCR using specific primers (**Table 2.1**). All the qPCR results were normalized by setting the mRNA level of groups treated with scrambled siRNAs but no actinomycin D as 100%. As shown in **Figure 2.7E**, the mRNA of Renilla luciferase modulated by WT CVB3 3'UTR has a decrease of 60% at 2 h and 85% at 4 h after actinomycin D treatment,

compared with 40% decrease at 2 h and 60% decrease at 4 h of the reporter modulated by mutant CVB3 3'UTR, indicating a more rapid decay of the mRNA with the WT ARE site when the new transcription is blocked. Moreover, when Hsp70-1 was knocked-down, a lower level of Renilla luciferase mRNA was detected in cells transfected with C49-WT-CVB3-3'UTR, but no significant changes were observed in cells transfected with C49-Mut-CVB3-3'UTR, supporting the previous finding that the mRNA with the WT ARE site is more sensitive to Hsp70-1 change and decay faster when Hsp70-1 level is low. These results indicate that Hsp70-1 stabilizes CVB3 genomic RNA and this function requires an ARE sequence.

It has been reported that Hsp70-1 stabilizes ARE-mRNA via sequestering AUF1 in the nucleus[319], and AUF1 isoforms $p37^{AUF1}$ and $p40^{AUF1}$ are involved in this process [331] . Thus, I further tested whether these two AUF1 isoforms play a role in stabilizing CVB3 genomic RNA during infection. To this end, I expressed either $p37^{AUF1}$ or $p40^{AUF1}$ by plasmid transfection in CVB3-infected HeLa cells and then measured viral genomic RNA during infection. The q-RT-PCR results showed that CVB3 genomic RNA was significantly decreased upon expression of these AUF1 isoforms although $p40^{AUF1}$ caused less decrease than $p37^{AUF1}$ (**Figure 2.7F**). However, when Hsp70-1 was co-transfected with AUF1, the decrease of viral genome was diminished (**Figure 2.7F**). These results demonstrate that $p37^{AUF1}$ or $p40^{AUF1}$ reduces the abundance of CVB3 genomic RNA while Hsp70-1 reverses such effect, indicating that Hsp70-1 stabilizes CVB3 genomic RNA via $p37^{AUF1}$ and $p40^{AUF1}$.

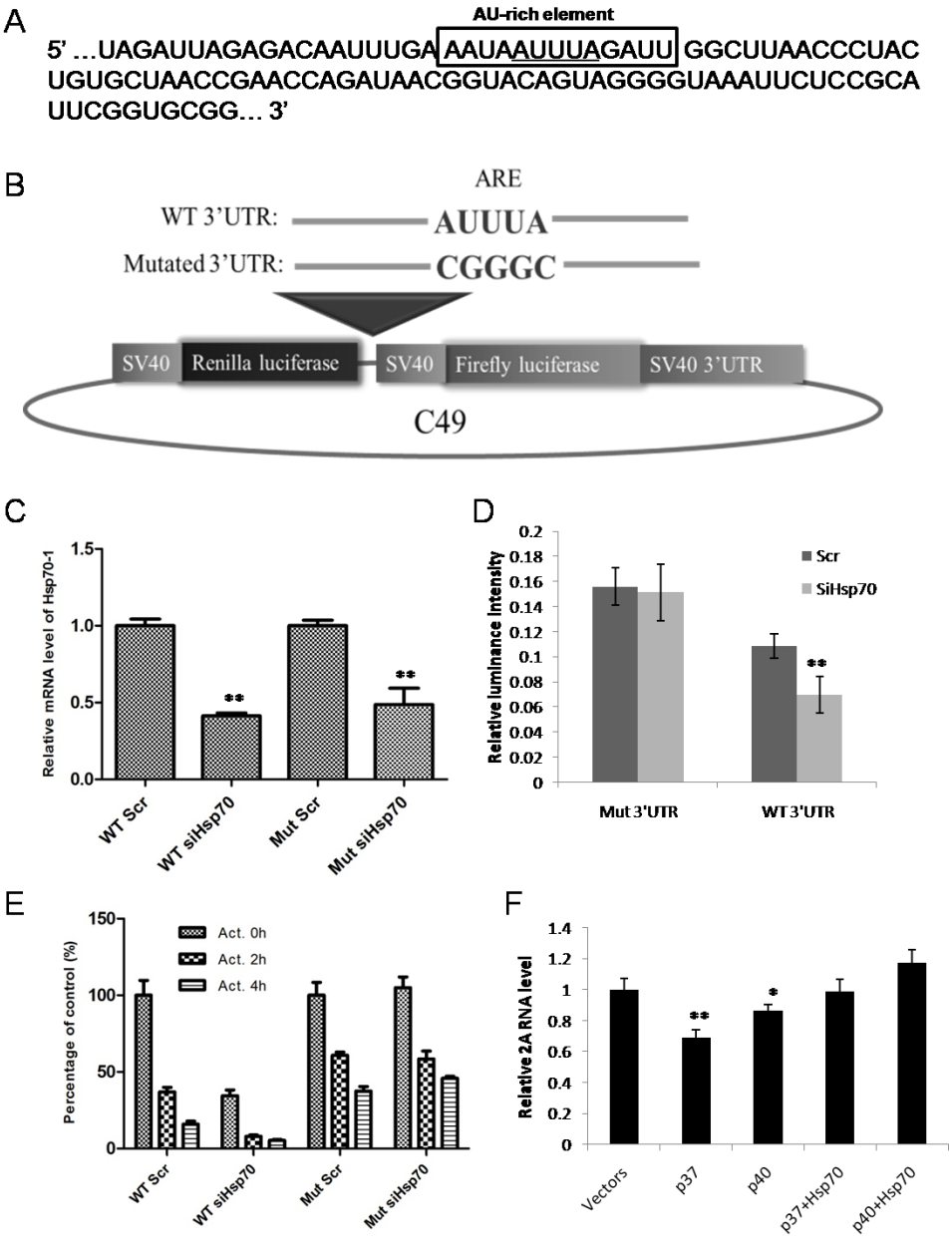
A
AU-rich element
5' ...UAGAUUAGAGACAAUUUGA AAUAAUUUAGAUU GGCUUAACCCUAC
UGUGCUAACCGAACCAGAUAACGGUACAGUAGGGGUAAAUUCUCCGCA
UUCGGUGCGG... 3'
B
ARE
WT 3'UTR: AUUUA
Mutated 3'UTR: CGGGC
SV40
Renilla luciferase
SV40
Firefly luciferase
SV40 3'UTR
C49
C
Relative mRNA level of Hsp70-1
1.5
1.0
0.5
0.0
**
**
WT Scr
WT siHsp70
Mut Scr
Mut siHsp70
D
Relative luminance intensity
0.2
0.18
0.16
0.14
0.12
0.1
0.08
0.06
0.04
0.02
0
Scr
SiHsp70
**
Mut 3'UTR
WT 3'UTR
E
Percentage of control (%)
150
100
50
0
Act. 0h
Act. 2h
Act. 4h
WT Scr
WT siHsp70
Mut Scr
Mut siHsp70
F
Relative 2A RNA level
1.4
1.2
1
0.8
0.6
0.4
0.2
0
**
*
Vectors
p37
p40
p37+Hsp70
p40+Hsp70

Figure 2.7. Hsp70-1 stabilizes CVB3 genomic RNA via the ARE site in the 3'UTR of CVB3 genome. (A) An AU-rich element is located in the 3'UTR of CVB3 genome. (B) Schematic structures of C49 luciferase reporter plasmid. WT and mutated CVB3 3'UTRs were amplified by PCR using specific primers and inserted into the downstream of Renilla luciferase coding region on the reporter plasmid, generating C49-WT-CVB3-3'UTR and C49-Mut-CVB3-3'UTR. (C) HeLa cells were co-transfected with different combinations of plasmids and siRNA: C49-WT-CVB3-3'UTR and scrambled siRNAs (WT Scr), C49-WT-CVB3-3'UTR and Hsp70-1 siRNAss (WT siHsp70), C49-Mut-CVB3-3'UTR and scrambled siRNAs (Mut Scr) or C49-Mut-CVB3-3'UTR and Hsp70-1 siRNAss (Mut siHsp70). The knockdown efficiency of Hsp70-1 by siRNA was determined by qPCR detection of Hsp70-1 mRNA. The results were normalized by GAPDH mRNA and the relative mRNA levels of Hsp70-1 in Scr siRNA-treated cells were set as 1.0. (D) Luciferase assay. HeLa cells were co-transfected with the C49 plasmids containing WT or mutated CVB3 3'UTR and Hsp70-1 siRNAs (siHsp70) or scrambled siRNA (Scr). At 48 h pt, cell lysates were collected and subjected to luciferase assay. Relative luciferase activities (Renilla/firefly) are shown as means ± SD (n=9). (E) HeLa cells were transfected with the same plasmids and siRNAs as those in (C) and (D). The transfected cells were treated with 2.5 μg/mL of actinomycin D for 2h (Act. 2h) or 4h (Act. 4h). The same cells treated with 0.1% DMSO (Act. 0h) served as a control. The rate of mRNA decay was determined by qPCR detection of the Hsp70-1 mRNA. The results were normalized by GAPDH mRNA and the relative mRNA levels of Hsp70-1 in Scr siRNA-treated cells without actinomycin D treatment were set as 100%. (F) HeLa cells were co-transfected with different plasmid combinations: Vectors (pFLAG + pEGFP), p37 (pFLAG-p37AUF1 + pEGFP), p40 (pFLAG-p40AUF1 + pEGFP), p37 + Hsp70 (pFLAG-p37AUF1 + pEGFP-Hsp70-1), and p40 + Hsp70 (pFLAG-p40AUF1 + pEGFP-Hsp70-1). At 36 h pt, the cells were infected with CVB3 at 10 MOI for 6 h and then viral genomic RNA was measured by q-RT-PCR detection of CVB3 2A RNA. The RNA levels of 2A were normalized against the mRNA levels of GAPDH and shown as means ± SD (n=6, $p < 0.01$).

2.5 Discussion

Hsp70 is one of the best characterized chaperon proteins in the Hsp70 family. Its expression is regulated by various cellular stress conditions including viral infection. Accumulating evidence indicates that the mutual regulation of viruses and Hsp70 is critical for viral replication and the pathogenesis of virus-induced diseases. On one hand, viral infections, such as foot-and-mouth disease virus (FMDV) [332] and rotavirus [333], induce up-regulation of Hsp70. On the other hand, Hsp70 expression plays different roles in viral replication, for example, the positive regulation in rabies virus [333], Japanese encephalitis virus [334] and porcine circovirus [335] and the negative regulation in vesicular stomatitis virus [336], human immunodeficiency virus-1 [337] and rotavirus [333]. However, such study has not been conducted in coxsackievirus infection and particularly has never distinguished the roles of Hsp70-1 and Hsp70-2 in viral replication.

In this study, we aim to understand the mutual regulation between Hsp70 and CVB3. Our results showed that Hsp70-1, not Hsp70-2, is upregulated during CVB3 infection in cells of different origins, though the induction level is much lower than that in heat shock, which is probably due to the expression inhibition of some transcriptional and translational factors during CVB3 infection. In searching for the underlying mechanism, we focused our attention on HSF1, the transcriptional factor of Hsp70-1. By siRNA-mediated knocking-down of HSF1, we found that HSF1 is responsible for CVB3-induced up-regulation of Hsp70-1. However, no significant upregulation except a molecular-weight shift of HSF1 band was observed in the virus-infected samples, indicating that the transcriptional activity of HSF1 may be enhanced by certain post-translational modifications. Thus, we tried to determine HSF1 phosphorylation and found that HSF1 was indeed phosphorylated at Ser230. This result is consistent with previous report that phosphorylation of Ser230 activates transcriptional activity of HSF1 [209]. CaMKII is the upstream

kinase of HSF1 [209], which is activated via phosphorylation at Thr286 in an elevated Ca2+/CaM condition and responsible for phosphorylation of HSF1. Thus we drew our attention on CaMKII. We found that CaMKII was phosphorylated at Thr286 during CVB3 infection. Correspondingly, our results showed that KN62, a specific inhibitor of CaMKII-calcium/calmodulin binding [326], inhibited phosphorylation of HSF1 at Ser230 and thus Hsp70-1 production during CVB3 infection. The family of CaMKIIs contains four isoforms, α, β, γ and δ [328]. Since α and β isoforms are almost exclusively expressed in the brain and the γ and δ are the predominant isoforms in the heart [329], we focused our identification on γ and δ isoforms. By siRNA-targeted gene silencing, we finally identified CaMKIIγ as the responsible isoform for HSF1 phosphorylation at Ser230 during CVB3 infection. These data suggest that CVB3-induced Hsp70-1 upregulation is via selective phosphorylation of HSF1 at Ser230, which is catalyzed by CaMKIIγ.

There are several other phosphorylation sites on HSF-1, among which we focused on the ERK1/2-regulated phosphorylation of HSF1 at Ser307 as this phosphorylation can inhibit the transcriptional activity of HSF1 [314]. However, this event was blocked during later time points of CVB3 infection, contributing to the enhancement of HSF1 activity and Hsp70-1 upregulation. Our previous study showed that ERK1/2 is activated at two separate phases although the later phase is dominant during CVB3 infection [316]. Here, we showed that ERK1/2 activation at the first phase was capable of inducing phosphorylation of HSF1 at Ser307 though the second phase of ERK1/2 activation was not. This is likely due to nuclear translocation of HSF1, which isolates HSF1 from ERK1/2, at late time points of CVB3 infection.

Having determined the up-regulation of Hsp70-1 during CVB3 infection, we next invested the effects of Hsp70-1 upregulation on CVB3 infection. By both the siRNA-mediated gene silencing

and plasmid-mediated overexpression of Hsp70-1, we confirmed that Hsp70-1 expression benefits CVB3 replication at the levels of transcription and translation. These data suggest that Hsp70-1 upregulation generates a positive feedback loop on CVB3 replication. This signaling pathway is summarized in **Figure 2.8**. Then the question was how Hsp70-1 favors CVB3 replication. One of our hypotheses was that Hsp70-1 protects viral genomic RNA from exonuclease-driven degradation, considering Hsp70-1 is closely related to mRNA turnover [5]. Many cellular mRNAs contain an ARE sequence in their 3'UTR. Association of ARE-binding protein (AUPBs) with these mRNAs promotes rapid mRNA degradation. AUF1, one of the best-characterized AUBPs, binds to many ARE-mRNAs and assembles other factors necessary to recruit the mRNA degradation machineries. These factors include eIF4G, PABP, Hsp70-1 and many unknown proteins [192]. During normal physiological conditions, AUF1 interacts simultaneously with eIF4G and ARE, while PABP binds both eIF4G and poly(A) tail. However during the active normal translation of ARE-containing mRNAs, the ribosome might relocate AUF1, which could bind PABP, thus causing exposure of the poly-A tail to deadenylases to initiate decay. During cellular stress or infection, the association of Hsp70-1 with AUF1 may disrupt or block the AUF-PABP interaction, leaving PABP free to remain bound to poly-A tail, thus masking it from ribonuclease [193]. This mechanism for stabilizing the viral mRNA has been reported in DNA virus infection [338]. By sequence screening, we found that the genomic RNA of CVB3 harbors an ARE site within its 3'UTR. To verify whether this ARE site plays a role in Hsp70-1-mediated stabilization of CVB3 genomic RNA, we performed luciferase assay and mRNA turnover assay using reporter plasmids containing CVB3 3'UTR with a WT or mutant ARE site. In the luciferase activity assay, we found that only the reporter regulated by the WT CVB3 ARE site is sensitive to Hsp70-1 level, supported by the result that the reporter signal was

significantly reduced when Hsp70-1 was knocked-down but no significant change was observed in the mutant control. In the mRNA turnover assay, the decay of the luciferase mRNA was detected directly and the results showed that the mRNA containing CVB3 3'UTR with WT ARE had a more rapid decay rate and its level was positively correlated with Hsp70-1 level, supporting that Hsp70-1 stabilizes the RNA with CVB3 3'UTR via the ARE site. We further determined whether AUF1 is involved in the process via ectopic expression of different AUF1 isoforms. We found that expression of $p37^{AUF1}$ and $p40^{AUF1}$ decreased the abundance of CVB3 genomic RNA; however such decrease was suppressed by expression of Hsp70-1, indicating that the stability of CVB3 genomic RNA is negatively regulated, at least in part, by AUF1-mediated RNA decay, whereas Hsp70-1 plays a role in counteracting this process**.**

CVB3 infection is the primary cause of viral myocarditis, an inflammatory heart disease. Lesions of the heart caused by CVB3 infection are not only due to viral replication in cardiomyocytes, but also resulted from virus-induced exaggerated immune responses. Hsp70-1 has been reported to be secreted upon induction and act as an immune stimulator leading to immune infiltration [336, 339, 340]. Thereby, we believe that CVB3-induced upregulation of Hsp70-1 not only favors viral replication, but also enhances immune infiltration during the development of myocarditis, both of which lead to exacerbation of the disease. Thus, Hsp70-1 chaperone is a rational pharmaceutical target for viral myocarditis.

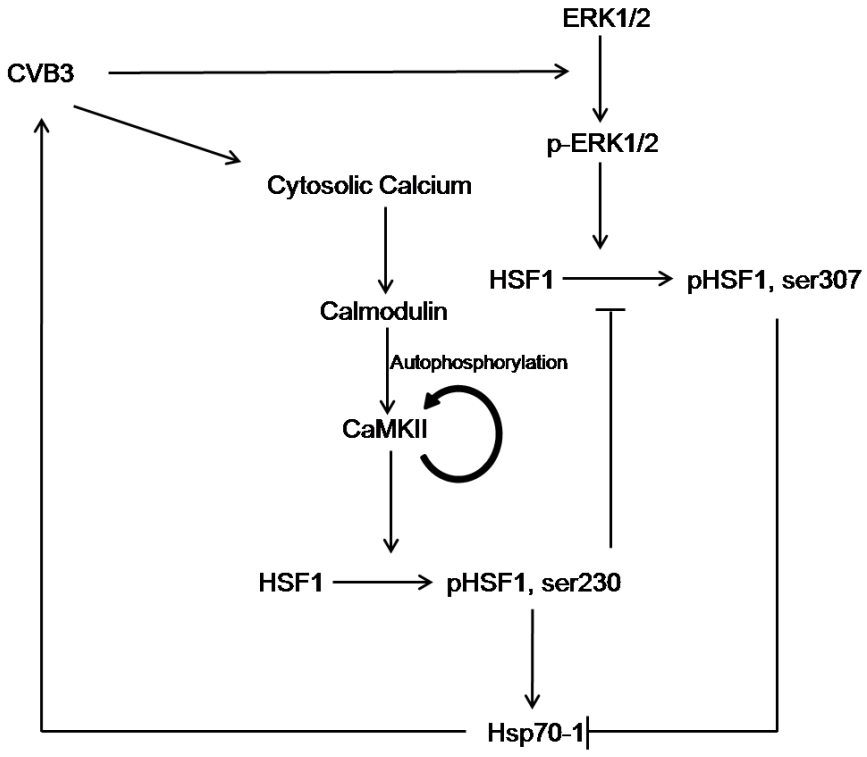

Figure 2.8. A putative model of the mutually beneficial regulation of CVB3 and Hsp70-1. CVB3 infection elevates the level of cytosolic calcium and activates CaMKII via inducing auto-phosphorylation of CaMKII at Thr286. The active CaMKII further phosphorylates HSF1 at Ser230 to enhance the transcription of Hsp70-1. On the other hand, HSF1 activation causes the nuclear translocation of HSF1 and thus blocks the ERK1/2-catalyzed phosphorylation of HSF1 at Ser307, a negative regulatory process of Hsp70-1 transcription, thus further contributing to Hsp70-1 upregulation. Finally, the upregulated Hsp70 in turn positively feedbacks on CVB3 replication.

Chapter 3 CVB3 and Nuclear Factor of Activated T-cells 5

3.1 Background and Rationale

3.1.1 NFAT5-related signals in heart diseases

NFAT5 is a master transcriptional factor (~170 kDa) activated in hypertonic stress, which promotes cell survival against the stress by inducing the expression of different tonicity-responsive genes via binding to the TonE [341]. As mentioned earlier, in mammals, hypertonic environment is almost exclusively found in the kidney on which most NFAT5 studies were conducted, while the function of NFAT5 in other organs has been barely studied regardless of the ubiquitous expression in almost all organs [298, 299]. Recently, a few reports have suggested the possible protective role of NFAT5 in some conditions of heart injury. For instance, degradation of NFAT5 is induced in cardiomyocytes treated with doxorubicin, a commonly used anti-tumor agent, and such decrease of NFAT5 exacerbates myocyte death upon doxorubicin treatment [300]. In certain clinical trials, HSS, a common inducing agent of hypertonic stress, was used as an auxiliary supplement to improve cardiac function in heart diseases [293, 294].

3.1.2 NFAT5 and CVB3

CVB3 infection activates p38 MAPK, which is the upstream signals upregulating NFAT5 expression [257, 298]. However, in Chapter 2, the detection of NFAT5 proteins during CVB3 infection showed a sudden disappearance of NFAT5 at 5 h pi in HeLa cells (**Figure 2.2C**) and knockdown of NFAT5 increased CVB3 proteins synthesis (**Figure 2.2E**). These results indicated a post-transcriptional inhibition of NFAT5, which may benefits CVB3 infection.

Among the signals downstream of NFAT5, NFκB has been reported to promote host cell viability in CVB3 infection [304]. In addition, iNOS, which is induced by NFAT5 [305], exerts

inhibitory effect on CVB3 replication and decreases mouse mortality rate after viral infection [307]. These findings inspired me to link NFAT5 and CVB3-induced cell death and cardiac injury, a virgin field for the studies of both NFAT5 and CVB3-induced viral myocarditis.

3.2 Hypothesis and Specific Aims

The objective of this chapter is to investigate the mechanism underlying NFAT5 disappearance in CVB3 infection and its feedback role on viral replication. According to the pattern of NFAT5 decrease and the current knowledge, I **HYPOTHESIZE** that NFAT5 is cleaved and inactivated by CVB3 proteases 2A and 3C, which promotes CVB3 replication and viral-induced cell death.

The **SPECIFIC AIMS** for this chapter are as follows:

Aim 1: To determine CVB3-mediated cleavage of NFAT5

Aim 2: To determine the protease(s) responsible for NFAT5 cleavage and the cleavage site(s)

Aim 3: To investigate the effects of NFAT5 and its cleavage product(s) on CVB3 replication

Aim 4: To test the therapeutic effect of hypertonic reagents on CVB3 infection *in vitro* and in mice

3.3 Method and Materials

3.3.1 General techniques

All tissue culture, western blots, viral plaque assay, plasmid and siRNA transfection, and immunofluorescence staining were conducted in the same ways as described in Chapter 2. The qPCR was also conducted using the same reagents as those in Chapter 2 but with different primers (**Table 3.1**).

3.3.2 Antibodies

For western blot analysis in this chapter, the following primary antibodies were used: monoclonal rabbit anti-VP1, monoclonal rabbit anti-FLAG and monoclonal rabbit anti-myc (Thermo Fisher); monoclonal mouse anti-β-actin and polyclonal rabbit anti-NFAT5 (Santa Cruz).

In immunofluorescence staining of this chapter, monoclonal rabbit anti-myc (Thermo Fisher) was used as the primary antibody.

3.3.3 Constructs, molecular cloning and site-directed mutagenesis

pEGFP-myc-NFAT5 and pEGFP-myc-NFAT5-DBD were kind gifts from Dr. Anjana Rao (Addgene plasmid #13627 and #14112) [342]. The FLAG-p70-NFAT5 fragment was amplified by PCR using universe hot start high-fidelity DNA polymerase (Bimake) and pEGFP-myc-NFAT5 plasmid as the template. . The primers (NFAT5 F/Xho I and NFAT5 G503 R/Bam HI) used in this PCR are listed in **Table 3.1**. The PCR product was digested with Xho I and Bam HI and then inserted into pcDNA3.1(-) to generate the expression plasmid of p70-NFAT5 and pcDNA3.1(-)-p70-NFAT5.

The plasmid pEGFP-myc-NFAT5 was mutated at G503 and G650 by PCR-mediated site-directed mutagenesis using corresponding primers (**Table 3.1**) to generate pEGFP-myc-NFAT5^{G503A} and pEGFP-myc-NFAT5^{G650A}, respectively. Briefly, PCR reaction using mutagenesis primers and pEGFP-myc-NFAT5 template was conducted using the same DNA polymerase kit as described above, and then the PCR product was transformed to DH5α competent *E. coli* cells. The transformed cells were plated onto Luria broth (LB) plates containing 50 μg/mL kanamycin and incubated overnight at 37 °C. On the next day, individual

bacterium colonies were picked and the plasmid was extracted using High-Speed Plasmid Mini Kit (Froggabio). The mutation sites were verified by DNA sequencing using primers NFAT5 G503 Seq and NFAT5 G650 Seq (**Table 3.1**).

Table 3.1. Primers used in Chapter 3

Experiment	Primer	Sequence
Q-RT-PCR	Human Hsp70-2 forward	TGTTTGTCTTTGAGGTGGAC
	Human Hsp70-2 reverse	AAGAATTCTAATGAACATATCGG TTG
	Human NFAT5 forward	GAAGTGGACATTGAAGGCACT
	Human NFAT5 reverse	CTGGCTTCGACATCAGCATT
	Human TauT forward	AGATCATCATAGGCCAGTACAC
	Human TauT reverse	TAGACATTCAGGAGGGACACA
	Human iκB forward	GATCCGCCAGGTGAAGGG
	Human iκB reverse	GCAATTTCTGGCTGGTTGG
	Human iNOS forward	GCAGAATGTGACCATCATGG
	Human iNOS reverse	ACAACCTTGGTGTTGAAGGC
	Human GAPDH forward	AATCCCATCACCATCTTCCA
	Human GAPDH reverse	TGGACTCCACGACGTACTCA
	Mouse GAPDH forward	GGCAAATTCAACGGCACAGT
	Mouse GAPDH reverse	AGATGGTGATGGGCTTCCC
	CVB3 2A forward	ATCAAGTTGCGTGCTGTG
	CVB3 2A reverse	TGCGAAATGAAAGGAGTGT
Molecular cloning	NFAT5 F/XhoI	AGCTCTCGAGATGGGCGGTGCTT GCAGCTCC
	NFAT5 G503 R/BamHI	AGCTGGATCCTTACTTATCGTCGT CATCCTTGTAATCAGTAGTTTTCA TTGCTTTC
	NFAT5 G503A F	GGCCATGAAAGCAATGAAAACTA CTGCATGTAATTTAGATAAGGTA AATATTATCCC
	NFAT5 G503A R	GGGATAATATTTACCTTATCTAAA TTACATGCAGTAGTTTTCATTGCT TTCATGGCC
	NFAT5 G650A F	GATATTACAGTCAGATGCTACAG TGGTTAATTTGTCAC
	NFAT5 G650A R	GTGACAAATTAACCACTGTAGCA TCTGACTGTAATATC
	NFAT5 G503 Seq	ACTTACACTCCAGACCC
	NFAT5 G650 Seq	TGACAACTATTCAAACCC

3.3.4 Reporter construction and dual luciferase assay

The NFAT5 reporter plasmid pGL-TonE-luciferase and the control Renilla reporter plasmid pRL were kind gifts from Dr. Anjana Rao (Addgene plasmid # 14110) [342] and Dr. Norbert Perrimon (Addgene plasmid # 37380) [343], respectively. In this plasmid, sequence containing TonE from promoter region of human aldose reductase (AR) gene, a typical downstream gene of NFAT5 [279], is inserted at the upstream of firefly luciferase coding region, and thus the expression of firefly luciferase is regulated by NFAT5 activity [342]. We cotransfected pGL-TonE-luciferase, pRL and plasmids expressing full-length (FL) NFAT5 or p70-NFAT5 into HeLa cells. At 48 h pt, the cell lysates were used for luciferase assay on a Tecan GENios fluorescence reader to determine the relative luciferase activity (Firefly/Renilla) by using the Dual-Luciferase® Reporter Assay System (Promega) as per the manufacturer's instructions. Each treatment was verified by three biological repeats.

3.3.5 Chemical inhibitor treatment

Cells were serum starved overnight and treated with caspase-3 inhibitor Z-VAD in DMSO (Cedarlane Labs) (25 μM), proteasome inhibitor MG132 in DMSO (Sigma) (10 μM) or equal volume of DMSO (0.1% in culture medium) (Sigma) starting from 30 min prior to infection. For iNOS inhibitor 1400W, the cell culture medium was replaced with serum-free medium containing 1 mM of 1400W or equal volume of ultrapure water (0.1% in culture medium) (Thermo Fisher) 24 h prior to infection. Cells were then infected with CVB3 at 10 MOI for 1 h. After infection, cells were washed with PBS and replenished with serum-free medium with Z-VAD, MG132 or 1400W.

For hypertonic reagent treatment on HeLa cells, sodium chloride (100 mM) and mannitol (100 – 200 mM) were dissolved directly in DMEM medium without FBS to generate hypertonic mediums. The cell culture medium was replaced with the hypertonic mediums 2 h prior to infection. Then the cells were infected with CVB3 diluted in the hypertonic mediums.

3.3.6 HSS treatment on mice

Male A/J mice (4-week old) were purchased from Jackson Laboratory. Animal experiment protocol was approved by the Animal Care Committee of Faculty of Medicine, University of British Columbia. Mice were infected by IP injection with 10^5 pfu of CVB3 or sham-infected with PBS. During the infection period, the mice were treated by IP injection with 0.9%, 5% or 7.5% NaCl solution in a dose of 10 mL/kg daily. Heart tissues were collected at day 6 pi after euthanasia in CO2, fixed in 10% buffered formalin, embedded in paraffin and subjected to H&E staining as described in Chapter 2.

3.3.7 MTS cell viability assay

Cell morphology was observed and photographed at room temperature under a phase contrast microscope (TMS-F, Nikon) connected with a camera (Coolpix 8400, Nikon). Cell viability was further quantified by using a 3-(4-5-dimethylthiazol-2-yl)-5-(-3-carboxymethoxyphenyl)-2H-tetrazolium salt (MTS) assay kit following the manufacturer's instructions (Promega). Briefly, cells were incubated with MTS solution for 2 h. Absorbency of formazan was measured at 492 nm using enzyme-linked immunosorbent assay (ELISA) plate reader. The results were normalized to sham-infected control which was set as a viability of 100%.

3.4 Results

3.4.1 CVB3 infection decreases NFAT5 in protein level but not mRNA level

We first detected the change of NFAT5 in SV40 human cardiomyocytes. SV40 cardiomyocytes were infected with CVB3 at a MOI of 20 or sham-infected with PBS and then the cells were subjected to protein and RNA extraction at 8 or 10 h pi. western blot analyses using antibodies against VP1 (CVB3 capsid protein) and NFAT5 were conducted to detect CVB3 infection and CVB3-induced NFAT5 protein reduction, respectively. **Figure 3.1A** shows that NFAT5 protein was highly expressed in sham-infected cardiomyocytes but disappeared at 8 h pi; however, the mRNA levels detected by qPCR using NFAT5-specific primers remained unchanged (**Figure 3.1B**). Similar results were observed in HeLa cells infected with CVB3 at 10 MOI, which showed a dramatic decrease of NFAT5 protein beginning at 4 h and disappeared at 5 h pi (**Figure 3.1C**), but qPCR showed no significant change of NFAT5 mRNA (**Figure 3.1D**). To test whether such change of NFAT5 occurred *in vivo*, we infected 4-week-old A/J mice with 10^5 pfu of CVB3 for six days and found that NFAT5 protein was decreased in the heart, a major susceptible organ to CVB3 (**Figure 3.1E**). All these results indicate that CVB3 infection mainly affects NFAT5 at protein level.

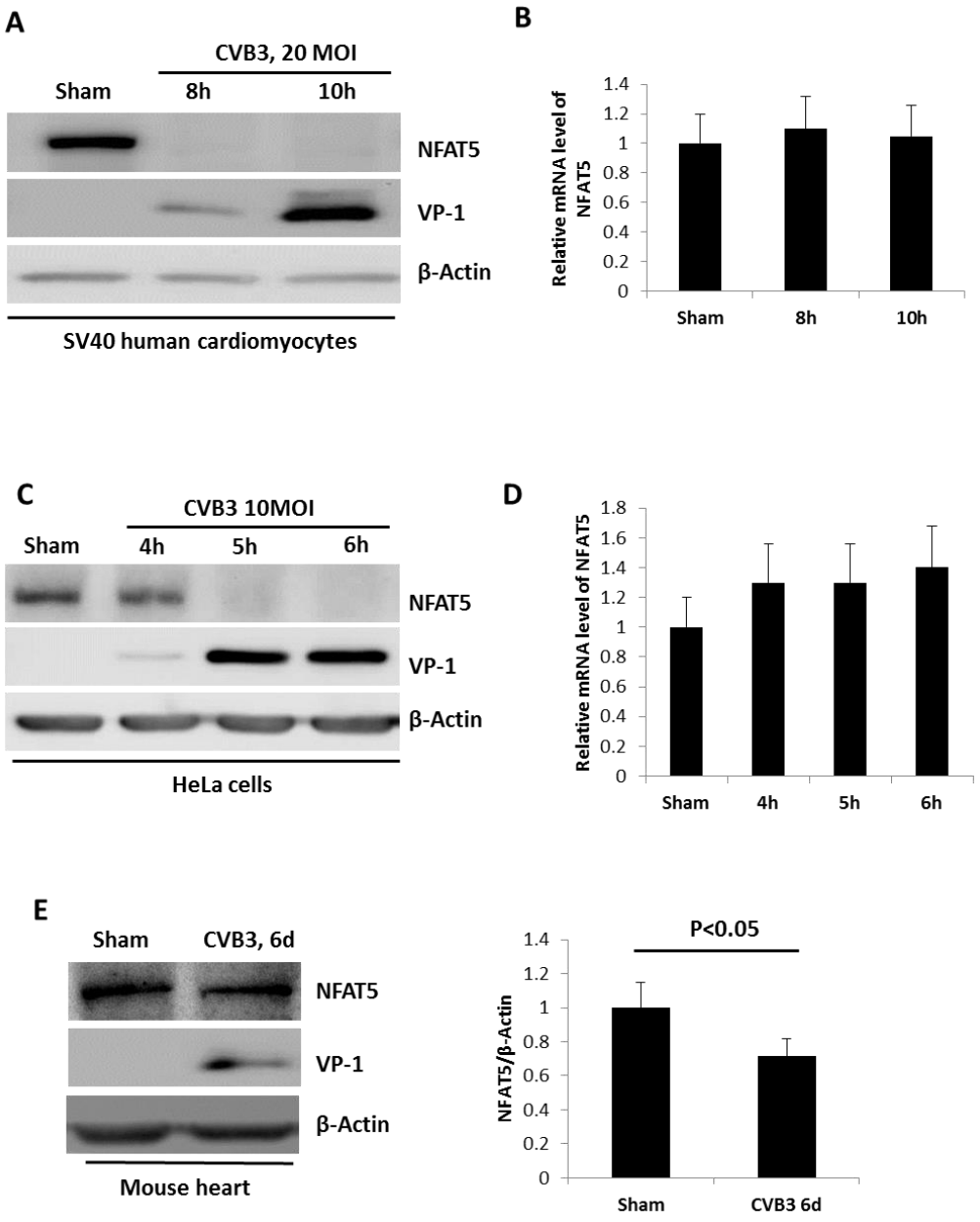

Figure 3.1. CVB3 infection reduces NFAT5 protein but not mRNA. SV40 human cardiomyocytes and HeLa cells were infected with CVB3 at 10 MOI or 20 MOI, respectively or sham-infected with PBS and harvested at indicated time points pi. Cellular proteins and RNAs were extracted for western blot analysis of NFAT5 protein **(A, C)** and qPCR measurement of NFAT5 mRNA **(B, D)**, respectively. **(E)** 4-week-old A/J mice were infected with CVB3 at 10^5 pfu (plaque forming unit) or sham-infected with PBS. At 6 days pi, the mice were sacrificed and the heart tissue was homogenized for western blot analysis of NFAT5 protein. β-actin was used as a loading control. Quantitation of NFAT5 protein was conducted by densitometry analysis using the NIH ImageJ program (right panel).

3.4.2 NFAT5 is cleaved by CVB3 proteases 2A and 3C

CVB3 infection promotes ubiquitin/proteasome-mediated protein degradation and induces caspase-3 activation [344, 345]. Since no change of NFAT5 mRNA was observed in CVB3 infection, we speculated that the decrease of NFAT5 protein might be due to proteasome-mediated degradation or caspase-3-mediated cleavage. To verify this hypothesis, we used 10 μM MG-132, a proteasome inhibitor, and 50 μM z-VAD-fmk, a pan-caspase inhibitor, to treat CVB3-infected HeLa cells. To our surprise, neither MG-132 nor z-VAD-fmk was capable of blocking the decrease of NFAT5 protein (**Figure 3.2A and B**). These results indicate that NFAT5 decrease is not resulted from proteasome-mediated degradation or caspase-3-mediated cleavage.

Then we hypothesized that NFAT5 was probably cleaved by CVB3 proteases 2A and/or 3C. To verify this hypothesis, we first detected the cleavage products of NFAT5 by western blot analysis using an N-terminal antibody of NFAT5 and observed a ~70 kDa band appearing at 4 h pi, coinciding with the reduction of 170 kDa FL NFAT5 (**Figure 3.2C**). However, a non-specific band at ~70 kDa also appeared in sham-infected control (**Figure 3.2C, lane 1**). To confirm this cleavage, we constructed and transfected pEGFP-myc-NFAT5, a plasmid expressing NFAT5 tagged with a 6*myc peptide at its N-terminus, into HeLa cells infected with CVB3. By immunoblotting using an anti-myc antibody, we observed a ~76 kDa band at 4 h pi (**Figure 3.2D**), suggesting that the 70 kDa band is truly the N-terminal cleavage product of NFAT5 (p70-NFAT5) since the total MW of six myc tags is ~6 kDa. Then we continued to determine which viral protease cleaved NFAT5 during CVB3 infection. For this aim, we transfected HeLa cells expressing myc-NFAT5 with plasmid pIRES-2A or pIRES-3C, which expresses 2A or 3C, respectively. At 36 h pt, by immunoblotting using a myc antibody, we observed that FL myc-NFAT5 decreased in both 2A- and 3C-transfected cells, but myc-p70-NFAT5 appeared only in

2A-transfected cells, which is similar to that in CVB3-infected cells; while 3C-transfected cells showed two weak bands of ~120 kDa and ~150 kDa (**Figure 3.2E**). These results demonstrate that both 2A and 3C cleave NFAT5 but only 2A cleavage produces the p70-NFAT5 fragment.

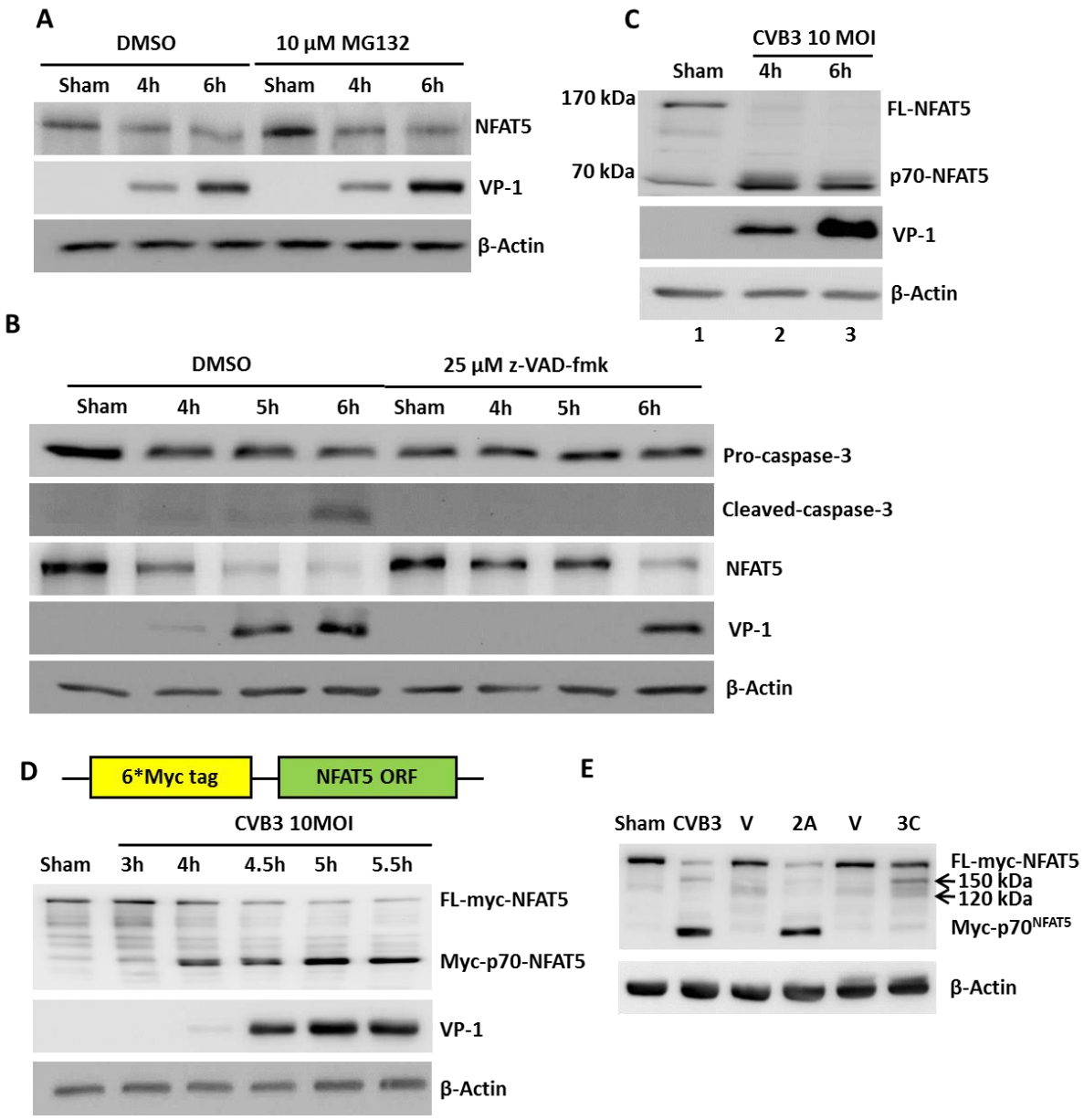

Figure 3.2. NFAT5 is cleaved by viral proteases 2A and 3C. HeLa cells were treated with 10 μmol/L MG132 **(A)** or 25 μmol/L z-VAD-fmk **(B)** and then infected with CVB3 at 10 MOI. At indicated time points pi, the cellular proteins were subjected to western blot analysis of NFAT5 and other proteins using the indicated antibodies. β-actin was used as a loading control. **(C)** HeLa cells were infected by CVB3 at 10 MOI for 4 and 6 h and then subjected to western blot analysis using an antibody against the N-terminal epitope of NFAT5. **(D)** HeLa cells transfected with a plasmid expressing the 6*myc-NFAT5 fusion protein (upper panel) were infected with CVB3 or sham-infected as described above and subjected to western blot analysis using an antibody against myc tag (lower panel). **(E)** HeLa cells expressing myc-NFAT5 were transfected with pIRES-2A (2A), pIRES-3C (3C) or vector only (V). At 48 h post transfection (pt), the cells were subjected to western blot analysis using an antibody against myc tag. The cells infected with CVB3 or sham-infected with PBS were used as controls. Arrows indicate the 3C cleavage bands.

3.4.3 CVB3 protease 2A cleaves NFAT5 at G503

According to the structure domains of NFAT5 protein, p70-NFAT5 covers one third of all amino acids (aa) of the whole protein, which contains five of the seven functional domains of NFAT5 (**Figure 1.7**). Interestingly, the aa 175 – 471 within the N-terminal fragment of NFAT5 has been proven to function as a dominant negative mutant of NFAT5 [267, 346], implying the potential influence of p70-NFAT5 on NFAT5 activity. Therefore, we focused our study on p70-NFAT5, the 2A cleavage product of NFAT5. To locate the exact cleavage site of 2A on NFAT5, we utilized the program NetPicoRNA 1.0 [347] to analyze the whole aa sequence of NFAT5 and predicted the peptide bond just before G503 as the top candidate locus of 2A cleavage (**Figure 3.3A**). The aa sequence around G503 is similar to the reported recognition motifs of CVB3 2A protease [348], which are conserved among different species (**Figure 3.3B**), indicating a high possibility of G503 as the 2A cleavage site. To verify the prediction, we mutated G503 of myc-NFAT5 to alanine (A) and constructed the expressing plasmid pEGFP-myc-NFAT5^{G503A}. Meanwhile, we made another mutant plasmid pEGFP-myc-NFAT5^{G650A} as a control. We transfected the two mutants as well as wild-type (WT) NFAT5 into HeLa cells separately, and then infected with CVB3. Immunoblotting using an anti-myc antibody showed no band of myc-p70-NFAT5 in NFAT5^{G503A}-transfected cells, and instead, it showed a similar 3C cleavage pattern on WT NFAT5 (**Figure 3.3C, arrows**) as seen in **Figure 3.2E**, indicating that upon G503 mutation, 2A can no longer cleave NFAT5. As for NFAT5^{G650A} control, we observed the same myc-p70-NFAT5 band as seen in WT NFAT5 cells (**Figure 3.3C**), suggesting that the mutagenesis procedure did not bring any influence on NFAT5 cleavage. This result was further confirmed by 2A plasmid transfection, which showed no cleavage of FL-myc- NFAT5^{G503A} upon

2A expression (**Figure 3.3D**). These data suggest that G503 is the only cleavage site of CVB3 protease 2A on NFAT5.

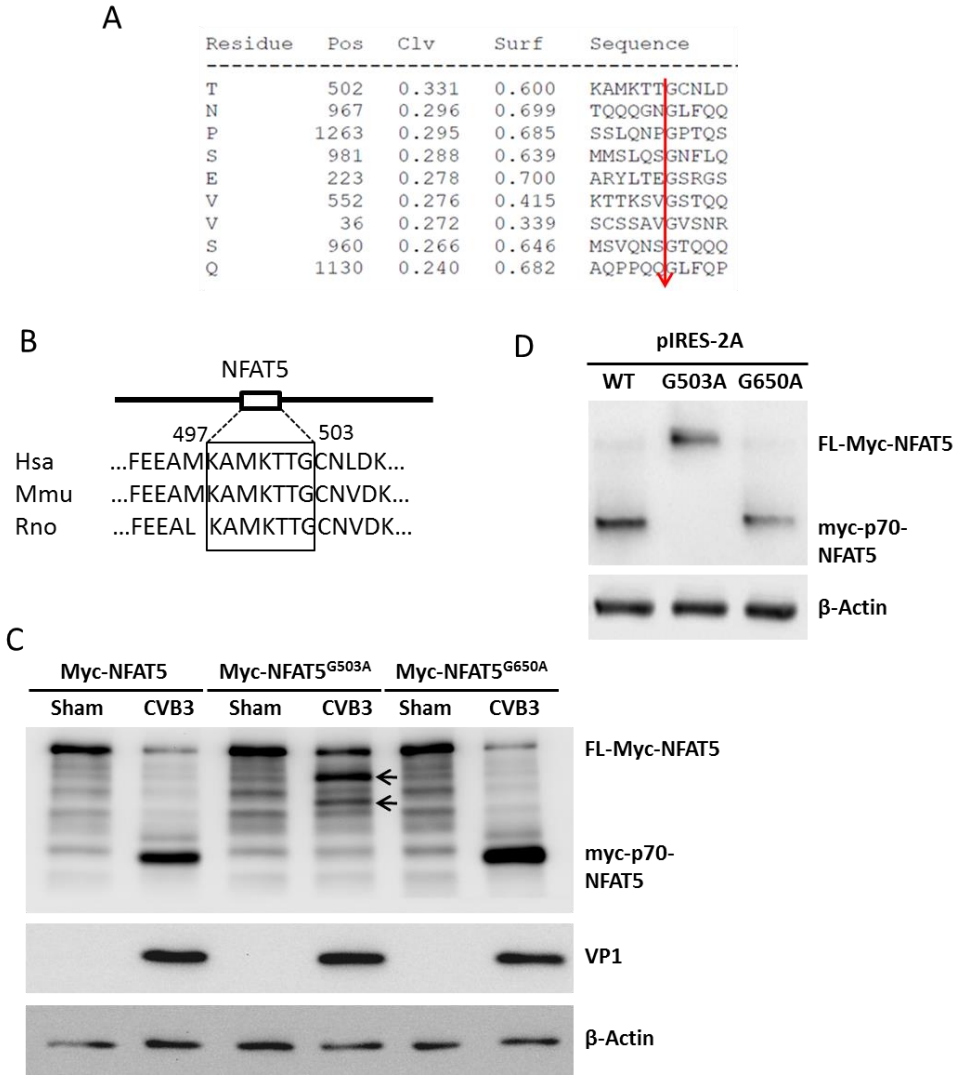

Figure 3.3. NFAT5 is cleaved by viral protease 2A at G503. (A) The potential 2A cleavage sites predicted by using the NetPicoRNA 1.0 program showing the cleavage position (Pos), cleavage score (Clv) and surface score (Surf). The arrow indicates the exact cleavage loci. **(B)** Alignment of the sequences around G503 of NFAT5 from different species. **(C)** HeLa cells were transfected with a plasmid expressing myc-NFAT5, myc-NFAT5^{G503A} or myc-NFAT5^{G650A} and then infected with CVB3 at 10 MOI for 6 h. Then the cell lysates were subjected to western blot analysis using an anti-myc antibody. Arrows indicate the 3C cleavage bands. **(D)** HeLa cells were co-transfected with pIRES-2A and a plasmid expressing WT or mutant NFAT5 as described above in (B). At 48 h pt, the cell lysates were subjected to western blot analysis using an anti-myc antibody.

3.4.4 NFAT5 inhibits CVB3 replication

Having confirmed the cleavage of NFAT5 by CVB3 protease, our next focus was to study the effect of NFAT5 and NFAT5 cleavage on CVB3 replication. Firstly, we knocked down NFAT5 expression using specific siRNAs in HeLa cells and then infected the cells with CVB3. At 4 and 6 h pi, we detected VP1 to evaluate the viral replication in the cells. The immunoblotting results showed a 15-fold increase of VP1 in NFAT5-knockdown cells compared to control cells treated with scrambled siRNAs at 4 h pi. At 6 h pi, there was a 20% but still statistically significant increase of VP1 level when NFAT5 was knocked down (**Figure 3.4A**). These results imply a potential anti-CVB3 activity of NFAT5. To further verify this speculation, we detected the VP1 in CVB3-infected cells overexpressing WT NFAT5, and observed a >50% decrease of VP1 in NFAT5-overexpressed cells compared to vector-transfected control cells (**Figure 3.4B, lane-2 & -3 vs. lane-5 & -6)**. More interestingly, in the cells overexpressing the non-cleavable NFAT5^{G503A}, the VP1 was decreased even more by ~80% compared to vector-transfected control cells (**Figure 3.4B, lane-2 & -3 vs. lane-8 & -9**). This result can be explained by the speculation that FL NFAT5 plays a role in suppression of CVB3 replication and cleavage product p70-NFAT5 may play a dominant negative effect on NFAT5's activity. To verify this conjecture, we constructed a FLAG-tagged p70-NFAT5 plasmid and overexpressed p70-NFAT5 in HeLa cells infected with CVB3. As expected, a ~4-fold increase of VP1 was observed in p70-NFAT5-overexpressed cells compared to vector only control (**Figure 3.4C**). In addition to VP1 level, we also detected the changes of CVB3 RNA and viral progeny release when FL NFAT5 or p70-NFAT5 was overexpressed. The qPCR results using primers flanking the coding region of CVB3 2A showed that NFAT5 decreased viral RNA level while p70-NFAT5 increased it (**Figure 3.4D**), which correlated well with the levels of VP1 showing in **Figure 3.4C**. For viral particle

formation, plaque assay showed that FL NFAT5 significantly decreased the viral particle release in the extracellular medium, but p70-NFAT5 reversed this decrease almost to the vector control level (**Figure 3.4E**). All together, these results suggest that FL NFAT5 inhibits viral replication and the N-terminal cleavage product p70-NFAT5 is capable of reversing such inhibition.

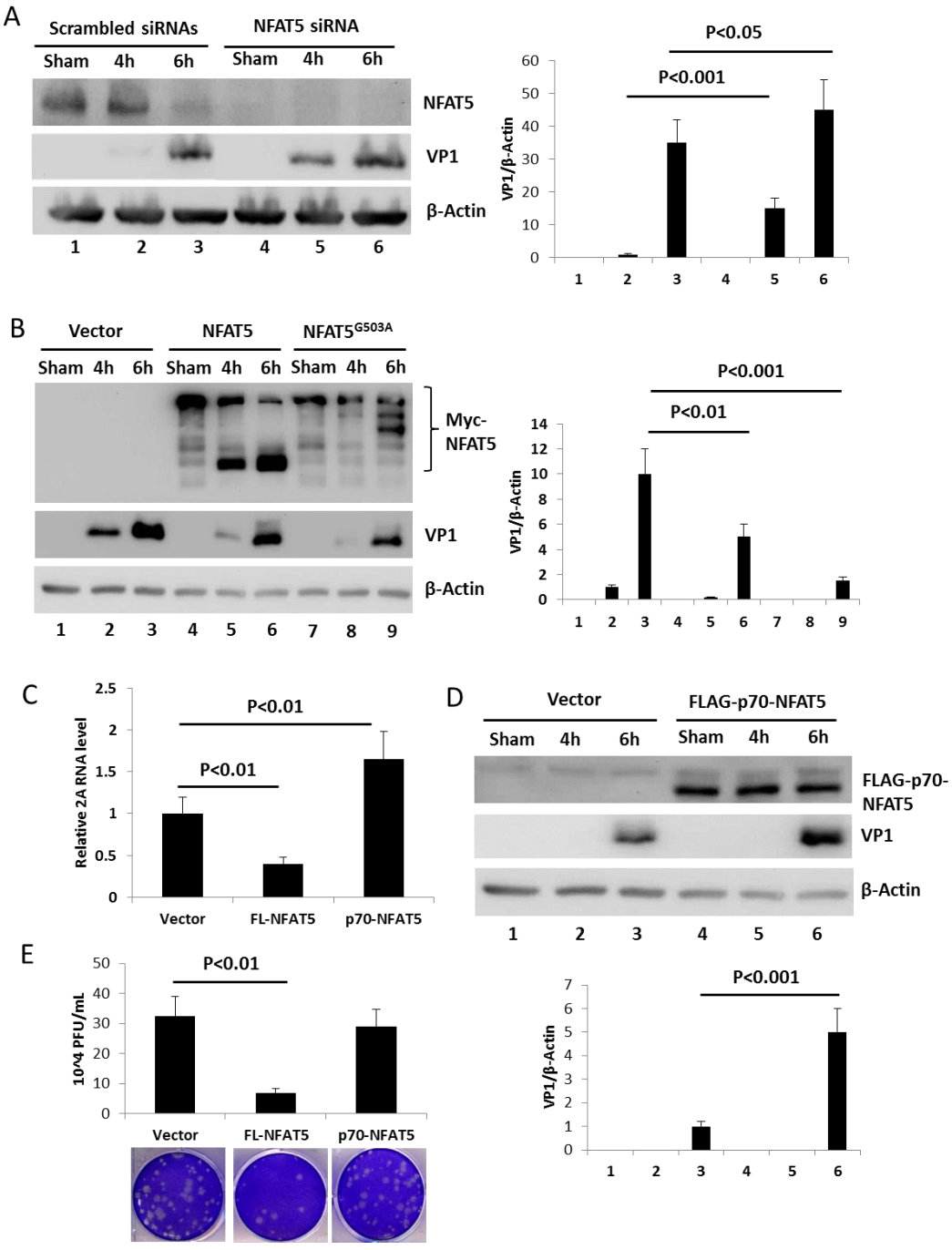

Figure 3.4. NFAT5 inhibits CVB3 replication while the N-terminal cleavage product p70-NFAT5 promotes CVB3 replication. (A) HeLa cells were transfected with NFAT5 siRNAs or scrambled control siRNAs and then infected with CVB3. At 4 and 6 h pi, the cell lysates were subjected to western blot analysis of VP1. Quantitation of VP1 was conducted by densitometry scan using the NIH ImageJ program and normalized against β-actin control (right panel). **(B)** HeLa cells were transfected with plasmids expressing WT myc-NFAT5 or myc-NFAT5^{G503A}, infected with CVB3 and then harvested for VP1 detection and quantification as described above (right panel). **(C)** HeLa cells were transfected with plasmids expressing p70-NFAT5 tagged with FLAG and then infected with CVB3 for VP1 detection and quantification (right panel) as described above. **(D, E)** HeLa cells were transfected with plasmids expressing FL-NFAT5 or p70-NFAT5 and then infected with CVB3. At 6 h pi, the cellular RNAs were extracted for qPCR measurement of CVB3 genomic RNA level **(D)** and the medium was collected for plaque assay to measure viral progeny release **(E)**.

3.4.5 The 2A cleavage product p70-NFAT5 shows dominant negative effect on NFAT5

It has been reported that the N-terminal DNA-binding domain (aa 175 – 471) of NFAT5 (NFAT5 DBD) has a dominant negative effect on NFAT5 activity [26]. In this study, we first showed that the N-terminal cleavage product p70-NFAT5 emerges a positive effect on CVB3 replication to counteract the FL NFAT5 activity. Therefore, we speculated that p70-NFAT5 could be a dominant negative mutant of NFAT5. To verify this, we first determined the effect of p70-NFAT5 on the nuclear translocation of endogenous NFAT5, a key step of NFAT5 activation [349]. As shown in **Figure 3.5A**, in cells transfected with pEGFP-myc-NFAT5, we observed a translocation of myc-NFAT5 from the cytoplasm to the nucleus, however when p70-NFAT5 was overexpressed via pcDNA3.1(-)-p70-NFAT5 transfection, such redistribution of myc-NFAT5 was significantly decreased. To further confirm the change of NFAT5 activity upon p70-NFAT5 overexpression, we cotransfected pGL-TonE-luciferase or pRL and plasmids expressing FL NFAT5, p70-NFAT5 or NFAT5 DBD into HeLa cells and then performed luciferase assay. We found that FL NFAT5 enhanced luciferase expression more than 100% while p70-NFAT5 reduced it by ~25% and such dominant negative effect of p70-NFAT5 was quite similar to that of

NFAT5 DBD (**Figure 3.5B**). To further confirm the NFAT5 activity on its downstream genes upon p70-NFAT5 overexpression with or without CVB3 infection, we detected the mRNA levels of taurine transporter (TauT) [280] and sodium/myo-inositol transporter (SMIT), two genes directly regulated by NFAT5 [281, 282]. In sham-infected cells, we observed ~60% increase of TauT mRNA when FL NFAT5 overexpressed and a ~40% decrease when p70-NFAT5 overexpressed (**Figure 3.5C**). As for SMIT mRNA, we observed a ~40% increase and a ~20% decrease when FL NFAT5 and p70-NFAT5 were overexpressed, respectively (**Figure 3.5D**). In CVB3-infected cells, we also observed the same trend of the altered mRNA expression but the rate of the differential expression is much smaller than those in sham-infected cells (**Figure 3.5C, D**), probably due to the generation of p70-NFAT5 by 2A cleavage during infection. These results suggest the dominant negative effect of p70-NFAT5 on NFAT5 in both sham-infected and CVB3-infected cells.

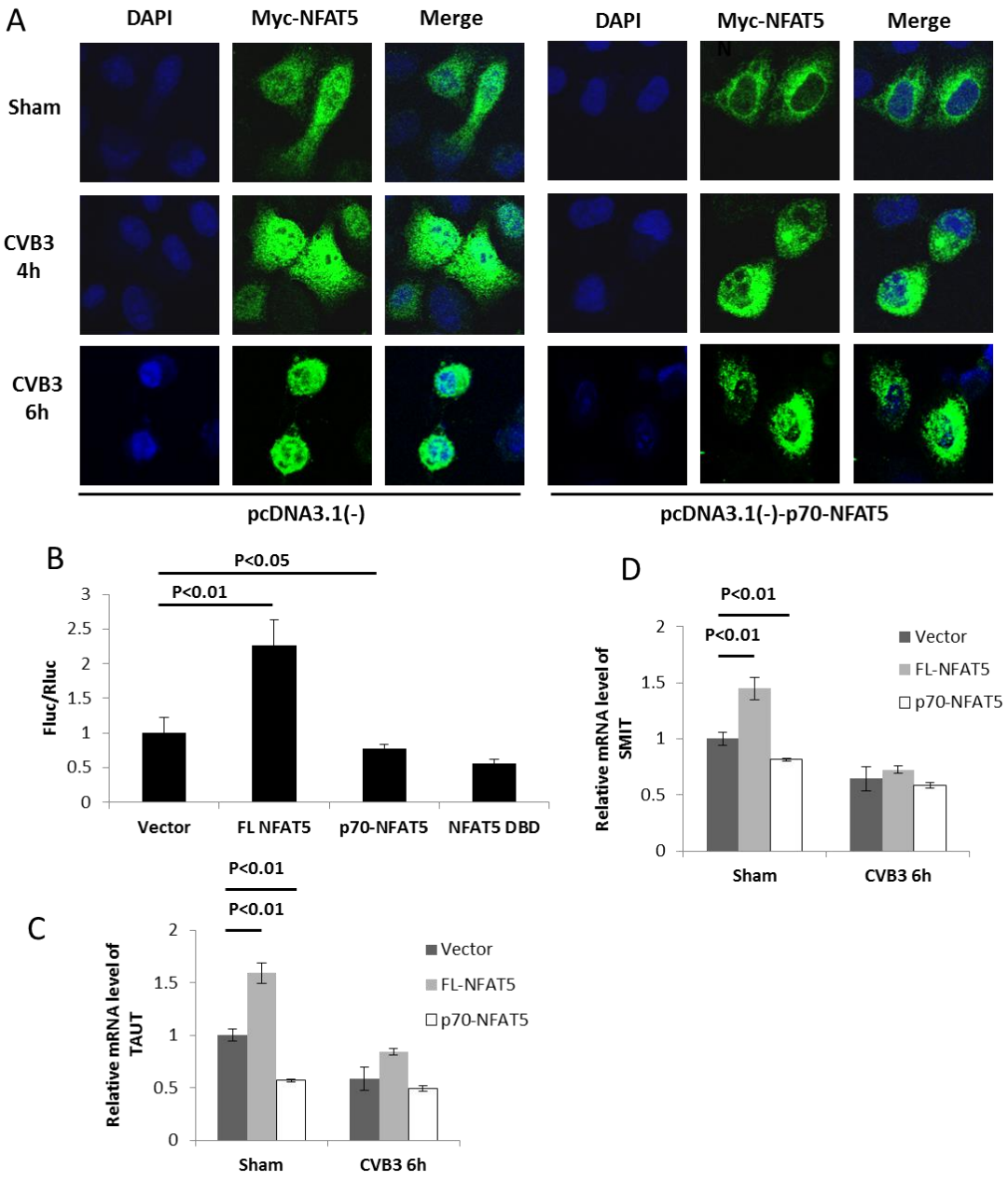

Figure 3.5. p70-NFAT5 acts as a dominant negative fragment of NFAT5. (A) HeLa cells were co-transfected with pEGFP-myc-NFAT5 and pcDNA3.1(-)-p70-NFAT5 or pcDNA3.1(-) empty vector. Then the cells were infected with CVB3. At 4 and 6 h pi, the cells were fixed and immunostained using a specific antibody against NFAT5 and observed by confocal microscopy. **(B)** HeLa cells were co-transfected the luciferase reporter constructs pGL-TonE-luciferase or pRL with the plasmids expressing FL NFAT5, p70-NFAT5, NFAT5 DBD or pEGFP empty vector. At 48 h pt, the cell lysates were subjected to dual luciferase assay. The relative activity (FLu/RLu) was determined after normalized against the vector control. **(C, D)** HeLa cells were transfected with plasmids expressing FL NFAT5 or p70-NFAT5 and then infected with CVB3. At 6 h pi, the cellular RNAs were extracted for qPCR measurement of mRNA level of TauT **(C)** and SMIT **(D)**. Vector-transfected cells were used as a control.

3.4.6 NFAT5 inhibits CVB3 replication via inducing expression of iNOS

Having uncovered the anti-CVB3 activity of NFAT5, we next aimed to reveal the underlying mechanism. Considering that NFAT5 is a transcriptional factor, we speculated that the anti-CVB3 activity might be attributed to the downstream genes regulated by NFAT5. Among these downstream genes of NFAT5, molecular chaperones, such as Hsp70, and NFκB are reported to be related to CVB3 infection [350, 351], but our results showed no significant changes ($p>0.05$) in Hsp70-2 expression and NFκB activity (indicated by iκB expression) upon expression of FL NFAT5 or p70-NFAT5 in either sham-infected or CVB3-infected cells (**Figure 3.6A, B**). Nevertheless, the qPCR detection of mRNA level of iNOS showed a ~40% increase upon FL NFAT5 overexpression and a ~50% decrease when p70-NFAT5 overexpressed in both sham- and CVB3-infected cells (**Figure 3.6C**). It has been reported that nitric oxide generated by iNOS exerts anti-CVB3 activity probably due to inhibition of viral proteases [307, 352]. Therefore, we speculated that NFAT5 inhibits CVB3 replication via inducing the expression of iNOS. To verify this speculation, we treated the NFAT5-overexpressing cells with 4 mM 1400W, a specific inhibitor of iNOS [353], and found that 1400W could counteract the effect of NFAT5 overexpression and restore the VP1 to a level even more than the control (**Figure 3.6D, lane-9 vs. -7**). These data indicate that iNOS induction is essential for the anti-CVB3 effect of NFAT5.

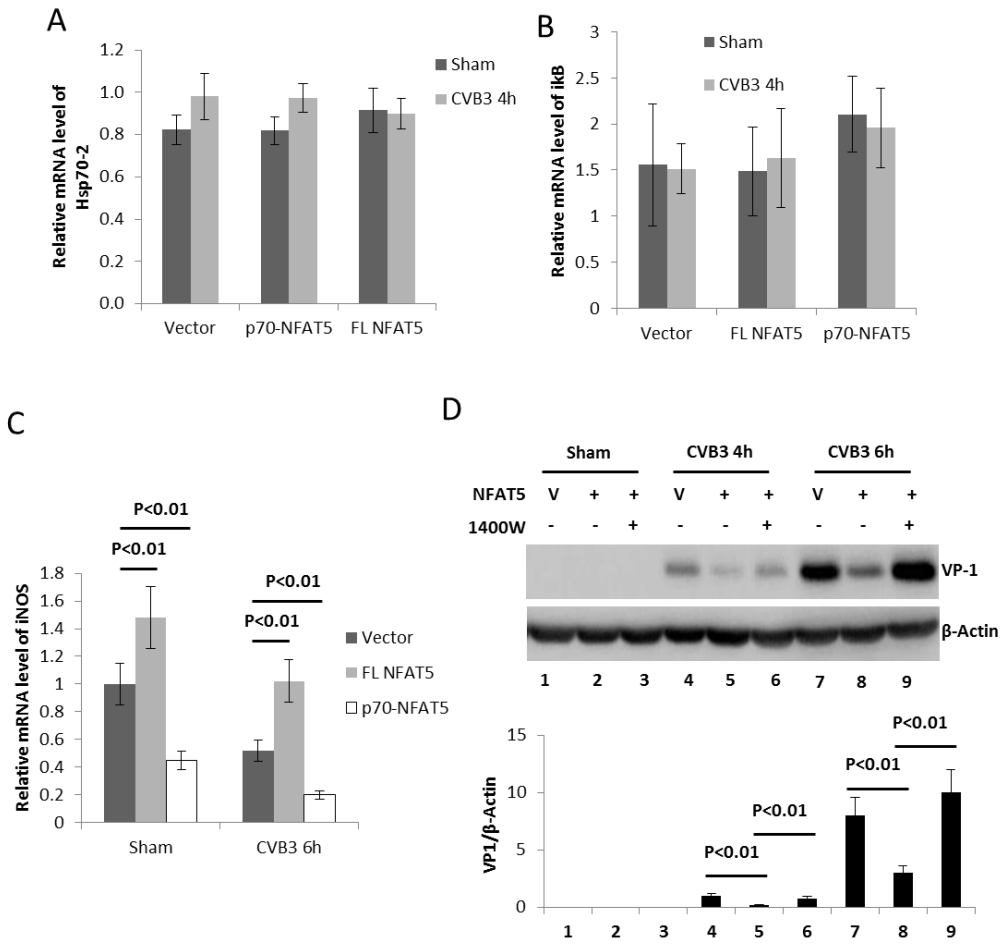

Figure 3.6. iNOS is essential for the anti-CVB3 effect of NFAT5. HeLa cells were transfected with plasmids expressing FL NFAT5 or p70-NFAT5 and then infected with CVB3. At 6 h pi, the cellular RNAs were extracted for qPCR measurement of mRNA level of Hsp70-2 **(A)**, iκB **(B)** and iNOS **(C)**. **(D)** HeLa cells transfected with pEGFP empty vector (V) or pEGFP-myc-NFAT5 were treated with 4 mmol/L 1400W or DMSO control and then infected with CVB3 for VP1 detection and quantification (lower panel) as described in Fig. 4A.

3.4.7 Hypertonic treatment inhibits viral replication and promotes cell survival in CVB3 infection

The above experiments showed that high level of NFAT5 is capable of inhibiting CVB3 replication. As a hypertonic responsive protein, NFAT5 can be induced by hypertonic stimulation, such as high concentration of NaCl, which may exert anti-CVB3 effect. We firstly tested the effect of hypertonic NaCl solution on CVB3 replication. At 24 h before infection, we replaced the cell medium with DMEM containing 100 mM excess NaCl, a concentration reported to be high enough to induce NFAT5 expression but not cytotoxic [177], and then infected the HeLa cells with CVB3. Such treatment resulted in an increase of NFAT5 expression (**Figure 3.7A, lane-1 vs. -4**). At 4 and 6 h pi, a dramatic decrease of VP1 was observed in cells treated by HSS compared to the mock-treated control (**Figure 3.7A, lanes 2-3 vs. lane 5-6**), suggesting that CVB3 replication was impaired by HSS treatment. To clarify whether such inhibition required NFAT5 or not, we added 25 μM rottlerin, an NFAT5 inhibitor[267], to the hypertonic medium, and observed that rottlerin decreased NFAT5 expression level and increased the VP1 level in HSS treatment (**Figure 3.7A, lanes 5-6 vs. lanes 8-9**), indicating an essential role of NFAT5 in HSS-mediated inhibition of CVB3. The anti-CVB3 effect of HSS was further verified by cell viability assay. By using either cell morphological images (**Figure 3.7B**) or MTS cell viability assay (**Figure 3.7C**), we observed a significant increase in cell viability by ~30% at 6 h pi compared to the mock-treatment control. Considering Na^+ and Cl^- ions can pass the cell membrane via facilitated diffusion [354] which may exert some unexpected effects on some signaling pathways other than NFAT5, we employed mannitol, a non-permeable hyperosmotic agent[355], to repeat the experiments. By using different concentrations (0, 100 and 200 mM) of mannitol, we found that NFAT5 was increased and VP1 was decreased in a mannitol concentration-dependent manner

and that the alterations of NFAT5 and VP1 expression were more significant than that in HSS treatment (**Figure 3.8A**). Furthermore, similar to HSS, hypertonic treatment with mannitol solutions of 100 or 200 mM also elevated the cell viability in CVB3 infection (**Figure 3.8B and C**). Altogether, our results suggest that hypertonic conditions inhibit CVB3 replication via NFAT5 induction.

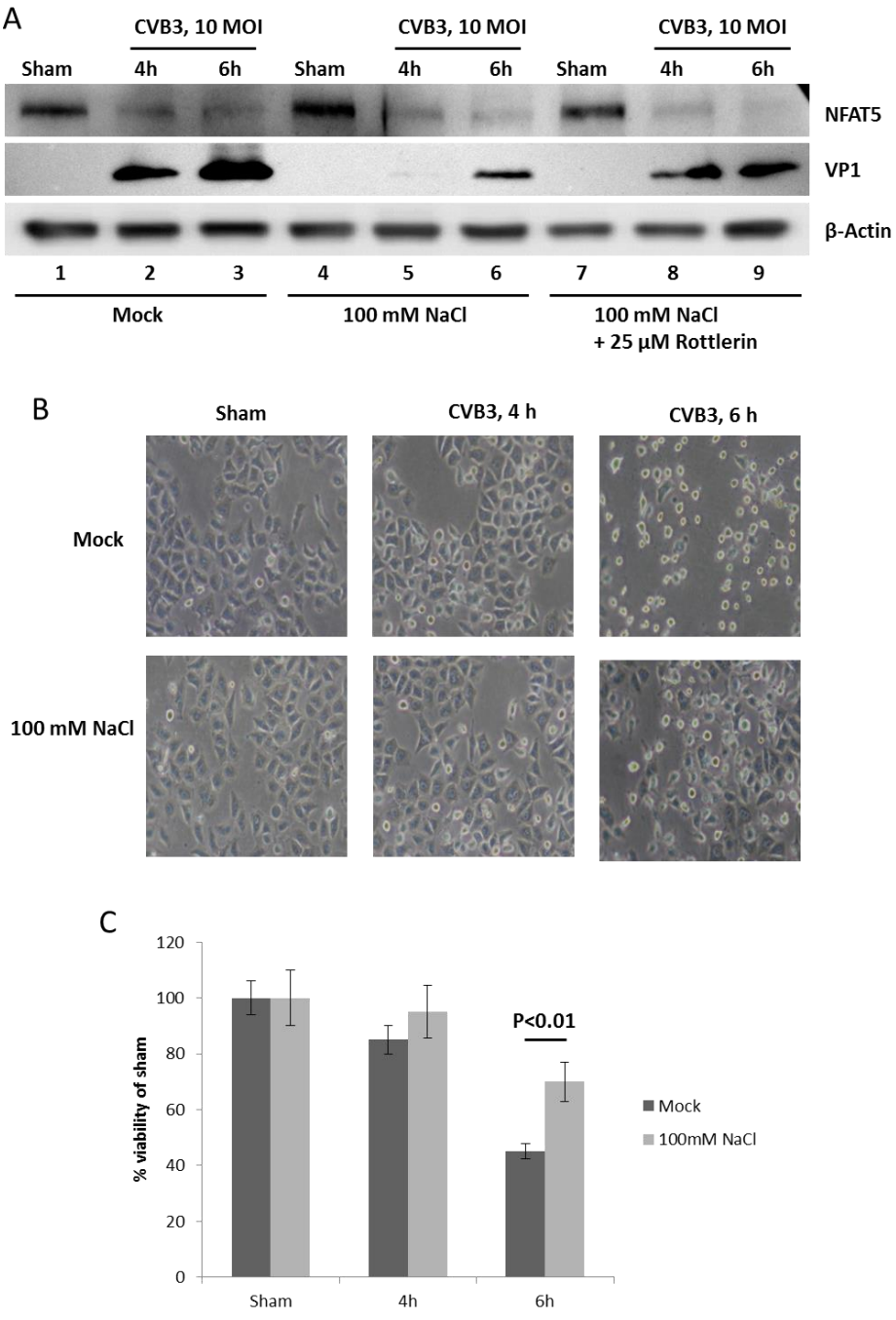

Figure 3.7. Hypertonic NaCl solution inhibits CVB3 replication and promote cell survival during CVB3 infection. HeLa cells were pre-treated with excess 100 mM NaCl or excess 100 mM NaCl + 25 μmol/L rottlerin for 4 h and then infected with CVB3. At 4 and 6 h pi, the cells were subjected to VP1 detection **(A)**, Phase contrast morphological imaging **(B)** and MTS cell viability assay **(C)**. Cell viability was determined by converting to the percentage of cell survival of the sham-treatment control, which was set as 100%.

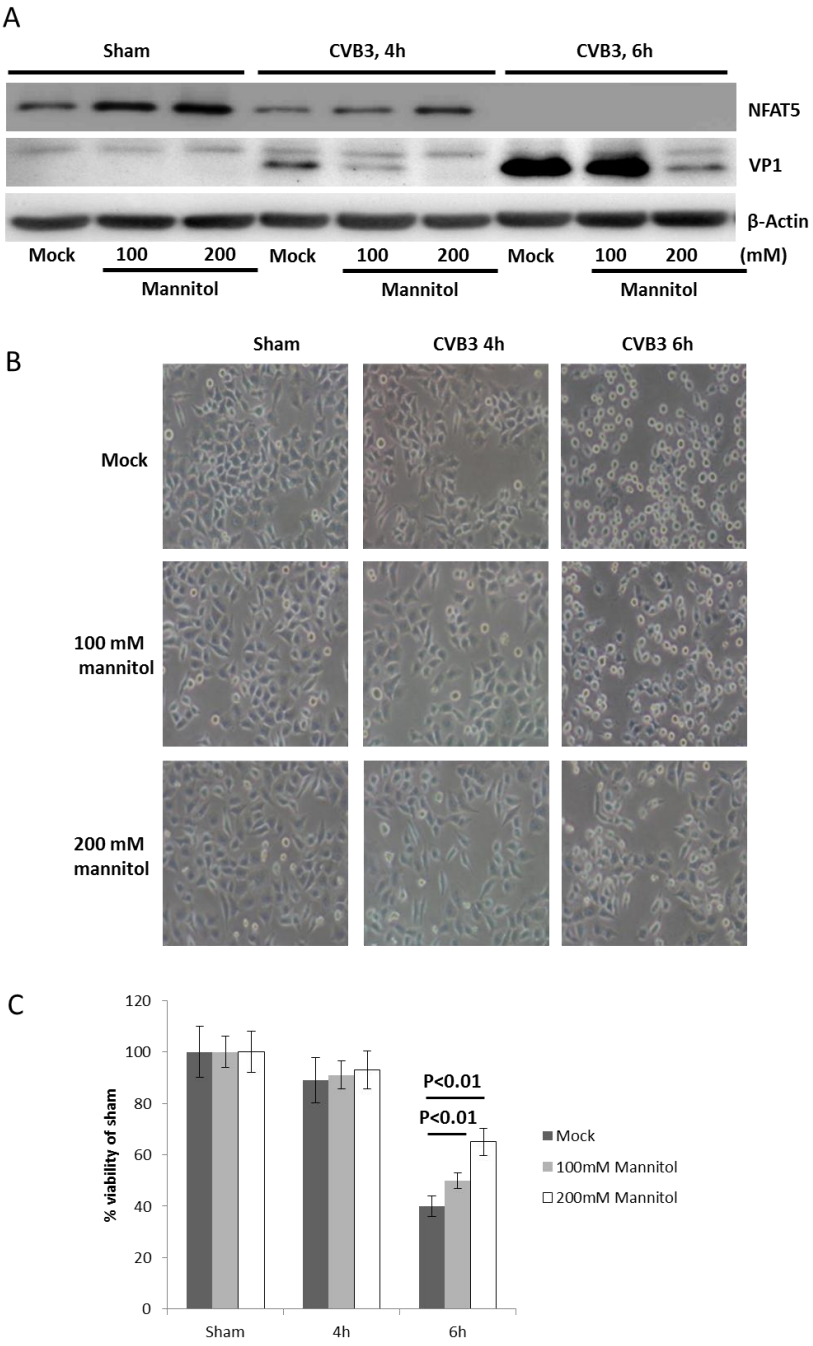

Figure 3.8. Hypertonic mannitol solutions inhibit CVB3 replication and promote cell survival during CVB3 infection. HeLa cells were treated with 100 mM or 200 mM mannitol solution after CVB3 infection or sham-infection. At 4 and 6 h pi, cells were subjected to VP1 detection by western blot analysis using the indicated antibodies (A), phase contrast microscopy imaging (B) and MTS cell viability assay (C). The cell viability was determined by converting to the percentage of cell survival of the sham-infection control, which was set as 100%.

3.4.8 Hypertonic saline lowers cardiac viral load and relieves tissue damage in mice

To test whether the anti-CVB3 effect of HSS treatment occurs *in vivo*, 30 A/J mice were divided into three groups and IP injected with 0.9% (normal saline solution, NSS), 5% and 7.5% HSS (10 mL/kg daily) for 6 consecutive days, respectively, and then the mice were challenged with CVB3 at 10^5 pfu/each. At 6 d pi, 3 of the 10 NSS-treated mice died and all HSS-treated mice survived. The live mice with different treatments were euthanized and the heart tissue was collected for viral detection and histological analysis. By immunoblotting and viral plaque assay, we found that HSS-treated mice showed higher NFAT5 level but lower levels of both VP1 expression and viral progeny release compared to the NSS-treated control (**Figure 3.9A, B**), indicating that the viral load was reduced by HSS treatment. The H&E staining of the myocardium tissue showed less tissue damage upon 5% HSS treatment compared to that in NSS treatment (**Figure 3.9C**). Note that since the 5% and 7.5% HSS showed similar effect on alleviating tissue injury, here we only show the H&E staining for the 5% HSS treatment. These data indicate that 5% HSS is capable of relieving tissue damage during CVB3 infection by induction of NFAT5.

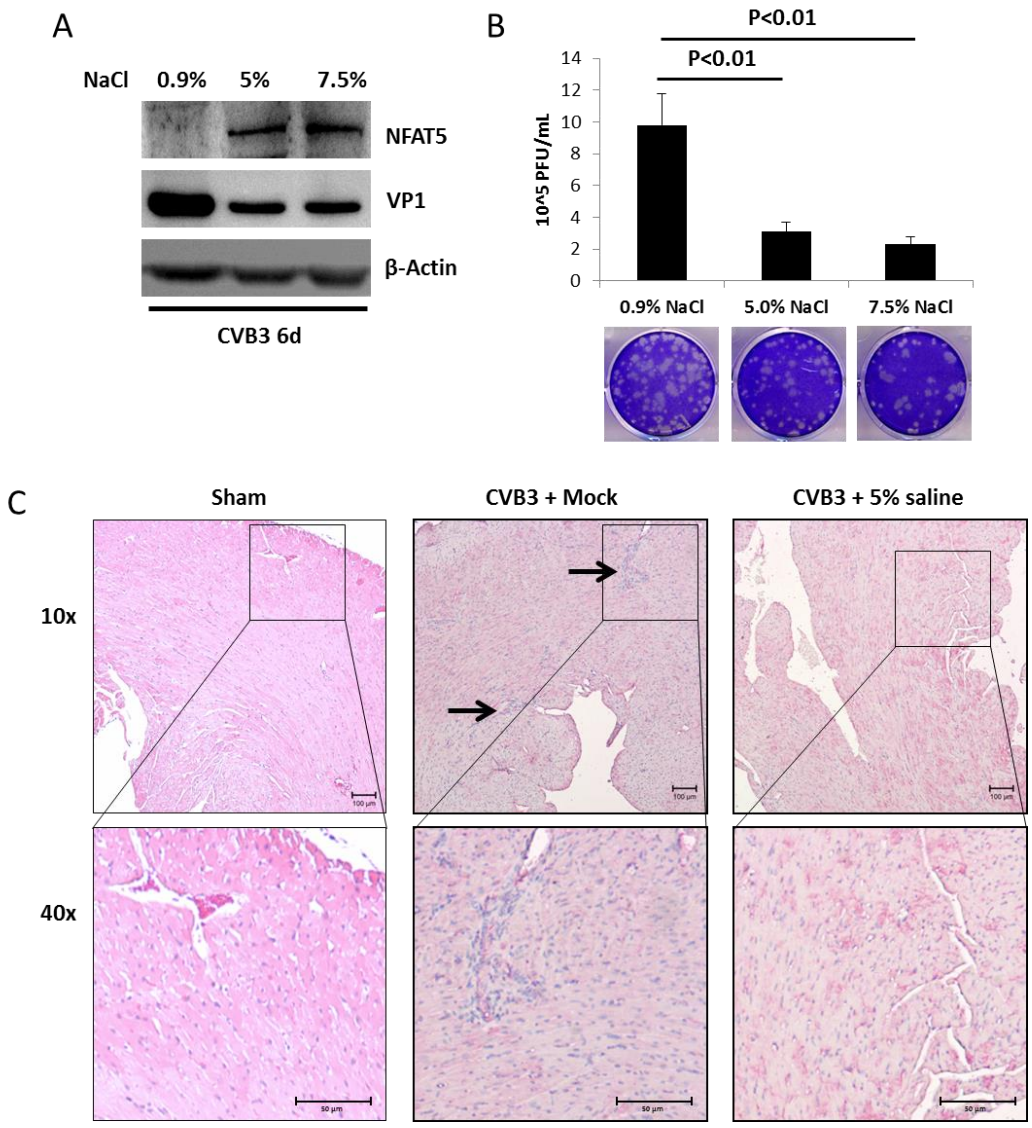

Figure 3.9. Hypertonic saline solution inhibits CVB3 replication and relieves mice heart tissue damage caused by viral infection. Four-week-old A/J mice were infected with CVB3 of 10^5 pfu. NaCl solution at 0.9%, 5% and 7.5% concentration was IP injected into the mice daily during the infection. At 6 d pi, the mice were euthanized and the heart tissues were harvested. Part of the heart tissue was homogenized for western blot analysis of VP1 **(A)** and plaque assay to determine viral particle formation **(B)**. **(C)** The remaining heart tissues from these mice were fixed, sectioned and H&E stained to evaluate the tissue damage. Sham-infected /mock-treated mice were the additional control.

3.5 Discussion

Viral protease-mediated cleavage of host proteins plays critical roles in viral replication and virus-induced tissue damage in picornavirus infections[159, 356-359]. Therefore, identifying these host proteins as potential drug targets is a rational strategy for the development of anti-picornavirus therapy. NFAT5 is a transcriptional factor activated in hypertonic stress conditions. Thus it can be modulated by changing the osmotic pressure of the extracellular fluid. However the hypertonic stress barely occurs in organs other than the kidney, thus few studies have linked NFAT5 to non-kidney diseases regardless of its ubiquitous expression in the body [298, 299], Despite the lack of direct evidence, several previous reports provided some clues on NFAT5's role associated with heart function. For instance, degradation of NFAT5 protein is a major cause of doxorubicin-induced cytotoxicity in cardiac myocytes[300]; NFAT5 is highly expressed in developing heart tissues[299] and is critical for heart development in children and young adults[360]. However, the role of NFAT5 in infectious and inflammatory heart diseases has never been delineated. Thus, in this study, we used CVB3 infection of cardiomyocyte cell line and A/J mice, a viral myocarditis model, to elucidate the role of NFAT5 in CVB3 replication and CVB3-induced myocarditis.

Firstly, we detected whether CVB3 infection would change NFAT5 level. It has been reported that NFAT5 expression is stimulated by p38 MAPK activation in hypertonic response [361]. Considering that CVB3 infection activates p38 MAPK via phosphorylation[150], we were expecting to see NFAT5 upregulation during CVB3 infection. Indeed, we observed significant increase of NFAT5 protein at early time points (~2 h pi) in HeLa cells infected with CVB3, but to our surprise, it decreased and disappeared rapidly after 4 h infection (**Fig. 3.10**). However, no NFAT5 mRNA decrease was observed during CVB3 infection, indicating that the reduction of

NFAT5 protein was not due to transcriptional arrest or mRNA degradation. Therefore, we switched our focus on the degradation and cleavage of NFAT5 protein during CVB3 infection. By MG132 and z-VAD-fmk test, we excluded the possibility of proteasome-mediated degradation and caspase-mediated cleavage of NFAT5, which are common causes of protein decrease during CVB3 infection[344, 362]. Then the most possible reason for NFAT5 reduction is the cleavage mediated by viral protease 2A and/or 3C. Using an antibody against the N-terminal of NFAT5, we observed a ~70 kDa cleavage band (p70-NFAT5) after CVB3 infection, which was further confirmed by cleavage of exogenous NFAT5 tagged with a 6*myc peptide at its N-terminus. By exogenous expression of 2A or 3C individually, we confirmed that both 2A and 3C were capable of cleaving NFAT5, but only 2A cleavage generated the 70 kDa N-terminal fragment p70-NFAT5, while 3C protease further chopped the C-terminal fragment downstream of 2A cleavage site. By bioinformatic prediction and mutagenic verification, we identified G503 as the only cleavage site of 2A on NFAT5 and such cleavage generated the p70-NFAT5. Based on this data, we further focused our studies only on p70-NFAT5 since most of the functional domains of NFAT5, including nucleus-cytoplasm localization sequence and DNA binding domain [4], are clustered in the N-terminal region, and especially, the N-terminal fragment of NFAT5 can act as a dominant negative mutant of NFAT5 [26].

We next detected the effect of NFAT5 and its cleavage product p70-NFAT5 on CVB3 replication. Our results showed that FL NFAT5 inhibited the synthesis of viral RNA and protein while p70-NFAT5 counteracted such role of NFAT5. These opposite effects of FL NFAT5 and p70-NFAT5 imply the dominant negative activity of p70-NFAT5 on FL NFAT5. This property was substantiated by i) TonE-reporter assay showing the FL NFAT5-enhanced luciferase expression and ii) qPCR detection showing the increased mRNA levels of SMIT and TAUT, two

effector genes of NFAT5. These data suggest that p70-NFAT5 has a dominant negative effect on FL NFAT5 in suppression of CVB3 replication.

The next issue we addressed was the mechansim underlying the anti-CVB3 effect of NFAT5. The direct downstream genes regulated by NFAT5 include organic osmolyte-related genes [270, 279-282], molecular chaperones [177], and iNOS [305]. The expression of transcription factor NFκB is not regulated by NFAT5, but NFAT5 modulates its transcriptional activity via binding to it [302], thus NFκB can also be considered as a downstream effector of NFAT5. Among these downstream proteins, the organic osmolyte-related genes, such as TAUT and SMIT, are mainly involved in osmotic regulation, and no antiviral effects or cardiac functions of these genes have been reported. Our previous study has shown that the chaperone protein Hsp70 promotes CVB3 replication via stabilizing the CVB3 genomic RNA [350], but in this current study, we did not observe significant change of Hsp70-2 expression, an Hsp70 family gene regulated by NFAT5[177], upon NFAT5 overexpression. Similar to Hsp70-2 expression, no significant change of NFκB activity was observed when NFAT5 was overexpressed although NFκB was reported to be activated during CVB3 infection [304]. However, iNOS expression was upregulated by the overexpression of FL NFAT5 and downregulated by the overexpression of p70-NFAT5 in either sham- or CVB3-infected cells. These data suggested iNOS as a potential candidate for our mechanism study. The expression of iNOS is induced by TLR activation, which requires NFAT5 activity [305]. CVB3 infection activates TLR expression [363], but high level of iNOS catalyzes production of nitric oxide, which impairs CVB3 replication via inhibition of viral proteases [307, 352]. Thus we hypothesized that CVB3 might cleave and inactivate NFAT5 to block the induction of iNOS. This hypothesis was supported by our experiment showing that treatment of cells with

iNOS inhibitor 1400W restored CVB3 replication blocked by overexpression of NFAT5 (**Fig. 3.6D**).

The anti-CVB3 effect of NFAT5 enables it as a potential drug target against CVB3 infection. As a hypertonicity-responsive protein, NFAT5 can be quickly induced by hypertonic solutions. HSS composed of high concentration of NaCl is the most commonly used inducer of NFAT5 due to its easy accessibility and safeness. In our experiments, HSS treatment significantly reduced viral replication and enhanced cell viability in CVB3-infected cells. In our *in vivo* test, A/J mice treated with HSS showed a lower viral load in heart tissue compared to the NSS-treated controls. Furthermore, the histological evaluation showed a lower level of heart tissue damage and immune infiltration in the HSS-treated mice, indicating that HSS treatment relieved the severity of CVB3-induced myocarditis. Though HSS is widely used to induce NFAT5, NaCl is an ionic osmolyte capable of entering cells and increasing intracellular ion concentration [354]. Excess intracellular ions lead to increased reactive oxygen species formation, cytoskeletal rearrangements, increased mitochondrial depolarization, decreased DNA replication and DNA repair [273, 274], which may affect CVB3 infection independent of NFAT5 pathway. To exclude the potential side effect of HSS, we also tested mannitol, a non-permeable hyperosmotic agent, in cell culture to induce NFAT5 and determined its effect on CVB3 replication. Interestingly, mannitol showed a similar anti-CVB3 effect as HSS, which decreased viral replication and enhanced cell survival during CVB3 infection.

In summary, our study uncovers a novel function of transcription factor NFAT5 in cardiac protection against CVB3 infection. CVB3 replication depends on different viral proteins generated by polyprotein cleavage mediated by viral protease 2A and 3C [364, 365]. However, the activity of viral proteases is probably inhibited by NFAT5 via promoting expression of its

downstream target protein iNOS, which enhances NO generation [307, 352, 366]. Since NFAT5 is cleaved by viral protease during infection, upregulation of NFAT5 expression is a rationale strategy to counteract CVB3 infection. Although HSS has already been used in treatment of non-infectious heart failure [367, 368], our successful testing of two solutions, HSS and mannitol, in anti-CVB3 infection is the first exploration in using the safe, low cost and easy accessible compounds to treat infectious heart disease, which has laid a solid foundation for further development.

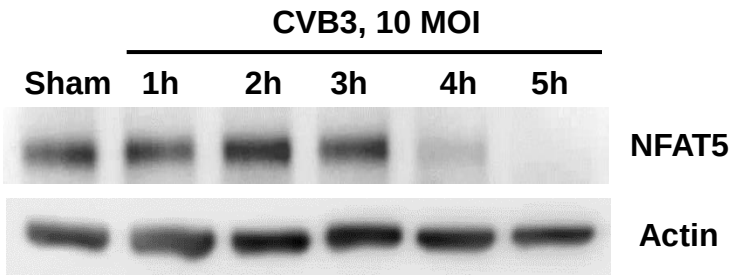

Figure 3.10. NFAT5 is upregulated at early stage of CVB3 infection. HeLa cells were infected with CVB3 at 10 MOI or sham-infected with PBS. At the indicated time points pi, cell lysates were used for Western blot analysis of NFAT5 protein using an antibody against the N-terminal epitope of NFAT5. β-actin was used as a loading control.

Chapter 4 Concluding Remarks

4.1 Summary and Conclusion

In this dissertation, I focused my studies on the mutual regulation of CVB3 and two typical SRPs, the heat-responsive protein Hsp70 and hypertonicity-responsive protein NFAT5. I have uncovered the alterations of these two SRPs in cellular level and activity during CVB3 infection and their feedback roles on CVB3 replication as well as the underlying mechanisms at the molecular level.

In Hsp70 project, I demonstrated that Hsp70-1, but not Hsp70-2, was upregulated during CVB3 infection. I further revealed a novel mechanism by which CVB3 infection activates CaMKIIγ and selectively phosphorylates HSF1 at Ser230, leading to enhanced Hsp70-1 transcription. Meanwhile, phosphorylation of Ser230 induces translocation of HSF1 from the cytosol to nucleus, thus blocking the ERK1/2-mediated phosphorylation of HSF1 at Ser307, a negative regulatory process on Hsp70-1 transcription, further contributing to upregulation of Hsp70-1. Finally, I determined that Hsp70-1 upregulation, in turn, facilitates CVB3 replication by stabilizing viral genomic RNA via cellular factor AUF1 and the ARE of CVB3 genome. These data indicate that Hsp70-related cellular chaperone system may be hijacked by CVB3 to favor its replication.

In NFAT5 project, I found that the reduction of NFAT5 expression during CVB3 infection is primarily due to post-translational cleavage at glycine (G) 503 of the protein by CVB3 protease. Such cleavage impaired NFAT5 activity due to the dominant negative effect of the ~70 kDa N-terminal cleavage product (p70-NFAT5). Ectopic expression of the FL NFAT5, especially a non-cleavable mutant NFAT5, resulted in strong inhibition of CVB3 replication, suggesting the antiviral effect of NFAT5. These data were further substantiated by siRNA-mediated gene

silencing of NFAT5, showing an increase of CVB3 replication. Mechanistic analyses revealed that iNOS, a protein downstream of NFAT5, was activated by FL NFAT5 but inhibited by p70-NFAT5 and that inhibition of iNOS by a specific inhibitor 1400W blocked the antiviral effect of NFAT5. In treatment studies using cell cultures, I found that HSS or mannitol, two potential inducers of NFAT5, significantly inhibited CVB3 replication. Finally, using a CVB3 myocarditis mouse model, I demonstrated that treating the infected mice with HSS significantly decreased viral load and alleviated heart tissue damage. In all, these data uncovered a novel cardiac protective role of NFAT5 against CVB3 infection, revealed the underlying mechanism by which NFAT5 protects the heart from CVB3 damage by activating iNOS and further verified the therapeutic potential of HSS and mannitol in the treatment of viral myocarditis.

In conclusion, CVB3 selectively utilizes host SRP system to benefit its own replication via either enhancing the expression of Hsp70-1 or cleaving and inhibiting NFAT5 activity, and thus these two SRPs can serve as potential targets for drug development against CVB3 infection and CVB3-induced myocarditis.

4.2 Significance

This study on Hsp70 has uncovered, for the first time, the differential regulation of Hsp70-1 and Hsp70-2, as well as the phosphorylation patterns of HSF-1 in CVB3 infection. Meanwhile, this study also determined the beneficial effect of Hsp70 on CVB3 replication via demonstrating a novel model in maintaining viral RNA stability through counteracting the Hsp70-AUF1-mediated RNA decay pathway. These results significantly contribute to the understanding of host-virus interactions during CVB3 infection and may probably inspire research on other picornaviruses. In addition, the finding of the interplay between CVB3 and Hsp70 may also

benefit therapeutic development. Since Hsp70 has a positive feedback effect on viral replication, this clearly indicates that Hsp70 is an ideal target for anti-CVB3 drug development. More importantly, RNA viruses, like CVB3, evolve rapidly and thus many drugs can be useless by newly emerging resistant variants. However, targeting the host protein (e.g., Hsp70) to inhibit CVB3 multiplication could be an alternative novel approach against RNA viruses. In addition, due to the pro-survival property of HSPs, many cancer cells have a high level of HSP expression. Thus the HSP chaperone inhibitors may not only be used for antiviral therapy but also for anticancer treatment. From this point of view, study of the mechanisms of Hsp70-mediated promotion of CVB3 replication will provide novel strategies for drug design.

NAFT5 is a cellular protective transcription factor responsible for chaperone gene transcription in response to hypertonic stress. Its role in kidney pathophysiology has been extensively studied. However, due to the surrounding non-hypertonic environment of the heart, research on NFAT5's role in myocardium has long been missing. Our study will fill a gap in this area of research. In addition, acute viral myocarditis is a big threat to public health due to rapid progress, leading to high morbidity and mortality, especially in children and young adults. A major barrier for the treatment of viral myocarditis is the lack of urgent measurements to control the disease development, particularly in rural area or developing countries. Our studies may provide a solution for this dilemma. The hypertonic saline solution is a low cost, non-toxic and easy use drug, which can be available in every clinic. Then patients will receive treatment immediately after diagnosis.

In all, the findings in this dissertation deepen the understanding of the modulation and roles of SRPs system in virus-host interactions, and also provide novel rationale for drug design to treat CVB3 infection and CVB3-induced myocarditis.

4.3 Limitations and Future Directions

Hsp70-1 and Hsp70-2 share more than 99% identity in their aa sequences and 84% homology in their gene sequences. The differences in nucleic acid sequences are mainly located in non-coding regions[369]. Thus, these two Hsp70s are usually considered as redundancy and named as Hsp70 indiscriminately. However, now increasing studies have demonstrated that Hsp70-1 and Hsp70-2 proteins play distinct roles in different situations, such as meiosis [370], carcinogenesis [371, 372], and obesity [373], indicating that the two proteins have more differences in their protein functions other than their induction patterns. However, the study of this dissertation only demonstrated the distinction of these two Hsp70s in regulation, but did not distinguish the functions and the two proteins. Actually, these two proteins are differently involved in apoptosis [374] and cell cycles [375], two cellular activities closely related to CVB3 replication, and more interestingly, I have shown in this dissertation that NFAT5, the transcriptional factor for Hsp70-2 but not Hsp70-1, exerted an anti-CVB3 activity opposite to the pro-virus effect of Hsp70-1. Considering these facts, it is probably worthy to study the individual function of each Hsp70 separately and uncover the underlying mechanisms of the functional difference of these two Hsp70s in CVB3 infection, if any. It may be surprising for two proteins with only two-aa difference to exert distinct functions, but any findings regarding this issue may significantly contribute to the understanding of the relationship between aa sequence and protein function.

In this dissertation, I attribute the positive feedback effect of Hsp70 on CVB3 to Hsp70-mediated stabilization of CVB3 genomic RNA only. However, as a multifunctional chaperone protein, Hsp70 probably influences CVB3 infection via other pathways. In a recent publication, to which I also contributed as a co-first author, we demonstrated that Hsp70 promotes CVB3 multiplication via enhancing viral RNA translation [376]. Briefly, Hsp70 benefits CVB3 translation

via two arms: 1) upregulation of IRES trans-acting factor lupus autoantigen protein and activation of eIF4E binding protein 1, a cap-dependent translation suppressor, to release translational machinery for viral IRES-driven translation; 2) enhancement of translation elongation via activation of eukaryotic elongation factor 2 (eEF2). This activation is regulated by Hsp70-mediated mTORC1-p70S6K-eEF2K cascade which requires cell division cycle protein 2 homolog (Cdc2, also called cyclin-dependent kinase 1). This study places Hsp70 in the center of the cellular network of molecular chaperones enhancing viral replication, demonstrating a great significance of Hsp70 in CVB3 replication. Since CVB3 replication and Hsp70 function are affected by numerous factors, it is reasonable to speculate that these factors share some overlaps, which may bridge Hsp70 and CVB3 replication. For example, Hsp70 may interact with viral polymerase 3D or other cellular RNA chaperone proteins (PCBP, PABP and hnRNP C) participating in viral RNA replication [377]; Hsp70 may also favor viral protein folding during rapid viral multiplication. Therefore, more pathways need to be characterized to better understand the roles of Hsp70 in CVB3 replication and established the interacting network of virus and molecular chaperones.

In the NFAT5 study of this dissertation, I mainly focused the anti-CVB3 effects of NFAT5 on CVB3 replication and CVB3-induced cell death, and further attributed the relief of myocarditis upon hypertonic treatment in mice to the induction of NFAT5 expression. However, in viral myocarditis, in addition to the direct cardiomyocyte damage caused by viral replication in the heart, the exaggerated immune response is also a critical cause of myocardium inflammation [52, 378-380]. As mentioned in 1.4.2, NFAT5 is an important immune modulator mainly reported in hypertonicity-related immune responses. NFAT5 is activated in T lymphocytes and bone-marrow-derived macrophages upon hypertonicity [381]. Deficiency of NFAT5 results in lymphoid

hypocellularity and impaired antigen-specific antibody responses, as well as reduction of lymphocyte proliferation under hypertonic conditions [284, 382]. In addition to immune cells, NFAT5 also regulates the expression of several proinflammatory cytokines, including TNFα and TL-β, in lymphocytes and macrophages exposed to hyperosmotic stress [283]. Considering that activation of macrophages and T lymphocytes as well as secretion of proinflammatory cytokines are key steps for immune infiltration in viral myocarditis [52, 53, 55], NFAT5 may play an important role in viral myovarditis via activation of immune responses. Thus, investigation focusing on NFAT5-induced immune response in CVB3 pathogenesis is worth conducting in-depth.

Bibliography

1. Zoll J, Heus HA, van Kuppeveld FJ, Melchers WJ. The structure-function relationship of the enterovirus 3'-utr. *Virus research*. 2009;139:209-216
2. Lin JY, Chen TC, Weng KF, Chang SC, Chen LL, Shih SR. Viral and host proteins involved in picornavirus life cycle. *Journal of biomedical science*. 2009;16:103
3. Kuhl U, Pauschinger M, Noutsias M, Seeberg B, Bock T, Lassner D, Poller W, Kandolf R, Schultheiss HP. High prevalence of viral genomes and multiple viral infections in the myocardium of adults with "idiopathic" left ventricular dysfunction. *Circulation*. 2005;111:887-893
4. Cheung CY, Ko BC. Nfat5 in cellular adaptation to hypertonic stress - regulations and functional significance. *Journal of molecular signaling*. 2013;8:5
5. Gratacos FM, Brewer G. The role of auf1 in regulated mrna decay. *Wiley Interdiscip Rev RNA*. 2010;1:457-473
6. Donaldson KA, Griffin DW, Paul JH. Detection, quantitation and identification of enteroviruses from surface waters and sponge tissue from the florida keys using real-time rt-pcr. *Water research*. 2002;36:2505-2514
7. Liu PP, Mason JW. Advances in the understanding of myocarditis. *Circulation*. 2001;104:1076-1082
8. Yajima T, Knowlton KU. Viral myocarditis: From the perspective of the virus. *Circulation*. 2009;119:2615-2624
9. Feldman AM, McNamara D. Myocarditis. *N Engl J Med*. 2000;343:1388-1398
10. Baughman KL. Diagnosis of myocarditis: Death of dallas criteria. *Circulation*. 2006;113:593-595
11. Kerr WW. Myocarditis. *California state journal of medicine*. 1904;2:369-371
12. Smith SC, Ladenson JH, Mason JW, Jaffe AS. Elevations of cardiac troponin i associated with myocarditis. Experimental and clinical correlates. *Circulation*. 1997;95:163-168
13. Franz WM, Remppis A, Kandolf R, Kubler W, Katus HA. Serum troponin t: Diagnostic marker for acute myocarditis. *Clin Chem*. 1996;42:340-341
14. Saphir O. Myocarditis - a general review, with an analysis of two hundred and forty cases. *Arch Pathol*. 1942;33:88-137
15. Aretz HT. Myocarditis: The dallas criteria. *Human pathology*. 1987;18:619-624
16. Aretz HT, Billingham ME, Edwards WD, Factor SM, Fallon JT, Fenoglio JJ, Jr., Olsen EG, Schoen FJ. Myocarditis. A histopathologic definition and classification. *Am J Cardiovasc Pathol*. 1987;1:3-14
17. Blauwet LA, Cooper LT. Myocarditis. *Progress in cardiovascular diseases*. 2010;52:274-288
18. Cooper LT, Jr. Myocarditis. *N Engl J Med*. 2009;360:1526-1538
19. Grist NR RD. Epidemiology of viral infections of the heart. In: Banatvala JE, ed. *Viral infection of the heart*. London: Edward Arnold; 1993:23-30.
20. Leonard EG. Viral myocarditis. *Pediatr Infect Dis J*. 2004;23:665-666
21. Kearney MT, Cotton JM, Richardson PJ, Shah AM. Viral myocarditis and dilated cardiomyopathy: Mechanisms, manifestations, and management. *Postgraduate medical journal*. 2001;77:4-10

22. Maron BJ, Towbin JA, Thiene G, Antzelevitch C, Corrado D, Arnett D, Moss AJ, Seidman CE, Young JB. Contemporary definitions and classification of the cardiomyopathies: An american heart association scientific statement from the council on clinical cardiology, heart failure and transplantation committee; quality of care and outcomes research and functional genomics and translational biology interdisciplinary working groups; and council on epidemiology and prevention. *Circulation*. 2006;113:1807-1816
23. Grumbach IM, Heim A, Pring-Akerblom P, Vonhof S, Hein WJ, Muller G, Figulla HR. Adenoviruses and enteroviruses as pathogens in myocarditis and dilated cardiomyopathy. *Acta cardiologica*. 1999;54:83-88
24. Kuhl U, Pauschinger M, Seeberg B, Lassner D, Noutsias M, Poller W, Schultheiss HP. Viral persistence in the myocardium is associated with progressive cardiac dysfunction. *Circulation*. 2005;112:1965-1970
25. Mahrholdt H, Wagner A, Deluigi CC, Kispert E, Hager S, Meinhardt G, Vogelsberg H, Fritz P, Dippon J, Bock CT, Klingel K, Kandolf R, Sechtem U. Presentation, patterns of myocardial damage, and clinical course of viral myocarditis. *Circulation*. 2006;114:1581-1590
26. Pankuweit S, Ruppert V, Eckhardt H, Strache D, Maisch B. Pathophysiology and aetiological diagnosis of inflammatory myocardial diseases with a special focus on parvovirus b19. *J Vet Med B Infect Dis Vet Public Health*. 2005;52:344-347
27. Tschope C, Bock CT, Kasner M, Noutsias M, Westermann D, Schwimmbeck PL, Pauschinger M, Poller WC, Kuhl U, Kandolf R, Schultheiss HP. High prevalence of cardiac parvovirus b19 infection in patients with isolated left ventricular diastolic dysfunction. *Circulation*. 2005;111:879-886
28. Bock CT, Klingel K, Kandolf R. Human parvovirus b19-associated myocarditis. *N Engl J Med*. 2010;362:1248-1249
29. Kuethe F, Lindner J, Matschke K, Wenzel JJ, Norja P, Ploetze K, Schaal S, Kamvissi V, Bornstein SR, Schwanebeck U, Modrow S. Prevalence of parvovirus b19 and human bocavirus DNA in the heart of patients with no evidence of dilated cardiomyopathy or myocarditis. *Clin Infect Dis*. 2009;49:1660-1666
30. Schenk T, Enders M, Pollak S, Hahn R, Huzly D. High prevalence of human parvovirus b19 DNA in myocardial autopsy samples from subjects without myocarditis or dilative cardiomyopathy. *J Clin Microbiol*. 2009;47:106-110
31. Koepsell SA, Anderson DR, Radio SJ. Parvovirus b19 is a bystander in adult myocarditis. *Cardiovascular pathology : the official journal of the Society for Cardiovascular Pathology*. 2012;21:476-481
32. Rotola A, Di Luca D, Cassai E, Ricotta D, Giulio A, Turano A, Caruso A, Muneretto C. Human herpesvirus 6 infects and replicates in aortic endothelium. *J Clin Microbiol*. 2000;38:3135-3136
33. Caruso A, Favilli F, Rotola A, Comar M, Horejsh D, Alessandri G, Grassi M, Di Luca D, Fiorentini S. Human herpesvirus-6 modulates rantes production in primary human endothelial cell cultures. *Journal of medical virology*. 2003;70:451-458
34. Crimeen-Irwin B, Ellis S, Christiansen D, Ludford-Menting MJ, Milland J, Lanteri M, Loveland BE, Gerlier D, Russell SM. Ligand binding determines whether cd46 is internalized by clathrin-coated pits or macropinocytosis. *The Journal of biological chemistry*. 2003;278:46927-46937

35. Poller W, Fechner H, Noutsias M, Tschoepe C, Schultheiss HP. Highly variable expression of virus receptors in the human cardiovascular system. Implications for cardiotropic viral infections and gene therapy. *Z Kardiol*. 2002;91:978-991
36. Bowles NE, Ni J, Kearney DL, Pauschinger M, Schultheiss HP, McCarthy R, Hare J, Bricker JT, Bowles KR, Towbin JA. Detection of viruses in myocardial tissues by polymerase chain reaction. Evidence of adenovirus as a common cause of myocarditis in children and adults. *J Am Coll Cardiol*. 2003;42:466-472
37. Calabrese F, Carturan E, Chimenti C, Pieroni M, Agostini C, Angelini A, Crosato M, Valente M, Boffa GM, Frustaci A, Thiene G. Overexpression of tumor necrosis factor (tnf)alpha and tnfalpha receptor i in human viral myocarditis: Clinicopathologic correlations. *Mod Pathol*. 2004;17:1108-1118
38. Ishikawa T, Zhu BL, Li DR, Zhao D, Maeda H. Epstein-barr virus myocarditis as a cause of sudden death: Two autopsy cases. *Int J Legal Med*. 2005;119:231-235
39. Beschorner WE, Baughman K, Turnicky RP, Hutchins GM, Rowe SA, Kavanaugh-McHugh AL, Suresch DL, Herskowitz A. Hiv-associated myocarditis. Pathology and immunopathology. *Am J Pathol*. 1990;137:1365-1371
40. Dennert R, Crijns HJ, Heymans S. Acute viral myocarditis. *European heart journal*. 2008;29:2073-2082
41. Zaoutis T, Klein JD. Enterovirus infections. *Pediatr Rev*. 1998;19:183-191
42. Singer M, Deutschman CS, Seymour CW, Shankar-Hari M, Annane D, Bauer M, Bellomo R, Bernard GR, Chiche JD, Coopersmith CM, Hotchkiss RS, Levy MM, Marshall JC, Martin GS, Opal SM, Rubenfeld GD, van der Poll T, Vincent JL, Angus DC. The third international consensus definitions for sepsis and septic shock (sepsis-3). *JAMA*. 2016;315:801-810
43. Deutschman CS, Tracey KJ. Sepsis: Current dogma and new perspectives. *Immunity*. 2014;40:463-475
44. Klingel K, Stephan S, Sauter M, Zell R, McManus BM, Bultmann B, Kandolf R. Pathogenesis of murine enterovirus myocarditis: Virus dissemination and immune cell targets. *Journal of virology*. 1996;70:8888-8895
45. Badorff C, Lee GH, Lamphear BJ, Martone ME, Campbell KP, Rhoads RE, Knowlton KU. Enteroviral protease 2a cleaves dystrophin: Evidence of cytoskeletal disruption in an acquired cardiomyopathy. *Nature medicine*. 1999;5:320-326
46. Huber SA, Budd RC, Rossner K, Newell MK. Apoptosis in coxsackievirus b3-induced myocarditis and dilated cardiomyopathy. *Annals of the New York Academy of Sciences*. 1999;887:181-190
47. Chow LH, Beisel KW, McManus BM. Enteroviral infection of mice with severe combined immunodeficiency. Evidence for direct viral pathogenesis of myocardial injury. *Laboratory investigation; a journal of technical methods and pathology*. 1992;66:24-31
48. Mann DL. The emerging role of innate immunity in the heart and vascular system: For whom the cell tolls. *Circulation research*. 2011;108:1133-1145
49. Fuse K, Chan G, Liu Y, Gudgeon P, Husain M, Chen M, Yeh WC, Akira S, Liu PP. Myeloid differentiation factor-88 plays a crucial role in the pathogenesis of coxsackievirus b3-induced myocarditis and influences type i interferon production. *Circulation*. 2005;112:2276-2285

50. Seko Y, Takahashi N, Yagita H, Okumura K, Yazaki Y. Expression of cytokine mrnas in murine hearts with acute myocarditis caused by coxsackievirus b3. *J Pathol*. 1997;183:105-108
51. Li J, Schwimmbeck PL, Tschope C, Leschka S, Husmann L, Rutschow S, Reichenbach F, Noutsias M, Kobalz U, Poller W, Spillmann F, Zeichhardt H, Schultheiss HP, Pauschinger M. Collagen degradation in a murine myocarditis model: Relevance of matrix metalloproteinase in association with inflammatory induction. *Cardiovasc Res*. 2002;56:235-247
52. Esfandiarei M, McManus BM. Molecular biology and pathogenesis of viral myocarditis. *Annu Rev Pathol*. 2008;3:127-155
53. Papageorgiou AP, Heymans S. Interactions between the extracellular matrix and inflammation during viral myocarditis. *Immunobiology*. 2012;217:503-510
54. Tomioka N, Kishimoto C, Matsumori A, Kawai C. Effects of prednisolone on acute viral myocarditis in mice. *J Am Coll Cardiol*. 1986;7:868-872
55. Godeny EK, Gauntt CJ. Involvement of natural killer cells in coxsackievirus b3-induced murine myocarditis. *Journal of immunology*. 1986;137:1695-1702
56. Klingel K, Hohenadl C, Canu A, Albrecht M, Seemann M, Mall G, Kandolf R. Ongoing enterovirus-induced myocarditis is associated with persistent heart muscle infection: Quantitative analysis of virus replication, tissue damage, and inflammation. *Proceedings of the National Academy of Sciences of the United States of America*. 1992;89:314-318
57. Kyu B, Matsumori A, Sato Y, Okada I, Chapman NM, Tracy S. Cardiac persistence of cardioviral rna detected by polymerase chain reaction in a murine model of dilated cardiomyopathy. *Circulation*. 1992;86:522-530
58. Gluck B, Schmidtke M, Merkle I, Stelzner A, Gemsa D. Persistent expression of cytokines in the chronic stage of cvb3-induced myocarditis in nmri mice. *Journal of molecular and cellular cardiology*. 2001;33:1615-1626
59. Mason JW, O'Connell JB, Herskowitz A, Rose NR, McManus BM, Billingham ME, Moon TE. A clinical trial of immunosuppressive therapy for myocarditis. The myocarditis treatment trial investigators. *The New England journal of medicine*. 1995;333:269-275
60. Fohlman J, Ilback NG, Friman G, Morein B. Vaccination of balb/c mice against enteroviral mediated myocarditis. *Vaccine*. 1990;8:381-384
61. Fohlman J, Pauksen K, Morein B, Bjare U, Ilback NG, Friman G. High yield production of an inactivated coxsackie b3 adjuvant vaccine with protective effect against experimental myocarditis. *Scandinavian journal of infectious diseases. Supplementum*. 1993;88:103-108
62. Braun H, Makarov VA, Riabova OB, Wutzler P, Schmidtke M. Amino acid substitutions at residue 207 of viral capsid protein 1 (vp1) confer pleconaril resistance in coxsackievirus b3 (cvb3). *Antivir Res*. 2011;90:A54-A55
63. Thibaut HJ, De Palma AM, Neyts J. Combating enterovirus replication: State-of-the-art on antiviral research. *Biochemical pharmacology*. 2012;83:185-192
64. McKinlay MA. Discovery and development of antipicornaviral agents. *Scandinavian journal of infectious diseases. Supplementum*. 1993;88:109-115
65. Turner RB, Dutko FJ, Goldstein NH, Lockwood G, Hayden FG. Efficacy of oral win 54954 for prophylaxis of experimental rhinovirus infection. *Antimicrobial agents and chemotherapy*. 1993;37:297-300

66. Kyto V, Saraste A, Fohlman J, Ilback NG, Harvala H, Vuorinen T, Hyypia T. Cardiomyocyte apoptosis after antiviral win 54954 treatment in murine coxsackievirus b3 myocarditis. *Scandinavian cardiovascular journal : SCJ*. 2002;36:187-192
67. Yanagawa B, Spiller OB, Proctor DG, Choy J, Luo H, Zhang HM, Suarez A, Yang D, McManus BM. Soluble recombinant coxsackievirus and adenovirus receptor abrogates coxsackievirus b3-mediated pancreatitis and myocarditis in mice. *The Journal of infectious diseases*. 2004;189:1431-1439
68. Kuhl U, Pauschinger M, Schwimmbeck PL, Seeberg B, Lober C, Noutsias M, Poller W, Schultheiss HP. Interferon-beta treatment eliminates cardiotropic viruses and improves left ventricular function in patients with myocardial persistence of viral genomes and left ventricular dysfunction. *Circulation*. 2003;107:2793-2798
69. Schmidt-Lucke C, Spillmann F, Bock T, Kuhl U, Van Linthout S, Schultheiss HP, Tschope C. Interferon beta modulates endothelial damage in patients with cardiac persistence of human parvovirus b19 infection. *The Journal of infectious diseases*. 2010;201:936-945
70. Kishimoto C, Shioji K, Kinoshita M, Iwase T, Tamaki S, Fujii M, Murashige A, Maruhashi H, Takeda S, Nonogi H, Hashimoto T. Treatment of acute inflammatory cardiomyopathy with intravenous immunoglobulin ameliorates left ventricular function associated with suppression of inflammatory cytokines and decreased oxidative stress. *International journal of cardiology*. 2003;91:173-178
71. Gullestad L, Aass H, Fjeld JG, Wikeby L, Andreassen AK, Ihlen H, Simonsen S, Kjekshus J, Nitter-Hauge S, Ueland T, Lien E, Froland SS, Aukrust P. Immunomodulating therapy with intravenous immunoglobulin in patients with chronic heart failure. *Circulation*. 2001;103:220-225
72. Folwaczny C, Born C, Loeschke K. Closure of an enterocutaneous fistula by high dose intravenous immune globuline therapy in a patient with x-linked agammaglobulinemia. *The American journal of gastroenterology*. 2001;96:1954-1955
73. Wallukat G, Muller J, Hetzer R. Specific removal of beta1-adrenergic autoantibodies from patients with idiopathic dilated cardiomyopathy. *The New England journal of medicine*. 2002;347:1806
74. Wallukat G, Reinke P, Dorffel WV, Luther HP, Bestvater K, Felix SB, Baumann G. Removal of autoantibodies in dilated cardiomyopathy by immunoadsorption. *International journal of cardiology*. 1996;54:191-195
75. Felix SB, Staudt A, Dorffel WV, Stangl V, Merkel K, Pohl M, Docke WD, Morgera S, Neumayer HH, Wernecke KD, Wallukat G, Stangl K, Baumann G. Hemodynamic effects of immunoadsorption and subsequent immunoglobulin substitution in dilated cardiomyopathy: Three-month results from a randomized study. *Journal of the American College of Cardiology*. 2000;35:1590-1598
76. Helwig FC, Schmidt CH. A filter-passing agent producing interstitial myocarditis in anthropoid apes and small animals. *Science*. 1945;102:31-33
77. Dalldorf G, Sickles GM. An unidentified, filtrable agent isolated from the feces of children with paralysis. *Science*. 1948;108:61-62
78. Melnick JL, Shaw EW, Curnen EC. A virus isolated from patients diagnosed as non-paralytic poliomyelitis or aseptic meningitis. *Proceedings of the Society for Experimental Biology and Medicine. Society for Experimental Biology and Medicine*. 1949;71:344-349

79. Pons-Salort M, Parker EP, Grassly NC. The epidemiology of non-polio enteroviruses: Recent advances and outstanding questions. *Current opinion in infectious diseases*. 2015;28:479-487
80. Landry ML, Madore HP, Fong CK, Hsiung GD. Use of guinea pig embryo cell cultures for isolation and propagation of group a coxsackieviruses. *Journal of clinical microbiology*. 1981;13:588-593
81. He W, Lu H, Zhao K, Song D, Gai X, Gao F. Complete genome sequence of a coxsackievirus b3 isolated from a sichuan snub-nosed monkey. *Journal of virology*. 2012;86:13134-13135
82. Marchant D, Si X, Luo H, McManus B, Yang D. The impact of cvb3 infection on host cell biology. *Current topics in microbiology and immunology*. 2008;323:177-198
83. Crowell RL, Landau BJ. A short history and introductory background on the coxsackieviruses of group b. *Current topics in microbiology and immunology*. 1997;223:1-11
84. Lim BK, Ju ES, Lao DH, Yun SH, Lee YJ, Kim DK, Jeon ES. Development of a enterovirus diagnostic assay system for diagnosis of viral myocarditis in humans. *Microbiology and immunology*. 2013;57:281-287
85. Baboonian C, Davies MJ, Booth JC, McKenna WJ. Coxsackie b viruses and human heart disease. *Current topics in microbiology and immunology*. 1997;223:31-52
86. Baboonian C, Treasure T. Meta-analysis of the association of enteroviruses with human heart disease. *Heart*. 1997;78:539-543
87. Dunn JJ, Chapman NM, Tracy S, Romero JR. Genomic determinants of cardiovirulence in coxsackievirus b3 clinical isolates: Localization to the 5' nontranslated region. *Journal of virology*. 2000;74:4787-4794
88. Martinez-Salas E, Francisco-Velilla R, Fernandez-Chamorro J, Lozano G, Diaz-Toledano R. Picornavirus ires elements: Rna structure and host protein interactions. *Virus research*. 2015;206:62-73
89. Gruez A, Selisko B, Roberts M, Bricogne G, Bussetta C, Jabafi I, Coutard B, De Palma AM, Neyts J, Canard B. The crystal structure of coxsackievirus b3 rna-dependent rna polymerase in complex with its protein primer vpg confirms the existence of a second vpg binding site on picornaviridae polymerases. *Journal of virology*. 2008;82:9577-9590
90. Lee YF, Nomoto A, Detjen BM, Wimmer E. A protein covalently linked to poliovirus genome rna. *Proceedings of the National Academy of Sciences of the United States of America*. 1977;74:59-63
91. Gamarnik AV, Andino R. Switch from translation to rna replication in a positive-stranded rna virus. *Genes & development*. 1998;12:2293-2304
92. Xiang W, Harris KS, Alexander L, Wimmer E. Interaction between the 5'-terminal cloverleaf and 3ab/3cdpro of poliovirus is essential for rna replication. *Journal of virology*. 1995;69:3658-3667
93. Bailey JM, Tapprich WE. Structure of the 5' nontranslated region of the coxsackievirus b3 genome: Chemical modification and comparative sequence analysis. *Journal of virology*. 2007;81:650-668
94. Herold J, Andino R. Poliovirus rna replication requires genome circularization through a protein-protein bridge. *Molecular cell*. 2001;7:581-591

95. van Ooij MJ, Glaudemans DH, Heus HA, van Kuppeveld FJ, Melchers WJ. Structural and functional integrity of the coxsackievirus b3 orir: Spacing between coaxial rna helices. *The Journal of general virology*. 2006;87:689-695
96. Klump WM, Bergmann I, Muller BC, Ameis D, Kandolf R. Complete nucleotide sequence of infectious coxsackievirus b3 cdna: Two initial 5' uridine residues are regained during plus-strand rna synthesis. *Journal of virology*. 1990;64:1573-1583
97. Preiss T, Hentze MW. Dual function of the messenger rna cap structure in poly(a)-tail-promoted translation in yeast. *Nature*. 1998;392:516-520
98. Preiss T, Muckenthaler M, Hentze MW. Poly(a)-tail-promoted translation in yeast: Implications for translational control. *RNA*. 1998;4:1321-1331
99. Massilamany C, Gangaplara A, Reddy J. Intricacies of cardiac damage in coxsackievirus b3 infection: Implications for therapy. *International journal of cardiology*. 2014;177:330-339
100. Bonderoff JM, Lloyd RE. Cvb translation: Lessons from the polioviruses. *Current topics in microbiology and immunology*. 2008;323:123-147
101. Bergelson JM, Mohanty JG, Crowell RL, St John NF, Lublin DM, Finberg RW. Coxsackievirus b3 adapted to growth in rd cells binds to decay-accelerating factor (cd55). *Journal of virology*. 1995;69:1903-1906
102. van Kuppeveld FJ, Galama JM, Zoll J, van den Hurk PJ, Melchers WJ. Coxsackie b3 virus protein 2b contains cationic amphipathic helix that is required for viral rna replication. *Journal of virology*. 1996;70:3876-3886
103. van Kuppeveld FJ, Hoenderop JG, Smeets RL, Willems PH, Dijkman HB, Galama JM, Melchers WJ. Coxsackievirus protein 2b modifies endoplasmic reticulum membrane and plasma membrane permeability and facilitates virus release. *The EMBO journal*. 1997;16:3519-3532
104. de Jong AS, de Mattia F, Van Dommelen MM, Lanke K, Melchers WJ, Willems PH, van Kuppeveld FJ. Functional analysis of picornavirus 2b proteins: Effects on calcium homeostasis and intracellular protein trafficking. *Journal of virology*. 2008;82:3782-3790
105. De Palma AM, Heggermont W, Lanke K, Coutard B, Bergmann M, Monforte AM, Canard B, De Clercq E, Chimirri A, Purstinger G, Rohayem J, van Kuppeveld F, Neyts J. The thiazolobenzimidazole tbze-029 inhibits enterovirus replication by targeting a short region immediately downstream from motif c in the nonstructural protein 2c. *Journal of virology*. 2008;82:4720-4730
106. Cornell CT, Kiosses WB, Harkins S, Whitton JL. Coxsackievirus b3 proteins directionally complement each other to downregulate surface major histocompatibility complex class i. *Journal of virology*. 2007;81:6785-6797
107. Pathak HB, Arnold JJ, Wiegand PN, Hargittai MR, Cameron CE. Picornavirus genome replication: Assembly and organization of the vpg uridylylation ribonucleoprotein (initiation) complex. *The Journal of biological chemistry*. 2007;282:16202-16213
108. Louis E.-C. Leong CTC, Bert L. Semler. Processing determinants and functions of cleavage products of picornavirus polyproteins. *Molecular Biology of Picornavirus*. 2002
109. Harris KS, Xiang W, Alexander L, Lane WS, Paul AV, Wimmer E. Interaction of poliovirus polypeptide 3cdpro with the 5' and 3' termini of the poliovirus genome. Identification of viral and cellular cofactors needed for efficient binding. *The Journal of biological chemistry*. 1994;269:27004-27014

110. Bell YC, Semler BL, Ehrenfeld E. Requirements for rna replication of a poliovirus replicon by coxsackievirus b3 rna polymerase. *Journal of virology*. 1999;73:9413-9421
111. Bergelson JM, Cunningham JA, Droguett G, Kurt-Jones EA, Krithivas A, Hong JS, Horwitz MS, Crowell RL, Finberg RW. Isolation of a common receptor for coxsackie b viruses and adenoviruses 2 and 5. *Science*. 1997;275:1320-1323
112. Tomko RP, Xu R, Philipson L. Hcar and mcar: The human and mouse cellular receptors for subgroup c adenoviruses and group b coxsackieviruses. *Proceedings of the National Academy of Sciences of the United States of America*. 1997;94:3352-3356
113. Ito M, Kodama M, Masuko M, Yamaura M, Fuse K, Uesugi Y, Hirono S, Okura Y, Kato K, Hotta Y, Honda T, Kuwano R, Aizawa Y. Expression of coxsackievirus and adenovirus receptor in hearts of rats with experimental autoimmune myocarditis. *Circulation research*. 2000;86:275-280
114. Honda T, Saitoh H, Masuko M, Katagiri-Abe T, Tominaga K, Kozakai I, Kobayashi K, Kumanishi T, Watanabe YG, Odani S, Kuwano R. The coxsackievirus-adenovirus receptor protein as a cell adhesion molecule in the developing mouse brain. *Brain research. Molecular brain research*. 2000;77:19-28
115. Cohen CJ, Shieh JT, Pickles RJ, Okegawa T, Hsieh JT, Bergelson JM. The coxsackievirus and adenovirus receptor is a transmembrane component of the tight junction. *Proceedings of the National Academy of Sciences of the United States of America*. 2001;98:15191-15196
116. Nicholson-Weller A, Wang CE. Structure and function of decay accelerating factor cd55. *The Journal of laboratory and clinical medicine*. 1994;123:485-491
117. Coyne CB, Bergelson JM. Virus-induced abl and fyn kinase signals permit coxsackievirus entry through epithelial tight junctions. *Cell*. 2006;124:119-131
118. Patel KP, Coyne CB, Bergelson JM. Dynamin- and lipid raft-dependent entry of decay-accelerating factor (daf)-binding and non-daf-binding coxsackieviruses into nonpolarized cells. *Journal of virology*. 2009;83:11064-11077
119. Chow M, Newman JF, Filman D, Hogle JM, Rowlands DJ, Brown F. Myristylation of picornavirus capsid protein vp4 and its structural significance. *Nature*. 1987;327:482-486
120. Yang D, Wilson JE, Anderson DR, Bohunek L, Cordeiro C, Kandolf R, McManus BM. In vitro mutational and inhibitory analysis of the cis-acting translational elements within the 5' untranslated region of coxsackievirus b3: Potential targets for antiviral action of antisense oligomers. *Virology*. 1997;228:63-73
121. Limpens RW, van der Schaar HM, Kumar D, Koster AJ, Snijder EJ, van Kuppeveld FJ, Barcena M. The transformation of enterovirus replication structures: A three-dimensional study of single- and double-membrane compartments. *mBio*. 2011;2
122. Romero-Brey I, Bartenschlager R. Membranous replication factories induced by plus-strand rna viruses. *Viruses*. 2014;6:2826-2857
123. Wong J, Zhang J, Si X, Gao G, Mao I, McManus BM, Luo H. Autophagosome supports coxsackievirus b3 replication in host cells. *Journal of virology*. 2008;82:9143-9153
124. Paul AV, van Boom JH, Filippov D, Wimmer E. Protein-primed rna synthesis by purified poliovirus rna polymerase. *Nature*. 1998;393:280-284
125. Flanegan JB, Baltimore D. Poliovirus-specific primer-dependent rna polymerase able to copy poly(a). *Proceedings of the National Academy of Sciences of the United States of America*. 1977;74:3677-3680

126. Nomoto A, Detjen B, Pozzatti R, Wimmer E. The location of the polio genome protein in viral rnas and its implication for rna synthesis. *Nature*. 1977;268:208-213
127. Goodfellow IG, Kerrigan D, Evans DJ. Structure and function analysis of the poliovirus cis-acting replication element (cre). *RNA*. 2003;9:124-137
128. Baltimore D, Girard M, Darnell JE. Aspects of the synthesis of poliovirus rna and the formation of virus particles. *Virology*. 1966;29:179-189
129. Carthy CM, Yanagawa B, Luo H, Granville DJ, Yang D, Cheung P, Cheung C, Esfandiarei M, Rudin CM, Thompson CB, Hunt DW, McManus BM. Bcl-2 and bcl-xl overexpression inhibits cytochrome c release, activation of multiple caspases, and virus release following coxsackievirus b3 infection. *Virology*. 2003;313:147-157
130. Paloheimo O, Ihalainen TO, Tauriainen S, Valilehto O, Kirjavainen S, Niskanen EA, Laakkonen JP, Hyoty H, Vihinen-Ranta M. Coxsackievirus b3-induced cellular protrusions: Structural characteristics and functional competence. *Journal of virology*. 2011;85:6714-6724
131. Robinson SM, Tsueng G, Sin J, Mangale V, Rahawi S, McIntyre LL, Williams W, Kha N, Cruz C, Hancock BM, Nguyen DP, Sayen MR, Hilton BJ, Doran KS, Segall AM, Wolkowicz R, Cornell CT, Whitton JL, Gottlieb RA, Feuer R. Coxsackievirus b exits the host cell in shed microvesicles displaying autophagosomal markers. *PLoS pathogens*. 2014;10:e1004045
132. Schroder M, Kaufman RJ. Er stress and the unfolded protein response. *Mutation research*. 2005;569:29-63
133. Lee AS. The er chaperone and signaling regulator grp78/bip as a monitor of endoplasmic reticulum stress. *Methods*. 2005;35:373-381
134. Feng J, Chen X, Sun X, Wang F. Expression of endoplasmic reticulum stress markers grp78 and chop induced by oxidative stress in blue light-mediated damage of a2e-containing retinal pigment epithelium cells. *Ophthalmic research*. 2014;52:224-233
135. Baumeister P, Luo S, Skarnes WC, Sui G, Seto E, Shi Y, Lee AS. Endoplasmic reticulum stress induction of the grp78/bip promoter: Activating mechanisms mediated by yy1 and its interactive chromatin modifiers. *Molecular and cellular biology*. 2005;25:4529-4540
136. Ni M, Zhang Y, Lee AS. Beyond the endoplasmic reticulum: Atypical grp78 in cell viability, signalling and therapeutic targeting. *The Biochemical journal*. 2011;434:181-188
137. Vembar SS, Brodsky JL. One step at a time: Endoplasmic reticulum-associated degradation. *Nature reviews. Molecular cell biology*. 2008;9:944-957
138. Benali-Furet NL, Chami M, Houel L, De Giorgi F, Vernejoul F, Lagorce D, Buscail L, Bartenschlager R, Ichas F, Rizzuto R, Paterlini-Brechot P. Hepatitis c virus core triggers apoptosis in liver cells by inducing er stress and er calcium depletion. *Oncogene*. 2005;24:4921-4933
139. Chan SW, Egan PA. Hepatitis c virus envelope proteins regulate chop via induction of the unfolded protein response. *FASEB journal : official publication of the Federation of American Societies for Experimental Biology*. 2005;19:1510-1512
140. Pavio N, Romano PR, Graczyk TM, Feinstone SM, Taylor DR. Protein synthesis and endoplasmic reticulum stress can be modulated by the hepatitis c virus envelope protein e2 through the eukaryotic initiation factor 2alpha kinase perk. *Journal of virology*. 2003;77:3578-3585

141. Tardif KD, Mori K, Kaufman RJ, Siddiqui A. Hepatitis c virus suppresses the ire1-xbp1 pathway of the unfolded protein response. *The Journal of biological chemistry*. 2004;279:17158-17164
142. Tirosh B, Iwakoshi NN, Lilley BN, Lee AH, Glimcher LH, Ploegh HL. Human cytomegalovirus protein us11 provokes an unfolded protein response that may facilitate the degradation of class i major histocompatibility complex products. *Journal of virology*. 2005;79:2768-2779
143. Isler JA, Skalet AH, Alwine JC. Human cytomegalovirus infection activates and regulates the unfolded protein response. *Journal of virology*. 2005;79:6890-6899
144. Zhang HM, Ye X, Su Y, Yuan J, Liu Z, Stein DA, Yang D. Coxsackievirus b3 infection activates the unfolded protein response and induces apoptosis through downregulation of p58ipk and activation of chop and srebp1. *Journal of virology*. 2010;84:8446-8459
145. Cohen PS, Schmidtmayerova H, Dennis J, Dubrovsky L, Sherry B, Wang H, Bukrinsky M, Tracey KJ. The critical role of p38 map kinase in t cell hiv-1 replication. *Mol Med*. 1997;3:339-346
146. Hirasawa K, Kim A, Han HS, Han J, Jun HS, Yoon JW. Effect of p38 mitogen-activated protein kinase on the replication of encephalomyocarditis virus. *Journal of virology*. 2003;77:5649-5656
147. McLean TI, Bachenheimer SL. Activation of cjun n-terminal kinase by herpes simplex virus type 1 enhances viral replication. *Journal of virology*. 1999;73:8415-8426
148. Shapiro L, Heidenreich KA, Meintzer MK, Dinarello CA. Role of p38 mitogen-activated protein kinase in hiv type 1 production in vitro. *Proceedings of the National Academy of Sciences of the United States of America*. 1998;95:7422-7426
149. Chang L, Karin M. Mammalian map kinase signalling cascades. *Nature*. 2001;410:37-40
150. Si X, Luo H, Morgan A, Zhang J, Wong J, Yuan J, Esfandiarei M, Gao G, Cheung C, McManus BM. Stress-activated protein kinases are involved in coxsackievirus b3 viral progeny release. *Journal of virology*. 2005;79:13875-13881
151. Chau DH, Yuan J, Zhang H, Cheung P, Lim T, Liu Z, Sall A, Yang D. Coxsackievirus b3 proteases 2a and 3c induce apoptotic cell death through mitochondrial injury and cleavage of eif4gi but not dap5/p97/nat1. *Apoptosis : an international journal on programmed cell death*. 2007;12:513-524
152. Lamphear BJ, Yan R, Yang F, Waters D, Liebig HD, Klump H, Kuechler E, Skern T, Rhoads RE. Mapping the cleavage site in protein synthesis initiation factor eif-4 gamma of the 2a proteases from human coxsackievirus and rhinovirus. *The Journal of biological chemistry*. 1993;268:19200-19203
153. Kerekatte V, Keiper BD, Badorff C, Cai A, Knowlton KU, Rhoads RE. Cleavage of poly(a)-binding protein by coxsackievirus 2a protease in vitro and in vivo: Another mechanism for host protein synthesis shutoff? *Journal of virology*. 1999;73:709-717
154. Amineva SP, Aminev AG, Palmenberg AC, Gern JE. Rhinovirus 3c protease precursors 3cd and 3cd' localize to the nuclei of infected cells. *The Journal of general virology*. 2004;85:2969-2979
155. Sharma R, Raychaudhuri S, Dasgupta A. Nuclear entry of poliovirus protease-polymerase precursor 3cd: Implications for host cell transcription shut-off. *Virology*. 2004;320:195-205

156. Clark ME, Lieberman PM, Berk AJ, Dasgupta A. Direct cleavage of human tata-binding protein by poliovirus protease 3c in vivo and in vitro. *Molecular and cellular biology*. 1993;13:1232-1237
157. Yalamanchili P, Weidman K, Dasgupta A. Cleavage of transcriptional activator oct-1 by poliovirus encoded protease 3cpro. *Virology*. 1997;239:176-185
158. Weidman MK, Yalamanchili P, Ng B, Tsai W, Dasgupta A. Poliovirus 3c protease-mediated degradation of transcriptional activator p53 requires a cellular activity. *Virology*. 2001;291:260-271
159. Yalamanchili P, Datta U, Dasgupta A. Inhibition of host cell transcription by poliovirus: Cleavage of transcription factor creb by poliovirus-encoded protease 3cpro. *Journal of virology*. 1997;71:1220-1226
160. Falk MM, Grigera PR, Bergmann IE, Zibert A, Multhaup G, Beck E. Foot-and-mouth disease virus protease 3c induces specific proteolytic cleavage of host cell histone h3. *Journal of virology*. 1990;64:748-756
161. Clark ME, Hammerle T, Wimmer E, Dasgupta A. Poliovirus proteinase 3c converts an active form of transcription factor iiic to an inactive form: A mechanism for inhibition of host cell polymerase iii transcription by poliovirus. *The EMBO journal*. 1991;10:2941-2947
162. Esfandiarei M, Luo H, Yanagawa B, Suarez A, Dabiri D, Zhang J, McManus BM. Protein kinase b/akt regulates coxsackievirus b3 replication through a mechanism which is not caspase dependent. *Journal of virology*. 2004;78:4289-4298
163. Yuan J, Zhang J, Wong BW, Si X, Wong J, Yang D, Luo H. Inhibition of glycogen synthase kinase 3beta suppresses coxsackievirus-induced cytopathic effect and apoptosis via stabilization of beta-catenin. *Cell death and differentiation*. 2005;12:1097-1106
164. Ritossa F. A new puffing pattern induced by temperature shock and dnp in drosophila. *Experientia*. 1962;18:571-573
165. Matz JM, Blake MJ, Tatelman HM, Lavoi KP, Holbrook NJ. Characterization and regulation of cold-induced heat shock protein expression in mouse brown adipose tissue. *The American journal of physiology*. 1995;269:R38-47
166. Cao Y, Ohwatari N, Matsumoto T, Kosaka M, Ohtsuru A, Yamashita S. Tgf-beta1 mediates 70-kda heat shock protein induction due to ultraviolet irradiation in human skin fibroblasts. *Pflugers Archiv : European journal of physiology*. 1999;438:239-244
167. Laplante AF, Moulin V, Auger FA, Landry J, Li H, Morrow G, Tanguay RM, Germain L. Expression of heat shock proteins in mouse skin during wound healing. *The journal of histochemistry and cytochemistry : official journal of the Histochemistry Society*. 1998;46:1291-1301
168. De Maio A. Heat shock proteins: Facts, thoughts, and dreams. *Shock*. 1999;11:1-12
169. Kampinga HH, Hageman J, Vos MJ, Kubota H, Tanguay RM, Bruford EA, Cheetham ME, Chen B, Hightower LE. Guidelines for the nomenclature of the human heat shock proteins. *Cell stress & chaperones*. 2009;14:105-111
170. Schlesinger MJ. Heat shock proteins. *The Journal of biological chemistry*. 1990;265:12111-12114
171. Tavaria M, Gabriele T, Kola I, Anderson RL. A hitchhiker's guide to the human hsp70 family. *Cell stress & chaperones*. 1996;1:23-28
172. Morano KA. New tricks for an old dog: The evolving world of hsp70. *Annals of the New York Academy of Sciences*. 2007;1113:1-14

173. Jiang R, Gao B, Prasad K, Greene LE, Eisenberg E. Hsc70 chaperones clathrin and primes it to interact with vesicle membranes. *The Journal of biological chemistry*. 2000;275:8439-8447
174. Bercovich B, Stancovski I, Mayer A, Blumenfeld N, Laszlo A, Schwartz AL, Ciechanover A. Ubiquitin-dependent degradation of certain protein substrates in vitro requires the molecular chaperone hsc70. *The Journal of biological chemistry*. 1997;272:9002-9010
175. Mayer MP, Bukau B. Hsp70 chaperones: Cellular functions and molecular mechanism. *Cellular and molecular life sciences : CMLS*. 2005;62:670-684
176. Kojima R, Randall JD, Ito E, Manshio H, Suzuki Y, Gullans SR. Regulation of expression of the stress response gene, osp94: Identification of the tonicity response element and intracellular signalling pathways. *The Biochemical journal*. 2004;380:783-794
177. Woo SK, Lee SD, Na KY, Park WK, Kwon HM. Tonebp/nfat5 stimulates transcription of hsp70 in response to hypertonicity. *Molecular and cellular biology*. 2002;22:5753-5760
178. Hendershot LM, Valentine VA, Lee AS, Morris SW, Shapiro DN. Localization of the gene encoding human bip/grp78, the endoplasmic reticulum cognate of the hsp70 family, to chromosome 9q34. *Genomics*. 1994;20:281-284
179. Kober L, Zehe C, Bode J. Development of a novel er stress based selection system for the isolation of highly productive clones. *Biotechnology and bioengineering*. 2012;109:2599-2611
180. Wang X, Wang Q, Lin H, Li S, Sun L, Yang Y. Hsp72 and gp96 in gastroenterological cancers. *Clin Chim Acta*. 2013;417:73-79
181. Domanico SZ, DeNagel DC, Dahlseid JN, Green JM, Pierce SK. Cloning of the gene encoding peptide-binding protein 74 shows that it is a new member of the heat shock protein 70 family. *Molecular and cellular biology*. 1993;13:3598-3610
182. Mizukoshi E, Suzuki M, Loupatov A, Uruno T, Hayashi H, Misono T, Kaul SC, Wadhwa R, Imamura T. Fibroblast growth factor-1 interacts with the glucose-regulated protein grp75/mortalin. *The Biochemical journal*. 1999;343 Pt 2:461-466
183. Wadhwa R, Yaguchi T, Hasan MK, Mitsui Y, Reddel RR, Kaul SC. Hsp70 family member, mot-2/mthsp70/grp75, binds to the cytoplasmic sequestration domain of the p53 protein. *Experimental cell research*. 2002;274:246-253
184. Tsukamoto Y, Kuwabara K, Hirota S, Kawano K, Yoshikawa K, Ozawa K, Kobayashi T, Yanagi H, Stern DM, Tohyama M, Kitamura Y, Ogawa S. Expression of the 150-kd oxygen-regulated protein in human breast cancer. *Laboratory investigation; a journal of technical methods and pathology*. 1998;78:699-706
185. Mayer MP. Gymnastics of molecular chaperones. *Mol Cell*. 2010;39:321-331
186. Mashaghi A, Bezrukavnikov S, Minde DP, Wentink AS, Kityk R, Zachmann-Brand B, Mayer MP, Kramer G, Bukau B, Tans SJ. Alternative modes of client binding enable functional plasticity of hsp70. *Nature*. 2016;539:448-451
187. Fan CY, Lee S, Cyr DM. Mechanisms for regulation of hsp70 function by hsp40. *Cell stress & chaperones*. 2003;8:309-316
188. Ohtsuka K, Hata M. Molecular chaperone function of mammalian hsp70 and hsp40--a review. *International journal of hyperthermia : the official journal of European Society for Hyperthermic Oncology, North American Hyperthermia Group*. 2000;16:231-245

189. Wegele H, Muller L, Buchner J. Hsp70 and hsp90--a relay team for protein folding. *Rev Physiol Biochem Pharmacol*. 2004;151:1-44
190. Chen CY, Shyu AB. Au-rich elements: Characterization and importance in mrna degradation. *Trends in biochemical sciences*. 1995;20:465-470
191. Bolognani F, Perrone-Bizzozero NI. Rna-protein interactions and control of mrna stability in neurons. *Journal of neuroscience research*. 2008;86:481-489
192. Wilson GM, Sutphen K, Bolikal S, Chuang KY, Brewer G. Thermodynamics and kinetics of hsp70 association with a + u-rich mrna-destabilizing sequences. *J Biol Chem*. 2001;276:44450-44456
193. Lu JY, Bergman N, Sadri N, Schneider RJ. Assembly of auf1 with eif4g-poly(a) binding protein complex suggests a translation function in au-rich mrna decay. *Rna*. 2006;12:883-893
194. Hu S, Claud EC, Musch MW, Chang EB. Stress granule formation mediates the inhibition of colonic hsp70 translation by interferon-gamma and tumor necrosis factor-alpha. *Am J Physiol Gastrointest Liver Physiol*. 2010;298:G481-492
195. Petersen RB, Lindquist S. Regulation of hsp70 synthesis by messenger rna degradation. *Cell Regul*. 1989;1:135-149
196. Dellavalle RP, Petersen R, Lindquist S. Preferential deadenylation of hsp70 mrna plays a key role in regulating hsp70 expression in drosophila melanogaster. *Mol Cell Biol*. 1994;14:3646-3659
197. Luders J, Demand J, Hohfeld J. The ubiquitin-related bag-1 provides a link between the molecular chaperones hsc70/hsp70 and the proteasome. *The Journal of biological chemistry*. 2000;275:4613-4617
198. Sreedhar AS, Pardhasaradhi BV, Khar A, Srinivas UK. A cross talk between cellular signalling and cellular redox state during heat-induced apoptosis in a rat histiocytoma. *Free Radic Biol Med*. 2002;32:221-227
199. Saleh A, Srinivasula SM, Balkir L, Robbins PD, Alnemri ES. Negative regulation of the apaf-1 apoptosome by hsp70. *Nat Cell Biol*. 2000;2:476-483
200. Beere HM, Wolf BB, Cain K, Mosser DD, Mahboubi A, Kuwana T, Tailor P, Morimoto RI, Cohen GM, Green DR. Heat-shock protein 70 inhibits apoptosis by preventing recruitment of procaspase-9 to the apaf-1 apoptosome. *Nat Cell Biol*. 2000;2:469-475
201. Matsumori Y, Northington FJ, Hong SM, Kayama T, Sheldon RA, Vexler ZS, Ferriero DM, Weinstein PR, Liu J. Reduction of caspase-8 and -9 cleavage is associated with increased c-flip and increased binding of apaf-1 and hsp70 after neonatal hypoxic/ischemic injury in mice overexpressing hsp70. *Stroke*. 2006;37:507-512
202. Gupta S, Deepti A, Deegan S, Lisbona F, Hetz C, Samali A. Hsp72 protects cells from er stress-induced apoptosis via enhancement of ire1alpha-xbp1 signaling through a physical interaction. *PLoS biology*. 2010;8:e1000410
203. Anckar J, Sistonen L. Regulation of hsf1 function in the heat stress response: Implications in aging and disease. *Annual review of biochemistry*. 2011;80:1089-1115
204. Xavier IJ, Mercier PA, McLoughlin CM, Ali A, Woodgett JR, Ovsenek N. Glycogen synthase kinase 3beta negatively regulates both DNA-binding and transcriptional activities of heat shock factor 1. *J Biol Chem*. 2000;275:29147-29152
205. Knauf U, Newton EM, Kyriakis J, Kingston RE. Repression of human heat shock factor 1 activity at control temperature by phosphorylation. *Genes Dev*. 1996;10:2782-2793

206. Chu B, Zhong R, Soncin F, Stevenson MA, Calderwood SK. Transcriptional activity of heat shock factor 1 at 37 degrees c is repressed through phosphorylation on two distinct serine residues by glycogen synthase kinase 3 and protein kinases calpha and czeta. *J Biol Chem*. 1998;273:18640-18646
207. Dai R, Frejtag W, He B, Zhang Y, Mivechi NF. C-jun nh2-terminal kinase targeting and phosphorylation of heat shock factor-1 suppress its transcriptional activity. *J Biol Chem*. 2000;275:18210-18218
208. Park J, Liu AY. Jnk phosphorylates the hsf1 transcriptional activation domain: Role of jnk in the regulation of the heat shock response. *J Cell Biochem*. 2001;82:326-338
209. Holmberg CI, Hietakangas V, Mikhailov A, Rantanen JO, Kallio M, Meinander A, Hellman J, Morrice N, MacKintosh C, Morimoto RI, Eriksson JE, Sistonen L. Phosphorylation of serine 230 promotes inducible transcriptional activity of heat shock factor 1. *EMBO J*. 2001;20:3800-3810
210. Soncin F, Zhang X, Chu B, Wang X, Asea A, Ann Stevenson M, Sacks DB, Calderwood SK. Transcriptional activity and DNA binding of heat shock factor-1 involve phosphorylation on threonine 142 by ck2. *Biochem Biophys Res Commun*. 2003;303:700-706
211. Avruch J, Khokhlatchev A, Kyriakis JM, Luo Z, Tzivion G, Vavvas D, Zhang XF. Ras activation of the raf kinase: Tyrosine kinase recruitment of the map kinase cascade. *Recent progress in hormone research*. 2001;56:127-155
212. Davis RJ. Signal transduction by the jnk group of map kinases. *Cell*. 2000;103:239-252
213. Lopez-Bergami P, Habelhah H, Bhoumik A, Zhang W, Wang LH, Ronai Z. Rack1 mediates activation of jnk by protein kinase c [corrected]. *Molecular cell*. 2005;19:309-320
214. Lopez-Bergami P, Huang C, Goydos JS, Yip D, Bar-Eli M, Herlyn M, Smalley KS, Mahale A, Eroshkin A, Aaronson S, Ronai Z. Rewired erk-jnk signaling pathways in melanoma. *Cancer cell*. 2007;11:447-460
215. Erickson JR, Joiner ML, Guan X, Kutschke W, Yang J, Oddis CV, Bartlett RK, Lowe JS, O'Donnell SE, Aykin-Burns N, Zimmerman MC, Zimmerman K, Ham AJ, Weiss RM, Spitz DR, Shea MA, Colbran RJ, Mohler PJ, Anderson ME. A dynamic pathway for calcium-independent activation of camkii by methionine oxidation. *Cell*. 2008;133:462-474
216. Hudmon A, Schulman H. Structure-function of the multifunctional ca2+/calmodulin-dependent protein kinase ii. *Biochem J*. 2002;364:593-611
217. Rosenberg OS, Deindl S, Sung RJ, Nairn AC, Kuriyan J. Structure of the autoinhibited kinase domain of camkii and saxs analysis of the holoenzyme. *Cell*. 2005;123:849-860
218. Mosser DD, Duchaine J, Massie B. The DNA-binding activity of the human heat shock transcription factor is regulated in vivo by hsp70. *Mol Cell Biol*. 1993;13:5427-5438
219. Bloor S, Maelfait J, Krumbach R, Beyaert R, Randow F. Endoplasmic reticulum chaperone gp96 is essential for infection with vesicular stomatitis virus. *Proc Natl Acad Sci U S A*.107:6970-6975
220. Das S, Laxminarayana SV, Chandra N, Ravi V, Desai A. Heat shock protein 70 on neuro2a cells is a putative receptor for japanese encephalitis virus. *Virology*. 2009;385:47-57

221. Reyes-Del Valle J, Chavez-Salinas S, Medina F, Del Angel RM. Heat shock protein 90 and heat shock protein 70 are components of dengue virus receptor complex in human cells. *J Virol*. 2005;79:4557-4567
222. Triantafilou K, Fradelizi D, Wilson K, Triantafilou M. Grp78, a coreceptor for coxsackievirus a9, interacts with major histocompatibility complex class i molecules which mediate virus internalization. *Journal of virology*. 2002;76:633-643
223. Saphire AC, Guan T, Schirmer EC, Nemerow GR, Gerace L. Nuclear import of adenovirus DNA in vitro involves the nuclear protein import pathway and hsc70. *J Biol Chem*. 2000;275:4298-4304
224. Chromy LR, Oltman A, Estes PA, Garcea RL. Chaperone-mediated in vitro disassembly of polyoma- and papillomaviruses. *J Virol*. 2006;80:5086-5091
225. Niyaz Y, Zeiner M, Gehring U. Transcriptional activation by the human hsp70-associating protein hap50. *J Cell Sci*. 2001;114:1839-1845
226. Takahashi N, Sasaki R, Takahashi J, Takayama S, Reed JC, Andoh T. Bag-1m, an isoform of bcl-2-interacting protein bag-1, enhances gene expression driven by cmv promoter. *Biochem Biophys Res Commun*. 2001;286:807-814
227. Devireddy LR, Kumar KU, Pater MM, Pater A. Bag-1, a novel bcl-2-interacting protein, activates expression of human jc virus. *J Gen Virol*. 2000;81:351-357
228. Oglesbee MJ, Liu Z, Kenney H, Brooks CL. The highly inducible member of the 70 kda family of heat shock proteins increases canine distemper virus polymerase activity. *The Journal of general virology*. 1996;77 (Pt 9):2125-2135
229. Momose F, Naito T, Yano K, Sugimoto S, Morikawa Y, Nagata K. Identification of hsp90 as a stimulatory host factor involved in influenza virus rna synthesis. *J Biol Chem*. 2002;277:45306-45314
230. Chen YJ, Chen YH, Chow LP, Tsai YH, Chen PH, Huang CY, Chen WT, Hwang LH. Heat shock protein 72 is associated with the hepatitis c virus replicase complex and enhances viral rna replication. *J Biol Chem*. 2010;285:28183-28190
231. Choukhi A, Ung S, Wychowski C, Dubuisson J. Involvement of endoplasmic reticulum chaperones in the folding of hepatitis c virus glycoproteins. *Journal of virology*. 1998;72:3851-3858
232. Oh WK, Song J. Hsp70 functions as a negative regulator of west nile virus capsid protein through direct interaction. *Biochemical and biophysical research communications*. 2006;347:994-1000
233. Macejak DG, Sarnow P. Association of heat shock protein 70 with enterovirus capsid precursor p1 in infected human cells. *Journal of virology*. 1992;66:1520-1527
234. Oglesbee M, Ringler S, Krakowka S. Interaction of canine distemper virus nucleocapsid variants with 70k heat-shock proteins. *The Journal of general virology*. 1990;71 (Pt 7):1585-1590
235. Melville MW, Tan SL, Wambach M, Song J, Morimoto RI, Katze MG. The cellular inhibitor of the pkr protein kinase, p58(ipk), is an influenza virus-activated co-chaperone that modulates heat shock protein 70 activity. *The Journal of biological chemistry*. 1999;274:3797-3803
236. Agostini I, Popov S, Li J, Dubrovsky L, Hao T, Bukrinsky M. Heat-shock protein 70 can replace viral protein r of hiv-1 during nuclear import of the viral preintegration complex. *Experimental cell research*. 2000;259:398-403

237. Locke M, Tanguay RM, Klabunde RE, Ianuzzo CD. Enhanced postischemic myocardial recovery following exercise induction of hsp 72. *Am J Physiol*. 1995;269:H320-325
238. Meng X, Brown JM, Ao L, Banerjee A, Harken AH. Norepinephrine induces cardiac heat shock protein 70 and delayed cardioprotection in the rat through alpha 1 adrenoceptors. *Cardiovasc Res*. 1996;32:374-383
239. Plumier JC, Currie RW. Heat shock-induced myocardial protection against ischemic injury: A role for hsp70? *Cell Stress Chaperones*. 1996;1:13-17
240. Pshennikova MG, Belkina LM, Bakhtina LY, Baida LA, Smirin BV, Malyshev IY. Hsp70 stress proteins, nitric oxide, and resistance of august and wistar rats to myocardial infarction. *Bull Exp Biol Med*. 2001;132:741-743
241. Okubo S, Wildner O, Shah MR, Chelliah JC, Hess ML, Kukreja RC. Gene transfer of heat-shock protein 70 reduces infarct size in vivo after ischemia/reperfusion in the rabbit heart. *Circulation*. 2001;103:877-881
242. Amrani M, Corbett J, Boateng SY, Dunn MJ, Yacoub MH. Kinetics of induction and protective effect of heat-shock proteins after cardioplegic arrest. *Ann Thorac Surg*. 1996;61:1407-1411; discussion 1411-1402
243. Meng X, Brown JM, Ao L, Nordeen SK, Franklin W, Harken AH, Banerjee A. Endotoxin induces cardiac hsp70 and resistance to endotoxemic myocardial depression in rats. *Am J Physiol*. 1996;271:C1316-1324
244. Snoeckx LH, Cornelussen RN, Van Nieuwenhoven FA, Reneman RS, Van Der Vusse GJ. Heat shock proteins and cardiovascular pathophysiology. *Physiological reviews*. 2001;81:1461-1497
245. Heydari AR, Takahashi R, Gutsmann A, You S, Richardson A. Hsp70 and aging. *Experientia*. 1994;50:1092-1098
246. Berberian PA, Myers W, Tytell M, Challa V, Bond MG. Immunohistochemical localization of heat shock protein-70 in normal-appearing and atherosclerotic specimens of human arteries. *Am J Pathol*. 1990;136:71-80
247. Zhang J, Furukawa RD, Fremes SE. The beneficial effects of heat-shock for prolonged hypothermic storage. *J Surg Res*. 1996;63:314-319
248. Gulbahar MY, Kabak YB, Karayigit MO, Yarim M, Guvenc T, Parlak U. The expressions of hsp70 and alphab-crystallin in myocarditis associated with foot-and-mouth disease virus in lambs. *J Vet Sci*.12:65-73
249. Delcayre C, Samuel JL, Marotte F, Best-Belpomme M, Mercadier JJ, Rappaport L. Synthesis of stress proteins in rat cardiac myocytes 2-4 days after imposition of hemodynamic overload. *J Clin Invest*. 1988;82:460-468
250. Bongrazio M, Comini L, Gaia G, Bachetti T, Ferrari R. Hypertension, aging, and myocardial synthesis of heat-shock protein 72. *Hypertension*. 1994;24:620-624
251. Hamet P, Malo D, Tremblay J. Increased transcription of a major stress gene in spontaneously hypertensive mice. *Hypertension*. 1990;15:904-908
252. McKinsey TA, Olson EN. Dual roles of histone deacetylases in the control of cardiac growth. *Novartis Found Symp*. 2004;259:132-141; discussion 141-135, 163-139
253. Olson EN, Backs J, McKinsey TA. Control of cardiac hypertrophy and heart failure by histone acetylation/deacetylation. *Novartis Found Symp*. 2006;274:3-12; discussion 13-19, 152-155, 272-156

254. Hamamori Y, Schneider MD. Hats off to hop: Recruitment of a class i histone deacetylase incriminates a novel transcriptional pathway that opposes cardiac hypertrophy. *J Clin Invest*. 2003;112:824-826
255. Kook H, Lepore JJ, Gitler AD, Lu MM, Wing-Man Yung W, Mackay J, Zhou R, Ferrari V, Gruber P, Epstein JA. Cardiac hypertrophy and histone deacetylase-dependent transcriptional repression mediated by the atypical homeodomain protein hop. *J Clin Invest*. 2003;112:863-871
256. Kee HJ, Eom GH, Joung H, Shin S, Kim JR, Cho YK, Choe N, Sim BW, Jo D, Jeong MH, Kim KK, Seo JS, Kook H. Activation of histone deacetylase 2 by inducible heat shock protein 70 in cardiac hypertrophy. *Circ Res*. 2008;103:1259-1269
257. Portig I, Pankuweit S, Maisch B. Antibodies against stress proteins in sera of patients with dilated cardiomyopathy. *J Mol Cell Cardiol*. 1997;29:2245-2251
258. Wei YJ, Huang YX, Shen Y, Cui CJ, Zhang XL, Zhang H, Hu SS. Proteomic analysis reveals significant elevation of heat shock protein 70 in patients with chronic heart failure due to arrhythmogenic right ventricular cardiomyopathy. *Mol Cell Biochem*. 2009;332:103-111
259. Shaw JP, Utz PJ, Durand DB, Toole JJ, Emmel EA, Crabtree GR. Identification of a putative regulator of early t cell activation genes. *Science*. 1988;241:202-205
260. Rao A, Luo C, Hogan PG. Transcription factors of the nfat family: Regulation and function. *Annual review of immunology*. 1997;15:707-747
261. Hogan PG, Chen L, Nardone J, Rao A. Transcriptional regulation by calcium, calcineurin, and nfat. *Genes & development*. 2003;17:2205-2232
262. Graef IA, Chen F, Crabtree GR. Nfat signaling in vertebrate development. *Current opinion in genetics & development*. 2001;11:505-512
263. Jain J, Burgeon E, Badalian TM, Hogan PG, Rao A. A similar DNA-binding motif in nfat family proteins and the rel homology region. *The Journal of biological chemistry*. 1995;270:4138-4145
264. Chytil M, Verdine GL. The rel family of eukaryotic transcription factors. *Current opinion in structural biology*. 1996;6:91-100
265. Luo C, Shaw KT, Raghavan A, Aramburu J, Garcia-Cozar F, Perrino BA, Hogan PG, Rao A. Interaction of calcineurin with a domain of the transcription factor nfat1 that controls nuclear import. *Proceedings of the National Academy of Sciences of the United States of America*. 1996;93:8907-8912
266. Macian F. Nfat proteins: Key regulators of t-cell development and function. *Nat Rev Immunol*. 2005;5:472-484
267. Lopez-Rodriguez C, Aramburu J, Rakeman AS, Rao A. Nfat5, a constitutively nuclear nfat protein that does not cooperate with fos and jun. *Proceedings of the National Academy of Sciences of the United States of America*. 1999;96:7214-7219
268. Tong EH, Guo JJ, Huang AL, Liu H, Hu CD, Chung SS, Ko BC. Regulation of nucleocytoplasmic trafficking of transcription factor orebp/tonebp/nfat5. *The Journal of biological chemistry*. 2006;281:23870-23879
269. Lee SD, Colla E, Sheen MR, Na KY, Kwon HM. Multiple domains of tonebp cooperate to stimulate transcription in response to hypertonicity. *The Journal of biological chemistry*. 2003;278:47571-47577
270. Miyakawa H, Woo SK, Dahl SC, Handler JS, Kwon HM. Tonicity-responsive enhancer binding protein, a rel-like protein that stimulates transcription in response to

hypertonicity. *Proceedings of the National Academy of Sciences of the United States of America*. 1999;96:2538-2542
271. Voet D, Voet JG, Pratt CW. *Fundamentals of biochemistry upgrade*. New York: Wiley; 2002.
272. Moeckel GW. Hypertonic stress and cell death. Focus on "multiple cell death pathways are independently activated by lethal hypertonicity in renal epithelial cells". *American journal of physiology. Cell physiology*. 2013;305:C1009-1010
273. Neuhofer W, Beck FX. Cell survival in the hostile environment of the renal medulla. *Annual review of physiology*. 2005;67:531-555
274. Dmitrieva NI, Burg MB. Hypertonic stress response. *Mutat Res*. 2005;569:65-74
275. Burg MB. Response of renal inner medullary epithelial cells to osmotic stress. *Comparative biochemistry and physiology. Part A, Molecular & integrative physiology*. 2002;133:661-666
276. Kino T, Takatori H, Manoli I, Wang Y, Tiulpakov A, Blackman MR, Su YA, Chrousos GP, DeCherney AH, Segars JH. Brx mediates the response of lymphocytes to osmotic stress through the activation of nfat5. *Science signaling*. 2009;2:ra5
277. Kelkar N, Standen CL, Davis RJ. Role of the jip4 scaffold protein in the regulation of mitogen-activated protein kinase signaling pathways. *Molecular and cellular biology*. 2005;25:2733-2743
278. Halterman JA, Kwon HM, Wamhoff BR. Tonicity-independent regulation of the osmosensitive transcription factor tonebp (nfat5). *American journal of physiology. Cell physiology*. 2012;302:C1-8
279. Ko BC, Turck CW, Lee KW, Yang Y, Chung SS. Purification, identification, and characterization of an osmotic response element binding protein. *Biochemical and biophysical research communications*. 2000;270:52-61
280. Ito T, Fujio Y, Hirata M, Takatani T, Matsuda T, Muraoka S, Takahashi K, Azuma J. Expression of taurine transporter is regulated through the tone (tonicity-responsive element)/tonebp (tone-binding protein) pathway and contributes to cytoprotection in hepg2 cells. *The Biochemical journal*. 2004;382:177-182
281. Bosman DK, Deutz NE, Maas MA, van Eijk HM, Smit JJ, de Haan JG, Chamuleau RA. Amino acid release from cerebral cortex in experimental acute liver failure, studied by in vivo cerebral cortex microdialysis. *Journal of neurochemistry*. 1992;59:591-599
282. Rim JS, Atta MG, Dahl SC, Berry GT, Handler JS, Kwon HM. Transcription of the sodium/myo-inositol cotransporter gene is regulated by multiple tonicity-responsive enhancers spread over 50 kilobase pairs in the 5'-flanking region. *The Journal of biological chemistry*. 1998;273:20615-20621
283. Lopez-Rodriguez C, Aramburu J, Jin L, Rakeman AS, Michino M, Rao A. Bridging the nfat and nf-kappab families: Nfat5 dimerization regulates cytokine gene transcription in response to osmotic stress. *Immunity*. 2001;15:47-58
284. Go WY, Liu X, Roti MA, Liu F, Ho SN. Nfat5/tonebp mutant mice define osmotic stress as a critical feature of the lymphoid microenvironment. *Proceedings of the National Academy of Sciences of the United States of America*. 2004;101:10673-10678
285. Nuss DL, Koch G. Differential inhibition of vesicular stomatitis virus polypeptide synthesis by hypertonic initiation block. *Journal of virology*. 1975;17:283-286

286. Docherty PA, Snider MD. Effects of hypertonic and sodium-free medium on transport of a membrane glycoprotein along the secretory pathway in cultured mammalian cells. *Journal of cellular physiology*. 1991;146:34-42
287. Nuss DL, Oppermann H, Koch G. Selective blockage of initiation of host protein-synthesis in rna-virus-infected cells. *Proceedings of the National Academy of Sciences of the United States of America*. 1975;72:1258-1262
288. Tershak DR. Peptide-chain initiation with lsc poliovirus is intrinsically more resistant to hypertonic environment than is peptide-chain initiation with mahoney virus and deletion mutants of mahoney virus. *Journal of virology*. 1978;28:1006-1010
289. Cherney CS, Wilhelm JM. Differential translation in normal and adenovirus type-5-infected human-cells and cell-free systems. *Journal of virology*. 1979;30:533-542
290. Ranjbar S, Tsytsykova AV, Lee SK, Rajsbaum R, Falvo JV, Lieberman J, Shankar P, Goldfeld AE. Nfat5 regulates hiv-1 in primary monocytes via a highly conserved long terminal repeat site. *PLoS pathogens*. 2006;2:e130
291. Ranjbar S, Jasenosky LD, Chow N, Goldfeld AE. Regulation of mycobacterium tuberculosis-dependent hiv-1 transcription reveals a new role for nfat5 in the toll-like receptor pathway. *PLoS pathogens*. 2012;8:e1002620
292. Lim YS, Shin KS, Oh SH, Kang SM, Won SJ, Hwang SB. Nonstructural 5a protein of hepatitis c virus regulates heat shock protein 72 for its own propagation. *Journal of viral hepatitis*. 2012;19:353-363
293. Paterna S, Di Pasquale P, Parrinello G, Fornaciari E, Di Gaudio F, Fasullo S, Giammanco M, Sarullo FM, Licata G. Changes in brain natriuretic peptide levels and bioelectrical impedance measurements after treatment with high-dose furosemide and hypertonic saline solution versus high-dose furosemide alone in refractory congestive heart failure: A double-blind study. *Journal of the American College of Cardiology*. 2005;45:1997-2003
294. Licata G, Di Pasquale P, Parrinello G, Cardinale A, Scandurra A, Follone G, Argano C, Tuttolomondo A, Paterna S. Effects of high-dose furosemide and small-volume hypertonic saline solution infusion in comparison with a high dose of furosemide as bolus in refractory congestive heart failure: Long-term effects. *American heart journal*. 2003;145:459-466
295. Gandhi S, Mosleh W, Myers RB. Hypertonic saline with furosemide for the treatment of acute congestive heart failure: A systematic review and meta-analysis. *International journal of cardiology*. 2014;173:139-145
296. Okuhara Y, Hirotani S, Naito Y, Nakabo A, Iwasaku T, Eguchi A, Morisawa D, Ando T, Sawada H, Manabe E, Masuyama T. Intravenous salt supplementation with low-dose furosemide for treatment of acute decompensated heart failure. *Journal of cardiac failure*. 2014;20:295-301
297. Zampieri FG, Caruso P. Acute treatment of uncompensated heart failure with 10% hypertonic saline and its subsequent effect on respiratory patterns. *Clinics*. 2011;66:717-718
298. Trama J, Lu Q, Hawley RG, Ho SN. The nfat-related protein nfatl1 (tonebp/nfat5) is induced upon t cell activation in a calcineurin-dependent manner. *J Immunol*. 2000;165:4884-4894

299. Maouyo D, Kim JY, Lee SD, Wu Y, Woo SK, Kwon HM. Mouse tonebp-nfat5: Expression in early development and alternative splicing. *American journal of physiology. Renal physiology*. 2002;282:F802-809
300. Ito T, Fujio Y, Takahashi K, Azuma J. Degradation of nfat5, a transcriptional regulator of osmotic stress-related genes, is a critical event for doxorubicin-induced cytotoxicity in cardiac myocytes. *The Journal of biological chemistry*. 2007;282:1152-1160
301. Mak MC, Lam KM, Chan PK, Lau YB, Tang WH, Yeung PK, Ko BC, Chung SM, Chung SK. Embryonic lethality in mice lacking the nuclear factor of activated t cells 5 protein due to impaired cardiac development and function. *PLoS One*. 2011;6:e19186
302. Roth I, Leroy V, Kwon HM, Martin PY, Feraille E, Hasler U. Osmoprotective transcription factor nfat5/tonebp modulates nuclear factor-kappab activity. *Mol Biol Cell*. 2010;21:3459-3474
303. Lawrence T. The nuclear factor nf-kappab pathway in inflammation. *Cold Spring Harb Perspect Biol*. 2009;1:a001651
304. Esfandiarei M, Boroomand S, Suarez A, Si X, Rahmani M, McManus B. Coxsackievirus b3 activates nuclear factor kappa b transcription factor via a phosphatidylinositol-3 kinase/protein kinase b-dependent pathway to improve host cell viability. *Cellular microbiology*. 2007;9:2358-2371
305. Buxade M, Lunazzi G, Minguillon J, Iborra S, Berga-Bolanos R, Del Val M, Aramburu J, Lopez-Rodriguez C. Gene expression induced by toll-like receptors in macrophages requires the transcription factor nfat5. *The Journal of experimental medicine*. 2012;209:379-393
306. Rastaldo R, Pagliaro P, Cappello S, Penna C, Mancardi D, Westerhof N, Losano G. Nitric oxide and cardiac function. *Life Sci*. 2007;81:779-793
307. Lowenstein CJ, Hill SL, Lafond-Walker A, Wu J, Allen G, Landavere M, Rose NR, Herskowitz A. Nitric oxide inhibits viral replication in murine myocarditis. *J Clin Invest*. 1996;97:1837-1843
308. Iordanskiy S, Zhao Y, Dubrovsky L, Iordanskaya T, Chen M, Liang D, Bukrinsky M. Heat shock protein 70 protects cells from cell cycle arrest and apoptosis induced by human immunodeficiency virus type 1 viral protein r. *Journal of virology*. 2004;78:9697-9704
309. Oglesbee MJ, Kenney H, Kenney T, Krakowka S. Enhanced production of morbillivirus gene-specific rnas following induction of the cellular stress response in stable persistent infection. *Virology*. 1993;192:556-567
310. Padmini E, Lavanya S. Over expression of hsp70 and hsf1 in endothelial cells during pre-eclamptic placental stress. *The Australian & New Zealand journal of obstetrics & gynaecology*. 2011;51:47-52
311. Dai Q, Zhang C, Wu Y, McDonough H, Whaley RA, Godfrey V, Li HH, Madamanchi N, Xu W, Neckers L, Cyr D, Patterson C. Chip activates hsf1 and confers protection against apoptosis and cellular stress. *The EMBO journal*. 2003;22:5446-5458
312. Liu G, Yang Y, Gu Q. [the effect of coxsackie virus b3 on intracellular calcium homeostasis in rat cardiomyocytes]. *Zhonghua Shi Yan He Lin Chuang Bing Du Xue Za Zhi*. 2000;14:113-116
313. Si X, McManus BM, Zhang J, Yuan J, Cheung C, Esfandiarei M, Suarez A, Morgan A, Luo H. Pyrrolidine dithiocarbamate reduces coxsackievirus b3 replication through inhibition of the ubiquitin-proteasome pathway. *Journal of virology*. 2005;79:8014-8023

314. Melling CW, Krause MP, Noble EG. Pka-mediated erk1/2 inactivation and hsp70 gene expression following exercise. *Journal of molecular and cellular cardiology*. 2006;41:816-822
315. Chu B, Soncin F, Price BD, Stevenson MA, Calderwood SK. Sequential phosphorylation by mitogen-activated protein kinase and glycogen synthase kinase 3 represses transcriptional activation by heat shock factor-1. *The Journal of biological chemistry*. 1996;271:30847-30857
316. Luo H, Yanagawa B, Zhang J, Luo Z, Zhang M, Esfandiarei M, Carthy C, Wilson JE, Yang D, McManus BM. Coxsackievirus b3 replication is reduced by inhibition of the extracellular signal-regulated kinase (erk) signaling pathway. *Journal of virology*. 2002;76:3365-3373
317. Henics T, Nagy E, Oh HJ, Csermely P, von Gabain A, Subjeck JR. Mammalian hsp70 and hsp110 proteins bind to rna motifs involved in mrna stability. *The Journal of biological chemistry*. 1999;274:17318-17324
318. He C, Schneider R. 14-3-3sigma is a p37 auf1-binding protein that facilitates auf1 transport and au-rich mrna decay. *EMBO J*. 2006;25:3823-3831
319. Laroia G, Cuesta R, Brewer G, Schneider RJ. Control of mrna decay by heat shock-ubiquitin-proteasome pathway. *Science*. 1999;284:499-502
320. Kishor A, Tandukar B, Ly YV, Toth EA, Suarez Y, Brewer G, Wilson GM. Hsp70 is a novel posttranscriptional regulator of gene expression that binds and stabilizes selected mrnas containing au-rich elements. *Mol Cell Biol*. 2013;33:71-84
321. van Ooij MJ, Polacek C, Glaudemans DH, Kuijpers J, van Kuppeveld FJ, Andino R, Agol VI, Melchers WJ. Polyadenylation of genomic rna and initiation of antigenomic rna in a positive-strand rna virus are controlled by the same cis-element. *Nucleic acids research*. 2006;34:2953-2965
322. Zeng XC, Bhasin S, Wu X, Lee JG, Maffi S, Nichols CJ, Lee KJ, Taylor JP, Greene LE, Eisenberg E. Hsp70 dynamics in vivo: Effect of heat shock and protein aggregation. *Journal of cell science*. 2004;117:4991-5000
323. Lund N, Milev MP, Wong R, Sanmuganantham T, Woolaway K, Chabot B, Abou Elela S, Mouland AJ, Cochrane A. Differential effects of hnrnp d/auf1 isoforms on hiv-1 gene expression. *Nucleic acids research*. 2012;40:3663-3675
324. Ye X, Zhang HM, Qiu Y, Hanson PJ, Hemida MG, Wei W, Hoodless PA, Chu F, Yang D. Coxsackievirus-induced mir-21 disrupts cardiomyocyte interactions via the downregulation of intercalated disk components. *PLoS pathogens*. 2014;10:e1004070
325. Kim D, Kim SH, Li GC. Proteasome inhibitors mg132 and lactacystin hyperphosphorylate hsf1 and induce hsp70 and hsp27 expression. *Biochem Biophys Res Commun*. 1999;254:264-268
326. Tokumitsu H, Chijiwa T, Hagiwara M, Mizutani A, Terasawa M, Hidaka H. Kn-62, 1-[n,o-bis(5-isoquinolinesulfonyl)-n-methyl-l-tyrosyl]-4-phenylpiperazi ne, a specific inhibitor of ca2+/calmodulin-dependent protein kinase ii. *J Biol Chem*. 1990;265:4315-4320
327. Yoon YJ, Kim JA, Shin KD, Shin DS, Han YM, Lee YJ, Lee JS, Kwon BM, Han DC. Kribb11 inhibits hsp70 synthesis through inhibition of heat shock factor 1 function by impairing the recruitment of positive transcription elongation factor b to the hsp70 promoter. *The Journal of biological chemistry*. 2011;286:1737-1747

328. Tombes RM, Faison MO, Turbeville JM. Organization and evolution of multifunctional ca(2+)/cam-dependent protein kinase genes. *Gene*. 2003;322:17-31
329. Backs J, Backs T, Neef S, Kreusser MM, Lehmann LH, Patrick DM, Grueter CE, Qi X, Richardson JA, Hill JA, Katus HA, Bassel-Duby R, Maier LS, Olson EN. The delta isoform of cam kinase ii is required for pathological cardiac hypertrophy and remodeling after pressure overload. *Proceedings of the National Academy of Sciences of the United States of America*. 2009;106:2342-2347
330. Peng W, Zhang Y, Zheng M, Cheng H, Zhu W, Cao CM, Xiao RP. Cardioprotection by camkii-deltab is mediated by phosphorylation of heat shock factor 1 and subsequent expression of inducible heat shock protein 70. *Circ Res*. 2010;106:102-110
331. Wagner BJ, DeMaria CT, Sun Y, Wilson GM, Brewer G. Structure and genomic organization of the human auf1 gene: Alternative pre-mrna splicing generates four protein isoforms. *Genomics*. 1998;48:195-202
332. Gulbahar MY, Kabak YB, Karayigit MO, Yarim M, Guvenc T, Parlak U. The expressions of hsp70 and alphab-crystallin in myocarditis associated with foot-and-mouth disease virus in lambs. *J Vet Sci*. 2011;12:65-73
333. Broquet AH, Lenoir C, Gardet A, Sapin C, Chwetzoff S, Jouniaux AM, Lopez S, Trugnan G, Bachelet M, Thomas G. Hsp70 negatively controls rotavirus protein bioavailability in caco-2 cells infected by the rotavirus rf strain. *J Virol*. 2007;81:1297-1304
334. Ye J, Chen Z, Zhang B, Miao H, Zohaib A, Xu Q, Chen H, Cao S. Heat shock protein 70 is associated with replicase complex of japanese encephalitis virus and positively regulates viral genome replication. *PloS one*. 2013;8:e75188
335. Liu J, Bai J, Zhang L, Jiang Z, Wang X, Li Y, Jiang P. Hsp70 positively regulates porcine circovirus type 2 replication in vitro. *Virology*. 2013;447:52-62
336. Kim MY, Ma Y, Zhang Y, Li J, Shu Y, Oglesbee M. Hsp70-dependent antiviral immunity against cytopathic neuronal infection by vesicular stomatitis virus. *Journal of virology*. 2013;87:10668-10678
337. Kumar M, Rawat P, Khan SZ, Dhamija N, Chaudhary P, Ravi DS, Mitra D. Reciprocal regulation of human immunodeficiency virus-1 gene expression and replication by heat shock proteins 40 and 70. *Journal of molecular biology*. 2011;410:944-958
338. Tan W, Schwartz S. The rev protein of human immunodeficiency virus type 1 counteracts the effect of an au-rich negative element in the human papillomavirus type 1 late 3' untranslated region. *Journal of virology*. 1995;69:2932-2945
339. Juhasz K, Lipp AM, Nimmervoll B, Sonnleitner A, Hesse J, Haselgruebler T, Balogi Z. The complex function of hsp70 in metastatic cancer. *Cancers*. 2013;6:42-66
340. Juhasz K, Thuenauer R, Spachinger A, Duda E, Horvath I, Vigh L, Sonnleitner A, Balogi Z. Lysosomal rerouting of hsp70 trafficking as a potential immune activating tool for targeting melanoma. *Current pharmaceutical design*. 2013;19:430-440
341. Kwon MS, Lim SW, Kwon HM. Hypertonic stress in the kidney: A necessary evil. *Physiology (Bethesda)*. 2009;24:186-191
342. Jauliac S, Lopez-Rodriguez C, Shaw LM, Brown LF, Rao A, Toker A. The role of nfat transcription factors in integrin-mediated carcinoma invasion. *Nature cell biology*. 2002;4:540-544

343. Nybakken K, Vokes SA, Lin TY, McMahon AP, Perrimon N. A genome-wide rna interference screen in drosophila melanogaster cells for new components of the hh signaling pathway. *Nat Genet*. 2005;37:1323-1332
344. Gao G, Wong J, Zhang J, Mao I, Shravah J, Wu Y, Xiao A, Li X, Luo H. Proteasome activator reggamma enhances coxsackieviral infection by facilitating p53 degradation. *Journal of virology*. 2010;84:11056-11066
345. Luo H, Zhang J, Cheung C, Suarez A, McManus BM, Yang D. Proteasome inhibition reduces coxsackievirus b3 replication in murine cardiomyocytes. *The American journal of pathology*. 2003;163:381-385
346. Esensten JH, Tsytsykova AV, Lopez-Rodriguez C, Ligeiro FA, Rao A, Goldfeld AE. Nfat5 binds to the tnf promoter distinctly from nfatp, c, 3 and 4, and activates tnf transcription during hypertonic stress alone. *Nucleic acids research*. 2005;33:3845-3854
347. Blom N, Hansen J, Blaas D, Brunak S. Cleavage site analysis in picornaviral polyproteins: Discovering cellular targets by neural networks. *Protein science : a publication of the Protein Society*. 1996;5:2203-2216
348. Wong J, Si X, Angeles A, Zhang J, Shi J, Fung G, Jagdeo J, Wang T, Zhong Z, Jan E, Luo H. Cytoplasmic redistribution and cleavage of auf1 during coxsackievirus infection enhance the stability of its viral genome. *FASEB journal : official publication of the Federation of American Societies for Experimental Biology*. 2013;27:2777-2787
349. Aramburu J, Drews-Elger K, Estrada-Gelonch A, Minguillon J, Morancho B, Santiago V, Lopez-Rodriguez C. Regulation of the hypertonic stress response and other cellular functions by the rel-like transcription factor nfat5. *Biochemical pharmacology*. 2006;72:1597-1604
350. Qiu Y, Ye X, Hanson PJ, Zhang HM, Zong J, Cho B, Yang D. Hsp70-1: Upregulation via selective phosphorylation of heat shock factor 1 during coxsackieviral infection and promotion of viral replication via the au-rich element. *Cellular and molecular life sciences : CMLS*. 2016;73:1067-1084
351. Sobotta K, Wilsky S, Althof N, Wiesener N, Wutzler P, Henke A. Inhibition of nuclear factor kappa b activation reduces coxsackievirus b3 replication in lymphoid cells. *Virus research*. 2012;163:495-502
352. Saura M, Zaragoza C, McMillan A, Quick RA, Hohenadl C, Lowenstein JM, Lowenstein CJ. An antiviral mechanism of nitric oxide: Inhibition of a viral protease. *Immunity*. 1999;10:21-28
353. Granados-Principal S, Liu Y, Guevara ML, Blanco E, Choi DS, Qian W, Patel T, Rodriguez AA, Cusimano J, Weiss HL, Zhao H, Landis MD, Dave B, Gross SS, Chang JC. Inhibition of inos as a novel effective targeted therapy against triple-negative breast cancer. *Breast Cancer Res*. 2015;17:25
354. Yu FH, Catterall WA. Overview of the voltage-gated sodium channel family. *Genome biology*. 2003;4:207
355. Malek AM, Goss GG, Jiang L, Izumo S, Alper SL. Mannitol at clinical concentrations activates multiple signaling pathways and induces apoptosis in endothelial cells. *Stroke*. 1998;29:2631-2640
356. Wang H, Lei X, Xiao X, Yang C, Lu W, Huang Z, Leng Q, Jin Q, He B, Meng G, Wang J. Reciprocal regulation between enterovirus 71 and the nlrp3 inflammasome. *Cell reports*. 2015;12:42-48

357. Li J, Yao Y, Chen Y, Xu X, Lin Y, Yang Z, Qiao W, Tan J. Enterovirus 71 3c promotes apoptosis through cleavage of pinx1, a telomere binding protein. *Journal of virology*. 2017;91
358. Hanson PJ, Ye X, Qiu Y, Zhang HM, Hemida MG, Wang F, Lim T, Gu A, Cho B, Kim H, Fung G, Granville DJ, Yang D. Cleavage of dap5 by coxsackievirus b3 2a protease facilitates viral replication and enhances apoptosis by altering translation of ires-containing genes. *Cell death and differentiation*. 2016;23:828-840
359. Deng H, Fung G, Shi J, Xu S, Wang C, Yin M, Hou J, Zhang J, Jin ZG, Luo H. Enhanced enteroviral infectivity via viral protease-mediated cleavage of grb2-associated binder 1. *FASEB journal : official publication of the Federation of American Societies for Experimental Biology*. 2015;29:4523-4531
360. Adachi A, Takahashi T, Ogata T, Imoto-Tsubakimoto H, Nakanishi N, Ueyama T, Matsubara H. Nfat5 regulates the canonical wnt pathway and is required for cardiomyogenic differentiation. *Biochem Biophys Res Commun*. 2012;426:317-323
361. Lee JH, Kim M, Im YS, Choi W, Byeon SH, Lee HK. Nfat5 induction and its role in hyperosmolar stressed human limbal epithelial cells. *Investigative ophthalmology & visual science*. 2008;49:1827-1835
362. Carthy CM, Granville DJ, Watson KA, Anderson DR, Wilson JE, Yang D, Hunt DW, McManus BM. Caspase activation and specific cleavage of substrates after coxsackievirus b3-induced cytopathic effect in hela cells. *Journal of virology*. 1998;72:7669-7675
363. Zhao Z, Cai TZ, Lu Y, Liu WJ, Cheng ML, Ji YQ. Coxsackievirus b3 induces viral myocarditis by upregulating toll-like receptor 4 expression. *Biochemistry. Biokhimiia*. 2015;80:455-462
364. Yang D, Yu J, Luo Z, Carthy CM, Wilson JE, Liu Z, McManus BM. Viral myocarditis: Identification of five differentially expressed genes in coxsackievirus b3-infected mouse heart. *Circulation research*. 1999;84:704-712
365. Melchers WJ, Hoenderop JG, Bruins Slot HJ, Pleij CW, Pilipenko EV, Agol VI, Galama JM. Kissing of the two predominant hairpin loops in the coxsackie b virus 3' untranslated region is the essential structural feature of the origin of replication required for negative-strand rna synthesis. *J Virol*. 1997;71:686-696
366. Forstermann U, Sessa WC. Nitric oxide synthases: Regulation and function. *European heart journal*. 2012;33:829-837, 837a-837d
367. Paterna S, Fasullo S, Parrinello G, Cannizzaro S, Basile I, Vitrano G, Terrazzino G, Maringhini G, Ganci F, Scalzo S, Sarullo FM, Cice G, Di Pasquale P. Short-term effects of hypertonic saline solution in acute heart failure and long-term effects of a moderate sodium restriction in patients with compensated heart failure with new york heart association class iii (class c) (smac-hf study). *The American journal of the medical sciences*. 2011;342:27-37
368. Tuttolomondo A, Pinto A, Parrinello G, Licata G. Intravenous high-dose furosemide and hypertonic saline solutions for refractory heart failure and ascites. *Semin Nephrol*. 2011;31:513-522
369. Daugaard M, Rohde M, Jaattela M. The heat shock protein 70 family: Highly homologous proteins with overlapping and distinct functions. *FEBS letters*. 2007;581:3702-3710

370. Govin J, Caron C, Escoffier E, Ferro M, Kuhn L, Rousseaux S, Eddy EM, Garin J, Khochbin S. Post-meiotic shifts in hspa2/hsp70.2 chaperone activity during mouse spermatogenesis. *The Journal of biological chemistry*. 2006;281:37888-37892
371. Jagadish N, Agarwal S, Gupta N, Fatima R, Devi S, Kumar V, Suri V, Kumar R, Sadasukhi TC, Gupta A, Ansari AS, Lohiya NK, Suri A. Heat shock protein 70-2 (hsp70-2) overexpression in breast cancer. *Journal of experimental & clinical cancer research : CR*. 2016;35:150
372. Daugaard M, Jaattela M, Rohde M. Hsp70-2 is required for tumor cell growth and survival. *Cell Cycle*. 2005;4:877-880
373. Mardan-Nik M, Pasdar A, Jamialahmadi K, Avan A, Mohebati M, Esmaily H, Biabangard-Zak A, Afzal Javan F, Rivandi M, Ferns GA, Ghayour-Mobarhan M. Association of heat shock protein70-2 (hsp70-2) gene polymorphism with obesity. *Annals of human biology*. 2016;43:542-546
374. Dix DJ, Allen JW, Collins BW, Mori C, Nakamura N, Poorman-Allen P, Goulding EH, Eddy EM. Targeted gene disruption of hsp70-2 results in failed meiosis, germ cell apoptosis, and male infertility. *Proceedings of the National Academy of Sciences of the United States of America*. 1996;93:3264-3268
375. Rohde M, Daugaard M, Jensen MH, Helin K, Nylandsted J, Jaattela M. Members of the heat-shock protein 70 family promote cancer cell growth by distinct mechanisms. *Genes & development*. 2005;19:570-582
376. Wang F, Qiu Y, Zhang HM, Hanson P, Ye X, Zhao G, Xie R, Tong L, Yang D. Heat shock protein 70 promotes coxsackievirus b3 translation initiation and elongation via akt-mtorc1 pathway depending on activation of p70s6k and cdc2. *Cellular microbiology*. 2017
377. Sean P, Semler BL. Coxsackievirus b rna replication: Lessons from poliovirus. *Curr Top Microbiol Immunol*. 2008;323:89-121
378. Weger S, Wendland M, Kleinschmidt JA, Heilbronn R. The adeno-associated virus type 2 regulatory proteins rep78 and rep68 interact with the transcriptional coactivator pc4. *Journal of virology*. 1999;73:260-269
379. Leuschner F, Katus HA, Kaya Z. Autoimmune myocarditis: Past, present and future. *Journal of autoimmunity*. 2009;33:282-289
380. Caforio AL, Marcolongo R, Jahns R, Fu M, Felix SB, Iliceto S. Immune-mediated and autoimmune myocarditis: Clinical presentation, diagnosis and management. *Heart failure reviews*. 2013;18:715-732
381. Morancho B, Minguillon J, Molkentin JD, Lopez-Rodriguez C, Aramburu J. Analysis of the transcriptional activity of endogenous nfat5 in primary cells using transgenic nfat-luciferase reporter mice. *BMC molecular biology*. 2008;9:13
382. Berga-Bolanos R, Drews-Elger K, Aramburu J, Lopez-Rodriguez C. Nfat5 regulates t lymphocyte homeostasis and cd24-dependent t cell expansion under pathologic hypernatremia. *Journal of immunology*. 2010;185:6624-6635